

Mohamed Khider University of Biskra Faculty of exact sciences Material sciences department

MASTER DISSERTATION

Domain of Material sciences Section of Physics Speciality of Materials Physics

Réf:

Presented by: **Ben khelifa Fouzia**

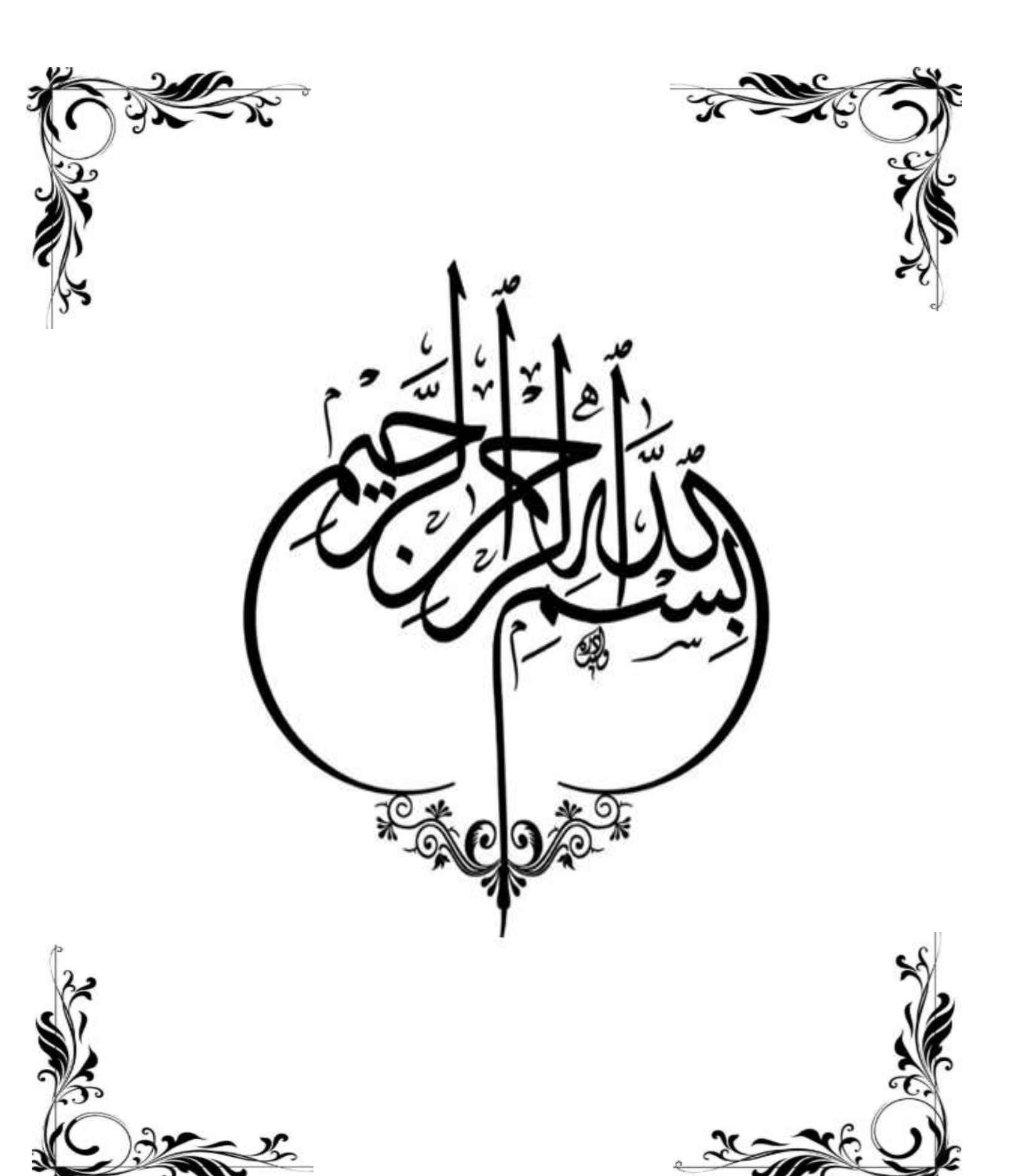
The: 26/05/2025

Effect of substrates on the properties of ZnO thin films elaborated with the solgel methode

Jury:

Mr . AbdelGhani Lakel
 MCA. University Med Khider of Biskra
 Chairman
 Mrs . Aicha Kater
 MAA. University Med Khider of Biskra
 Examiner
 Miss . Louiza Arab
 Pr. University Med Khider of Biskra
 Reporter

Academic Year: 2024/2025



Dedication

In the name of Allah, the Most Gracious, the Most Most Merciful, and may peace and blessings be upon His noble Messenger.

With great pride and appreciation, I dedicate this humble work to my dear parents: my beloved mother, **Khadija**, who has been my source of support and motivation toward success, and my dear father, **Issa**, who has been my pillar in continuing my academic journey and ensuring my academic journey and ensuring my higher education.

To my dear siblings, **Souad, Jamal**, and **Salim**, And their **children**.

To my dear uncle, **Mohamed**, who holds a special in my heart.

To all my friends and fellow students.

Fouzía

ACKNOWLEDGEMENTS

In the name of Allah, the Most Gracious, the Most Merciful. All praise is due to Allah His grace and generosity, granting us strength, patience, and perseverance to continue my journey in the pursuit of knowledge and to reach the academic ranks I have always dreamed of

I would like to express my gratitude and appreciation to everyone who contributed to the completion of this these, whether directly or indirectly.

I extend my sincere thanks and deep appreciation to my supervisor, professor Louiza Arab, who accompanied me throughout the completion of this theses with her dedication and continuous support.

I would like to extend my gratitude to all the members of the examination committee, including **prof Aicha Kater** from the University of Biskra and the chairman of the committee, **prof Abdel Ghani Lakel** from the University of Biskra, for their constructive criticism and valuable evaluations.

I would like to express my appreciation and gratitude to my friend, Ms. Latif Aya, and Ms. Messeddek Lobna, for their valuable guidance and their dedication in helping me complete my thesis in the best possible way

I extend my deepest thanks and gratitude to professor Nour El-Dín Sengouga, Head of the Laboratory of Metallic and Semiconductor Materials (LMSM) at the University of Biskra, and to the esteemed professor Toufik Tibermacine for their invaluable assistance. I also thank all the members and staff who contributed to the success of this achievement.

Dedication	I
Acknowledgements	II
Content table	III
List of Tables	VII
List of Figures	VIII
General Introduction	1
Chapter I: Bibliographic Research	
I.1. Introduction	4
I.2. What is Transparent Conducting Oxide?	4
I.2.1. Some properties of TCOs.	4
I.2.1.1. The electrical properties of TCO	5
I.2.1.2 . The optical properties of TCO	5
I.2.1.2.a. The transmittance T.	5
I.2.1.2.b. The reflection R.	5
I.2.1.2.c. The absorption factors A	6
I.2.2. Different types of defects in transparent conductive oxides(TCOs)	7
I.2.3. Transparent conductive oxide applications	8
I.3. The Zinc Oxide	9
I.3.1. History of zinc oxide "ZnO"	10
I.3.2. The choice of the studied semiconductor ZnO	11
I.3.3. Properties of Zinc Oxide	11
I.3.3.1. Physical Properties.	12
I.3.3.1.1. Crystallographic properties	12
I.3.3.1.2. electronic structure of a band	14
I.3.3.1.3. Optical and luminous characteristics	16
I.3.3.1.4Mechanical properties.	17
I.3.3.1.5. The piezoelectric effect.	18
I.3.3.1.6. Magnetic properties	18

I.3.3.2. Chemical Properties	18
I.3.4. Applications of Zinc Oxide	19
I.4. Nanotechnologies	20
I.4.1. Materials at the nanoscale	21
I.4.2. ZnO nanoparticles.	23
I.4.3. Morphology Controlled.	23
I.4.4. Properties of Zinc Oxide Nanostructures	24
I.4.4.1. Electronic properties of nanomaterials	24
I.4.4.2. Mechanical properties of nanomaterials	25
I.4.4.3. Piezoelectric properties of nanomaterials	25
I.4.4.4. Optical properties of nanomaterials	25
I.5. Brief history	26
I.5.1. What is a thin film?	26
I.5.2. Applications of Zinc Oxide thin films	27
I.5.3. Technological challenges of thin films	28
References	30
Chapter II. Elaboration and abayestavization methods	
Chapter II: Elaboration and characterization methods	
II .1. Introduction	36
II .2. Thin film Deposition Methods	36
II .3. Sol-gel method.	37
II .3.1. History of the sol-gel method.	37
II .3.2. Definition of the sol-gel.	38
II.3.3. The Sol-gel process.	38
II.3.3.1. The sol-gel transition	39
II.3.3.2. Reaction mechanisms.	40
II.3.3.2. a. Hydrolysis reaction.	40
II.3.3.2 b. Condensation reaction.	40
II.3.3.3. Gelation	41
II.3.3.4. Ageing	41

II.3.3.5. Drying	41
II.3.4. parameters influencing the reaction rate	42
II.3.5. Gel Drying.	42
II.3.6. Sol-gel deposition techniques.	43
II.3.6.1. Spin-coating.	44
II.3.6.2. Dip-coating.	46
II.3.7. Applications of the sol-gel method.	46
II.3.8. Advantages of the sol-gel method	47
II.3.9. Drawbacks of the sol-gel method.	47
II.4. Characterization techniques.	48
II.4.1. X-ray Diffraction.	48
II.4.1.a. Apparatus	48
II.4.1.b. The X-ray diffraction measurement principle	49
II.4.1.c. Determination of interatomic distances and lattice parameters	49
II.4.1.d. Determination of grain size and stresses	50
II.4.2. Optical characterization.	52
II.4.2.1. absorption spectra.	55
II.4.2.2. Optical band gap (<i>Eg</i>)	55
II.4.2.3. Determination of the Urbach energy.	56
II.4.3. Electrical characterization.	56
II.4.3.1. Four probes technique.	56
References	59
Chapter III: Results and Discussion	
III .1. Introduction	62
III .2. Used apparatus (Spin coating)	62
III .3. Experimental details	63
III.3.1. Choice of deposition substrates.	63
III.3.2. Cleaning of the substrate	63

III.3.3. Preparation of Zinc Oxide	64
III.3.4. Drying and heat treatment of Thin Films	65
III.3.5. Adhesion quality test.	66
III.4. Results and discussion.	67
III.4.1. Structural characterization.	67
III.4.1.1. X-ray diffraction.	67
III.4.1.2. Analysis of X-ray spectra.	67
III.4.1.3. Determination of grain size	71
III.4.1.3.1. Effect of substrates on Zinc Oxide thin films	74
III.4.1.3.1.a. Variation of crystallin parameters with substrates grown on	74
III.4.1.3.1.b Variation of grain size with substrates grown on	75
III.4.1.3.2. Effect of gelation time on Zinc Oxide thin films	77
III.4.2. Optical characterization.	81
III.4.2.1. UV-visible.	81
III.4.2.1.1. Transmittance.	81
III.4.2.1.1.1. Effect of substrates on Zinc Oxide thin films	82
III.4.2.1.1.2. The Effect of gelation time on ZnO thin films	83
III.4.2.1.1.3. Effect of rest time of the solution on ZnO thin films	84
III.4.2.1.2. Optical band gap.	85
III.4.2.1.3. Urbach energy.	85
III.4.3. Electrical characterization	88
III.4.3.1. The four-point Technique	88
References	93
General Conclusion	97
Abstract	99
ملخص	99
Dágumá	100

List of Table

Table I-1: Expansion of the band gap of certain TCO 4
Table I-2: Properties of Zinc Oxide 12
Table I-3: Recapitalization of structural characteristics of ZnO 14
Table I-4: Some electrical properties of ZnO 16
Table I-5: The optical properties of Zinc Oxide 17
Table III-1: Structural parameters values of ZnO thin films grown on different substrates with gelation time $tg = 60 \text{ min}$ 74
Table III-2: Grain size, micro strains (ϵ), and dislocation densities (δ) of ZnO thin films grown on different substrates with gelation time tg = 60 min
Table III-3: Structural parameters values of ZnO thin films grown on different substrates with gelation time tg = 30 and 60 min.
Table III-5: Variation of the optical parameters of ZnO thin films with elaboration conditions87
Table III-6: Results of resistance and resistivity of ZnO thin films for different substrates used

List of figures

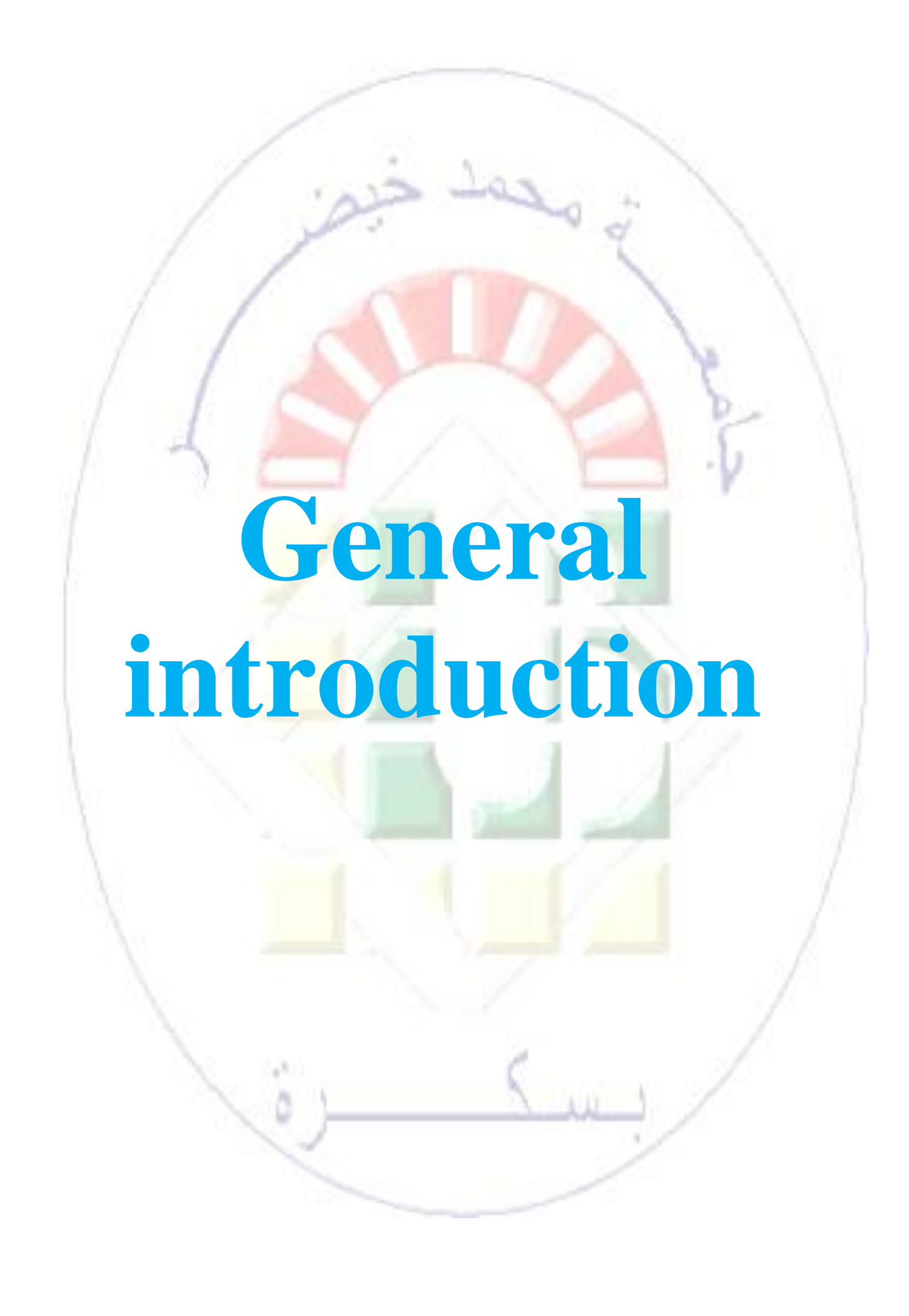
Figure 1-1: Optical window diagram for transparent conducting oxides (TCOs)7
Figure I-2: Location of the main defects intrinsic in the band gap of ZnO
Figure I-3: Some applications of TCOs9
Figure I-4: A natural form of Zinc oxide "Zincite"
Figure I-5: Evolution of the number of publications and patents per year of ZnO from 1920 to
201111
Figure I-6: Representation of the crystalline structures of ZnO: (a) hexagonal wurtzite, (b) zinc
blende, (c) cubic rock salt. The large gray spheres represent zinc atoms and the small black spheres
represent oxygen atoms
Figure I-7:Wurtzite Structure of Zinc Oxide
Figure I-8: The energy band structure of zinc oxide (E=0, the maximum value corresponds to the
valence band)
Figure I-9: schematic representations of all the application of ZnO
Figure I-10: Schematic representation of the growth mechanism of ZnO NPs by wet chemical
methods
Figure I-11: Schematic illustrating the relative dimensions of nanoparticles
Figure I-12: Size range of nanoparticles compared to that of major chemical and biological
structures
Figure I-13: Various nanostructures of Zinc Oxide (ZnO)
Figure I-14: Variation of emission as a function of excitation wavelength
Figure I-15 : Schematic of a typical thin film material on a substrate structure
Figure I-16: Pictorials of some applications of ZnO (a) pure green and blue LEDs (b) TV (c)
Cathode Ray Tube and (d) Solar cells
Figure II-1: General methods for depositing a thin film
Figure II-2: Sol-gel synthesis
Figure II-3: Macroscopic characterizations of the peaks of the Sol-Gel transition40
Figure II-4: The main steps of preparation and deposition of thin films and powder by the sol-gel
process
Figure II-5: The four steps of spin coating

List of figures

Figure II-6: Stages of the dip-coating process: a) dipping of the substrate into the coating solu	ıtion;
b) wet layer formation by withdrawing the substrate; c) gelation of the layer by solvent evapor	ation
	46
Figure II-7: Applications of sol gel method .	47
Figure II-8: Rigaku Mini Flex 600 type diffractometer	49
Figure II-9: Schematic of X-ray diffraction	49
Figure II-10: The extraction of the full width at half maximum (β) from X-ray diffra	ction
peak	51
Figure II-11: The principle of operation of UV-visible	53
Figure II-12: The determination of thickness using Optical interference curves	54
Figure II-13: Appearing form of radiation passes through the sample on a glass substrate	54
Figure II-14: Determination of the optical gap according to the Tauc method	56
Figure II-15: Representative diagram of the principle of the four-point method	58
Figure III-1: Spin coating.	62
Figure III-2: Flow chart of sol—gel method for preparation of ZnO thin films.	65
Figure III-3: Furnace for heat treatment.	66
Figure III-4: Adhesion force test.	67
Figure III-5: X-ray diffraction ZnO/Glass.	68
Figure III-6: X-ray diffractograms of ZnO [98-006-5119] from the FASTM file	69
Figure III-7: X-ray diffraction patterns of ZnO thin films grown on p-type silicon substrate.	70
Figure III-8: Hexagonal crystal Structure of ZnO	71
Figure III-9: Gaussian extrapolation of the (101) peak shows the full width at half maximum	n and
the position of the peak	72
Figure III-10: Williamson-Hall plot for thin films of commercial Zinc Oxide	73
Figure III-11: Changes in the values of a and c as a function of substrates and FASTM	75
Figure III-12: Changes in grain size and dislocations as a function of Substrate.	76
Figure III-13: Variation of parameters a and c and with Substrate at gelation time tg =30 min	n .78
Figure III-14: Changes in the values of a and c as function of substrates and FASTM at gel	ation
time tg = 60 min	78
Figure III-15: Variations in grain size and dislocation values as a function of the substrate	es on
which they are deposited	80

List of figures

Figure III-16: UV-VIS Spectrophotometer (EVOLUTION 220)
Figure III-17: Optical transmittance spectra of ZnO thin films prepared on glass and ITO and Si-
P substrate.
Figure III-18: Optical transmittance spectra of ZnO thin films prepared at tg= 30 and 60 min 83
Figure III-19:Effect of rest time of the solution on ZnO thin films prepared on glass substrates
84
Figure III-20: Variation of $(\alpha h v)^2$ as a function of $(h v)$ for ZnO thin films for tg =60min85
Figure III-21: Graph of (Lnα) as a function of (hv) for thin films of pure ZnO86
Figure III-22: Variation of Eg and E ₀₀ for different Simple
Figure III-23: KEYSIGHT B1500A Semiconductor Device Analyzer
Figure III-24: Variation of Resistivity for different Simple
Figure III-25: Changes in electrical conductivity and Strain as a function of the substrate92



General introduction

Significant technological developments over the past decade have changed the way we live, work, and interact with each other. Every year, experts make predictions about emerging technologies, for example, in the future, advanced optoelectronic devices are expected to have small sizes, high performance, and high operation speeds. Nanostructured semiconductor materials are appropriate to realize these goals because they have some unique physical, chemical and optical properties as well as an interesting size. Therefore, they can be widely applied in optoelectronics, medicine, photo catalyst, electronics, and photonics [1].

TCOs (transparent conducive oxides) are unusual materials that exhibit two remarkable physical properties: high optical transparence in the visible range (over 80%) and high electrical conductivity approximately $10^3 \,\Omega cm^{-1}$ or more. For a fully transparent material, it must exhibit a wide band gab energy greater than the energy of visible light, for example exceeding 3,1(eV). Metals, for instance, are highly conductive but do not transmit visible light. In contrast, transparent materials, such as glass, are insulators. The high electrical conductivity is attributed to a high concentration of free charge carriers (electrons or holes) [2].

Zinc oxide is one of the important TCOs, which has caused a lot of ink to flow. For many years, the main applications of zinc oxide (ZnO) have been in the fields of chemical and pharmaceutical industries. It is important to note that ZnO in pigment form is strongly diffuses and absorbs ultraviolet radiation. It is a II-VI semiconductor with a wurtzite crystal structure, exhibiting a direct bandgap of 3.37 eV at room temperature, as well as a strong exciton binding energy of 60 meV [3].

ZnO nanostructures have been the most demanding material in the last few decades due to the exhibition of enormous applications of this material in various fields. These nanostructures can be controlled dimensionally through variations in hydrothermal process. Different ZnO nanostructures are attributed to different electronic properties which is favorable in the application of photo catalysis, sensing, energy harvesting etc [4].

Scientists have developed numerous methods to create nanoparticles with precise control over their shape, size, and structure. This fine-tuning enhances the properties of these

General introduction

nanomaterials. It's no wonder there are so many techniques for ZnO nanoparticle synthesis. These techniques include ball milling, co-precipitation, the sol-gel process, and hydrothermal synthesis. The chosen method depends on the desired application [5].

The objectives of this study are summarized in the most important points, which are:

- The first objective is to prepare thin films of zinc oxide (ZnO) using an efficient and easy to apply technique which is the sol-gel spin coating process. Sol-gel processes are particularly suitable for producing and preparing thin films with high precision and control at low temperatures.
- The second objective is to study the effect of glass, ITO, and silicon substrates on the structural, optical, and electrical properties of the ZnO thin films.

The research work is written and presented in three chapters, organized as follows:

Chapter one presents a general bibliographic study on Zinc Oxide (ZnO) covering all its fundamental aspects, including crystal lattice structures, electronic band structure, optical and electrical properties. Additionally, it explores the related nanomaterials in all their dimensions and characteristics. Finally, it addresses the nature of thin films and their technological applications.

Chapter two presents a brief overview of the different methods for depositing thin films, including Chemical Vapor Deposition (CVD) and Physical Vapor Deposition (PVD), with a focus on the sol-gel method used in this experimental work, and describes the thin film deposition process using the spin—coating device. The second part of the chapter, is devoted to the characterization techniques used to study the properties and features of the experimentally prepared thin films.

Chapter three presents the experimental work, including the elaboration of the ZnO thin films on different substrates and at two different gelation time. The lion's share of the chapter is devoted to results and discussion.

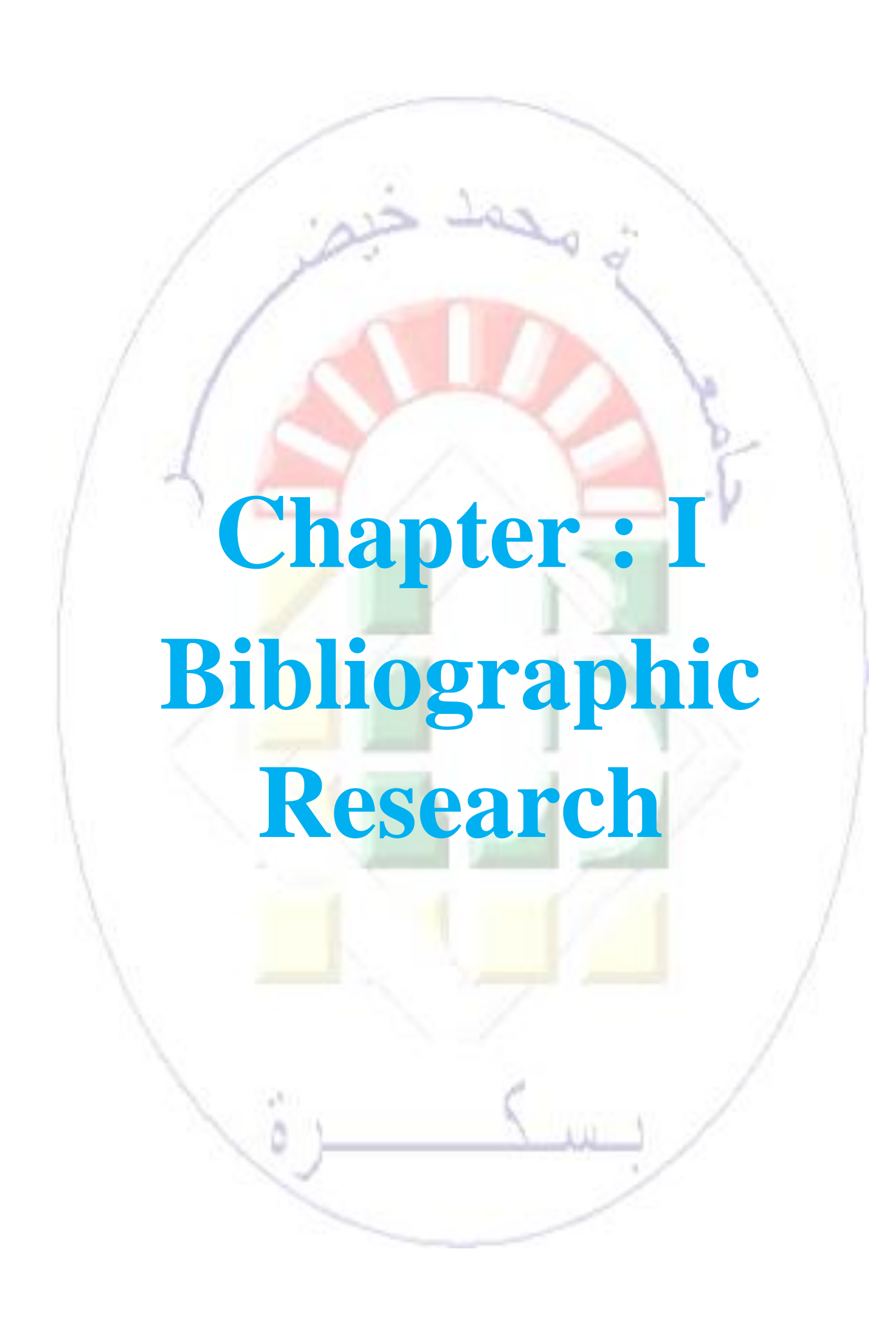
The manuscript ends with a general conclusion, which summarizes the important results found.



General introduction

References

- [1] R. N. E. H. Nezzal Hala, "Elaboration of pure and Bi-doped ZnO nano-powders with the solgel method", Master dessertation, Mohamed Khider University of Biskra-Algerai, 2022.
- [2] A. Amri, "Elaboration des couches minces à base de ZnO pour transistors couches minces TFTs", Doctoral Theses, Mohamed Khider University of Biskra-Algerie, 2024.
- [3] R. W. Boudiaf Yasmine, "Elaboration et Caractérisation des nanopoudres de ZnO pure et dopées avec le Ga par la méthode sol-gel", Master dessertation, Mohamed Khider University of Biskra-Algeria, 2020.
- [4] A. Kumar Sarkar, R. Borgohain, B. Agarwal, S. Baruah, "ZnO nanostructures advances in research and applications", Published by Nova Science Publishers, Inc.New York, P. 1-2, 2024.
- [5] A. Latif, "Elaboration of pure and doped ZnO powders with the sol gel method, Doctoral These", Mohamed Khider University of Biskra-Algerie, 2024.



I.1. Introduction

Over the past few years, transparent conductors have played and continue to play an increasingly significant role in the field of nanotechnology. Among these materials, zinc oxide (ZnO) is now one of the most studied oxides in literature due to its high availability in nature, non-toxicity to the environment, and high thermal stability [1]. Zinc oxide is covered in detail in the first chapter, with a focus on recent developments in key areas including electrical and optical characteristics, electronic band structure, and crystal structure. In addition, we will address the various forms of ZnO Oxide [2].

I.2. What is Transparent Conducting Oxide?

Transparent conductive oxide films (TCOs) have been extensively investigated due to their broad range of applications, such as transparent electrodes in solar cells and photovoltaic devices [3, 4]. Among the available TCOs, ZnO reveals itself as a potential candidate for optoelectronic applications, especially for solar cells, where it is used as a transparent and conducting top layer. In addition to being transparent, ZnO may turn into conductor type n if it has an excess of electrons in its network. This excess of electrons can be produced by either structural flaws that cause an imbalance in the oxygen's stoichiometry or by the proper doping [5].

 TCO
 band gap (eV)

 SnO2
 3, 6 - 4, 2

 ZnO
 3,2 - 3,3

 ITO
 4,2

 ZTO
 3

3-3,2

Table I-1: Expansion of the band gap of certain TCO [6].

I.2.1. Some properties of TCOs

TiO2

There are three different kinds of materials that may be made: transparent thin-film conductors, metal films, and metal semi-conductor films. Metal films, such as aluminum, silver, copper, silver, and gold, among others [6]. Among the properties of transparent conductive oxides, we mention.

I.2.1.1. The electrical properties of TCO

The electrical properties of TCOs are described by the physics of wide band gap semiconductors. The expression for the conductivity σ (Ω .cm)⁻¹ is given by the product of the charge carrier density N (cm⁻³), the charge carrier mobility μ (cm²V⁻¹s⁻¹), and the elementary electric charge of the electron **q** (C) as shown in equation (I-1) [7].

$$\sigma = \frac{1}{\rho} = N. q. \mu_n \tag{I-1}$$

The resistivity ρ , which is the inverse of the conductivity, is expressed in (Ω .cm). In the field of TCO, an important surface property is the square resistance $\mathbf{Rs}(\Omega)$, which is defined as the ratio between the resistivity ρ and the thickness **d** of the layer, according to the given relationship [7]

$$R_S = \frac{\rho}{d} \tag{I-2}$$

Although porter's mobility is a crucial component in enhancing conductivity, it is inherently dependent on diffusion mechanisms, making direct control challenging. Furthermore, these mechanisms often restrict mobility as porters' concentration increases. Therefore, one important parameter influencing conductivity is mobility [8].

I.2.1.2. The optical properties of TCO

Three fundamental phenomena govern the optical properties of materials: the transmission factor (T), the reflection factor (R), and the absorption factor (A) [9].

I.2.1.2.a. The transmittance T:

The transmittance is defined as the relationship between the intensity of light incident on a material's surface (\emptyset_0) and the intensity of light transmitted through it (\emptyset_T) [9].

$$T = \frac{\phi_T}{\phi_O}$$
 T%=100.T (I-3)

I.2.1.2.b. The reflection R:

The intensity of the reflected light (\emptyset_R) divided by the incident light intensity (\emptyset_0) at the material's surface is known as the reflectance [9].

$$R = \frac{\phi_R}{\phi_O} \qquad \qquad \text{R\%=100.R}$$

I.2.1.2.c. The absorption factors A:

The relationship between the intensity of the light absorbed (\emptyset_A) and the incident light intensity (\emptyset_0) is known as the absorption factor[9].

$$A = \frac{\phi_A}{\phi_O} \qquad \qquad \text{A\% = 100.A}$$

The following equation, based on the Beer-Lambert law, allows us to link the transmitted flux, the absorption coefficient (α) and the thickness of the layer (\mathbf{d}) [9].

$$T = (1 - R)e^{-\alpha d} \tag{I-6}$$

With:

T and **R**: Transmission and reflection of the transparent conductive oxide film. α being the absorption coefficient of the film, linked to the extinction coefficient k which translates the absorption of radiation by the material by the following relation:

$$K = \frac{\alpha\lambda}{4\pi} \tag{I-7}$$

 λ : is the wave length.

The extinction coefficient (\mathbf{k}) , refractive index (\mathbf{n}) , and energy gap (\mathbf{Eg}) may be inferred by measuring the thickness, transmission, and reflection of transparent conductive oxides [9].

Thus, materials capable of transmitting light with relatively little absorption and reflection are transparent. The figure I-1 shows a schematic diagram of the optical window of transparent conducting oxides.

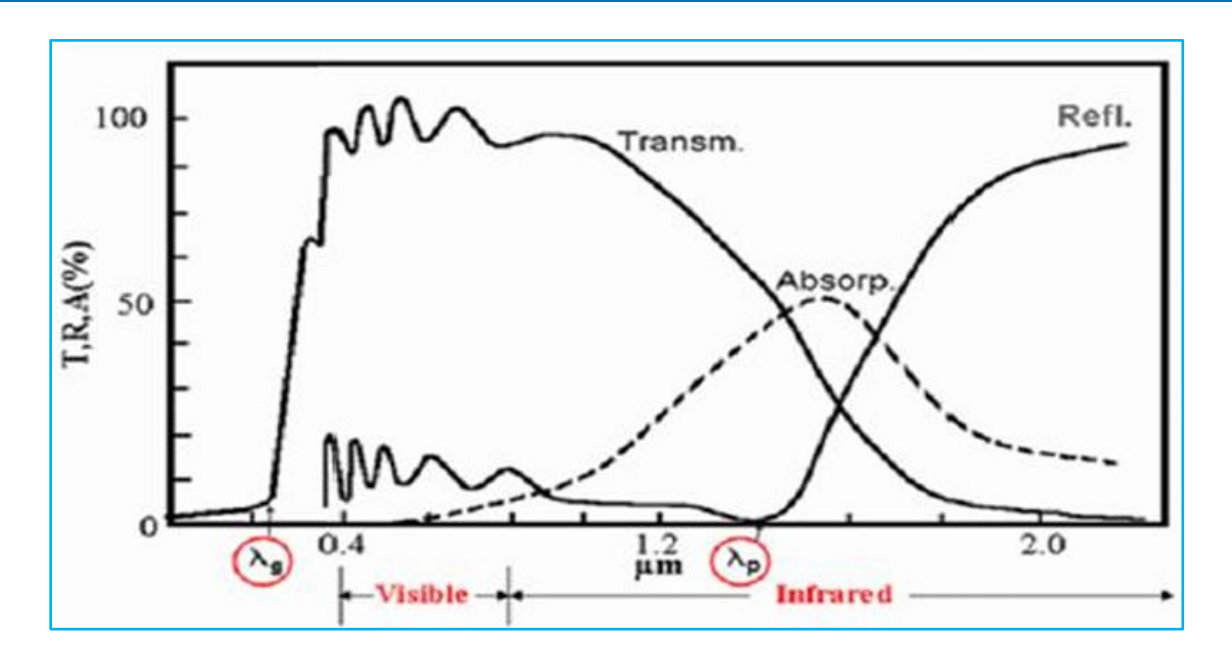


Figure I-1: Optical window diagram for transparent conducting oxides (TCOs) [6].

I.2.2. Different types of defects in transparent conductive oxides (TCOs)

Defects observed in transparent conducting oxides (TCOs) are dependent on the growth method and the conditions of elaboration of this material. Defects that can be observed include [10].

- Point defects (interstitials, vacancies, foreign atoms).
- Linear defects (dislocations and sub-grain boundaries).
- > Planar defects (twinning, grain boundaries).

There are other types of defects of thermal nature (phonon) or electrical (electrons, holes, excitons)(Figure I-2) [11].

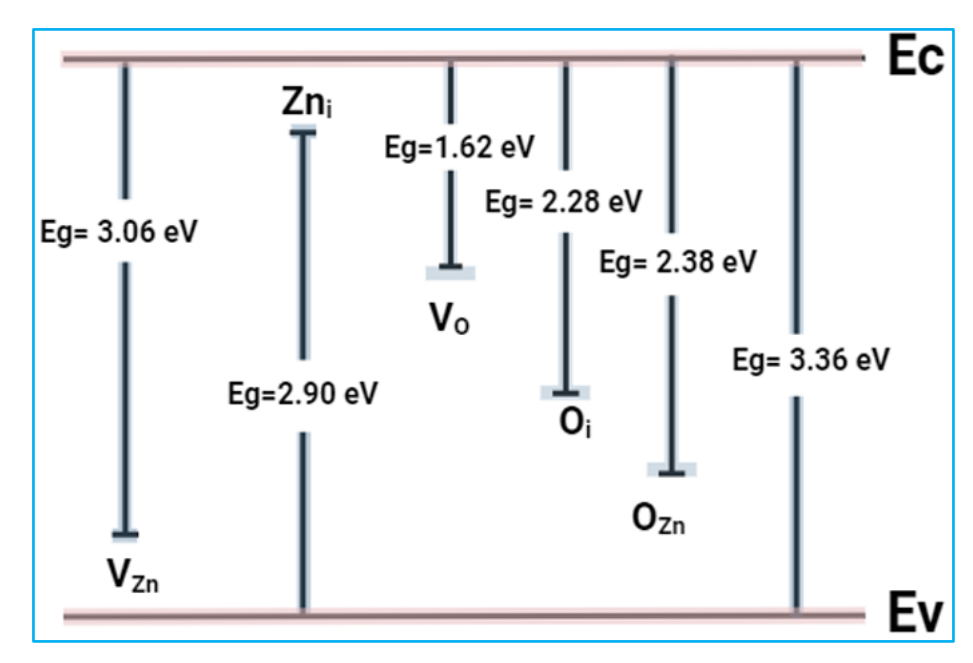


Figure I-2: Location of the main defects intrinsic in the band gap of ZnO [12].

I.2.3. Transparent conductive oxide applications

TCOs may be used in various applications due to their previously established features Figure I-3. The following list presents some materials' primary applications [6].

- Screens for plants.
- Laser cavity.
- Window anti-frost.
- Windows in houses, furnaces, etc. that reflect heat.
- **♣** Touch displays for control. Gas sensor.
- **Lesson** Electromagnetic protection.
- Electrostatic charge dissipation.
- ♣ The front contact that light must go through in order to enter the solar cell.



Figure I-3: Some applications of TCOs [13].

I.3. The Zinc Oxide

Zinc oxide has become an interesting research topic in recent years due to its optical and piezoelectric properties. ZnO is a II-VI group semiconductor with a wide bandgap (≈ 3.37 eV) and a high exciton energy (60 meV) at room temperature. It is a natural n-type semiconductor, its conductivity due to intrinsic defects such as zinc interstitials and oxygen vacancies. ZnO has a high mechanical and thermal stability. Moreover, ZnO is abundant on Earth, inexpensive, and non-toxic [14]. It is also known as zinc white or snow white, it is a white powder obtained by burning zinc vapor.

At ambient temperature, ZnO, a semiconductor with a broad bandgap, emits light in the ultraviolet (UV) spectrum at about 374 nm [15]. However, it is transparent in the near-infrared (IR) and visible spectrums [16]. There are several uses for zinc oxide, including as an addition in goods and materials including paint, ceramics, tires, glass, and plastic. Additionally, ZnO can be used in optoelectronics, cathodoluminescence, photoluminescence, and electroluminescence. Additionally, photocatalysis uses it to purify water (Figure I-4) [17].



Figure I-4: A natural form of Zinc oxide "Zincite" [18].

I.3.1. History of zinc oxide "ZnO"

In the field of research on materials with semiconductor properties, the first works undertaken on ZnO appeared in 1930 [19]. The main applications of zinc oxide are still today found in the fields of the chemical and pharmaceutical industries (paints, sunscreens...) Since the 1920s, ZnO was also used as a transducer in the receivers of the first wireless radios (piezoelectric effect). ZnO has been extensively studied since the early 1950s before being relatively neglected in the 1970s, to then experience a significant resurgence of interest starting in the 1990s due to its very attractive fundamental properties in the field of optoelectronics [20, 21].

Since ZnO and GaN have many structural and electrical characteristics, they are considered direct competitors in the realm of optoelectronics. The amount of scholarly publications published in recent years indicates that there is currently a greater interest in developing ZnO thin films and nanostructures Figure I-5. The data concerning publications obtained from the "Scopus" search engine and for patents from the "Orbit" database [22].

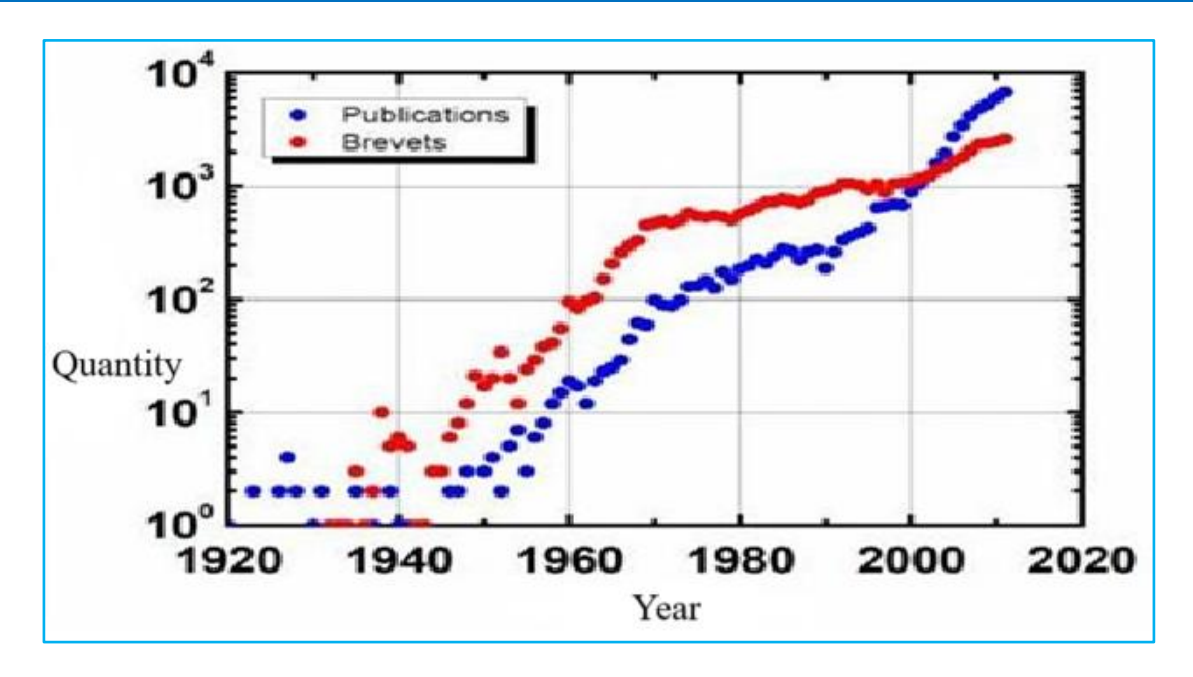


Figure I-5: Evolution of the number of publications and patents per year of ZnO from 1920 to 2011 [22].

I.3.2. The choice of the studied semiconductor ZnO

The main advantage of zinc oxide (ZnO) is that its components are non-toxic and very abundant on Earth. It is an undeniable asset because it helps reduce production costs. Zinc oxide is a material that belongs to the family of transparent conductive oxides (TCO) [23]. He shows great interest in the development of new applications in photonics. For example, it is a good candidate for transparent electrical contacts in the visible range (surface electrodes of solar panels, or very high-density optical discs), It is also used for the manufacture of lasers emitting in the blue or near ultraviolet. ZnO is a very promising material for optoelectronic applications. Its photoluminescence properties strongly depend on the surface state and the oxygen stoichiometry of the crystallites [24].

I.3.3. Properties of Zinc Oxide

Zinc oxide (ZnO) is a direct band gap semiconductor with great potential for a variety of applications, such as: optical waveguides, phosphors, transparent conductive oxides, chemical gas sensors, spin functional devices, UV-light emitters, and piezoelectric transducers. Its wide bandgap (3.37 eV at room temperature) makes ZnO a promising material for optoelectronic and

photonic applications in the UV, or blue spectral range [25]. Table I-2 shows the general properties of Zinc Oxide.

Table I-2: Properties of Zinc Oxide [26].

Properties	
Molecular formula	ZnO
Molar mass	81.408 g/mol
Appearance	White solid
Odor	odorless
Density	5.606 g/cm ³
Melting point	1975 °C (decomposes)
Boiling point	2360 °C
Solubility in water	0.16 mg/100 mL (30 °C)
Band gap	3.3 eV (direct)
Refractive index (nD)	2.0041

I.3.3.1. Physical Properties

I.3.3.1.1. Crystallographic properties

Zinc oxide is a semiconductor that can crystallize in the wurtzite structure, zinc blende, or even in the rocksalt NaCl structure, as shown in Figure I-6, where the gray spheres represent Zn atoms and the black ones represent oxygen atoms [27]. Under ambient conditions, the thermodynamically more stable phase is the Wurtzite phase, while the Zinc-blende structure of ZnO can only be stabilized by growth on cubic substrates and the rocksalt structure (NaCl) can be obtained at relatively high pressures [28].

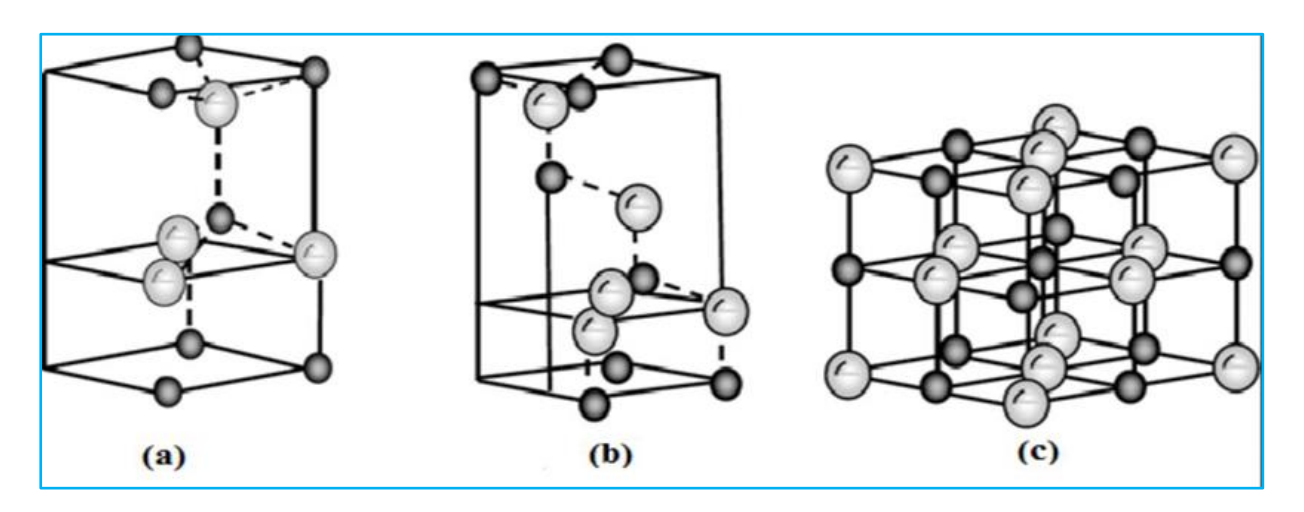


Figure I-6: Representation of the crystalline structures of ZnO: (a) hexagonal wurtzite, (b) zinc blende, (c) cubic rock salt. The large gray spheres represent zinc atoms and the small black spheres represent oxygen atoms [24].

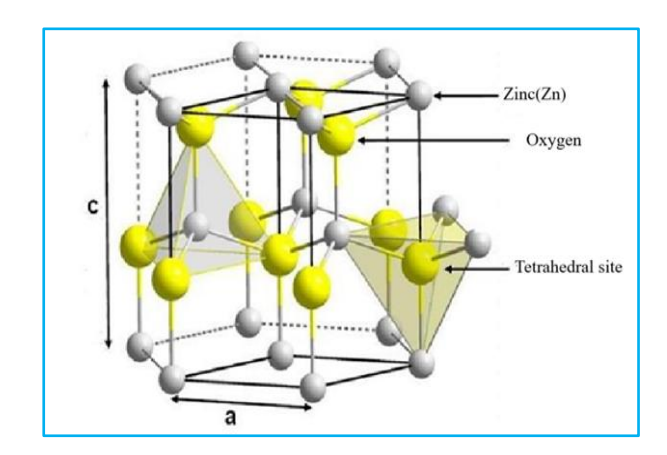
The wurtzite structure belongs to the space group P63mc. The O²-oxygen ions form a compact hexagonal lattice in which half of the tetrahedral sites are occupied by Zn²⁺cations Figure I-7 [29]. whose specific positions of the Zn and O atoms in the lattice are [30].

 0^{2-} : (0, 0, 0) (and its equivalents) et (2/3, 1/3, 1/2) (Inside the mesh).

 $\mathbf{Zn^{2+}}$: (0, 0, 3/8) ((and its equivalents) et (2/3, 1/3, 7/8) (Inside the mesh).

The ZnO crystal is characterized in the wurtzite structure by the lattice parameters

$$a=b=3.2499$$
 Å, $c=5.2060$ Å, $\alpha=\beta=90^{\circ},$ and $\gamma=120^{\circ}$ [27].



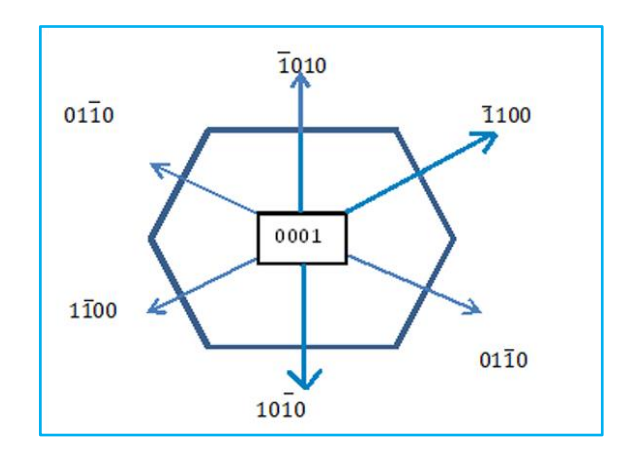


Figure I-7: Wurtzite Structure of Zinc Oxide [14].

The table below presents a summary of some structural characteristics of zinc oxide. The zinc and oxygen atoms occupy only 40% of the crystal volume, leaving voids with a radius of 0.95Å.

It is possible that, under certain conditions, excess zinc atoms can fit into these spaces, that is, in interstitial positions. This characteristic helps explain certain particular properties of zinc oxide related to phenomena such as: semi conductivity, photoconductivity, luminescence, as well as the catalytic and chemical properties of the material [27].

Table I-3: Recapitalization of structural characteristics of ZnO [24].

Lattice	Würtzite hexagon
Maille parameters	a=3.2499 Å c/a=1.6019
	c=5.2060 Å
The distance between \boldsymbol{O}^{-2} and $\boldsymbol{Z}\boldsymbol{n}^{+2}$ (the	Along the c axis d=1.96 Å
closest neighbors)	For the other three d=1.98 Å
Ionic radius for tetrahedral Covalent bond coordination	Zn neutre =1.31 Å; O neutre =0.66 Å
Ionic bond	Zn^{+2} = 0.60 Å; O^{-2} = 1.38 Å
Rayon crystallin for a tetraedrique	$Zn^{+2} = 0.74 \text{ Å}$
coordination	O^{-2} =1.24 Å

I.3.3.1.2. electronic structure of a band

It is recalled that the band electronic structures of oxygen and zinc are:

$$O:1S^22S^2 2P^4$$

Zn:
$$1S^2 2S^2 2P^6 3S^2 3P^6 3d^{10} 4S^2$$

ZnO is composed of zinc and oxygen, these two elements belong to columns (II-VI) respectively of the periodic table of chemical elements. Figure I-8 illustrates the appearance of the band structure of ZnO. In reality, six Γ bands result from the 2p states of oxygen; they are the lowest of the conduction bands and have a strong contribution from the 4s states of Zinc [31].

The reaction for the formation of zinc oxide is as follows [32].

$$Zn^{2+} 2e^{2-} + \frac{1}{2}O^2 \rightarrow ZnO$$

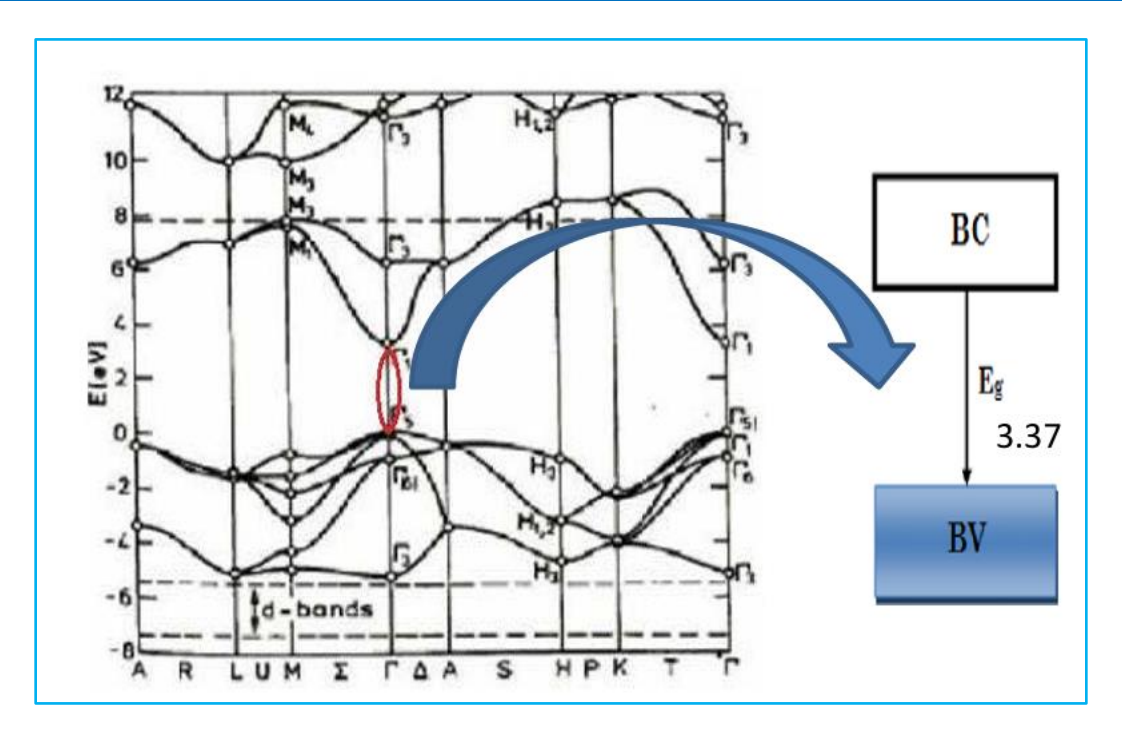


Figure I-8: The energy band structure of zinc oxide (E=0, the maximum value corresponds to the valence band) [17].

Zinc oxide has a high exciton binding energy of around 60 meV at 300 K, which is one of the reasons why ZnO is highly sought after, especially for making optoelectronic devices at room temperature [17].

Table I-4: Some electrical properties of ZnO [24, 18].

Nature of the forbidden band	Direct
Band gap width at 300°K	3.4 ± 0.02
Type of conductivity	n or p
electrons effective mass	$0.28 \text{ m}_0, m_0 = 9.11 \times 10^{-31} \text{kg}$
holes effective masse	$0.59 m_0, m_0 = 9.11 \times 10^{-31} \text{kg}$
Density of states in CB	$3.71 \times 10^{18} cm^{-3}$
Density of states in BV	$1.16 \times 10^{19} \ cm^{-3}$
Electron concentration (n)	10^{20} cm^{-3}
Holes concentration (p)	10 ¹⁹ cm ⁻³
Maximum resistivity	10^6 Ω.cm
Minimum resistivity	$10^{-1}\Omega$.cm
The mobility of n type	200 cm ² v ⁻¹ s ⁻¹ .
The molibility of p type	5-50 cm ² v ⁻¹ s ⁻¹
Static dielectric constant (ε _s)	7.9

I.3.3.1.3. Optical and luminous characteristics

In the form of a thin film, the refractive index and absorption coefficient of ZnO vary depending on the fabrication conditions. The refractive index has a value that varies between 1.90 and 2.20 according to different authors. The improvement of the stoichiometry of ZnO leads to a decrease in the absorption coefficient and an increase in the bandgap energy. Doped zinc oxide falls into the class of transparent conductive oxides known as TCO (transparent conductive oxide). Very lightly doped, it can be used in luminescence; under the action of a high-energy light beam (E > 3.4 eV) or an electron bombardment, zinc oxide emits photons; this phenomenon corresponds to luminescence. Depending on the preparation conditions and subsequent treatments, different photoluminescence bands have been observed: they range from near UV (350 nm) to visible (green radiation with a wavelength close to 550 nm) [33]. The intensity of the green emission strongly

depends on the preparation conditions and the annealing temperature, this intensity varies with the annealing temperature according to an Arrhenius law [6].

$$I = I_0 \exp(-\frac{Ea}{KTr})$$
 (I-8)

With:

I: output intensity

 I_0 : input intensity

K: Boltzmann constant

T_r: annealing temperature;

 $\mathbf{E_a}$: activation energy = 1.035 eV

Table I-5: The optical properties of Zinc Oxide [6].

dielectric constant	$\epsilon_{//}$ =8.7 ϵ_{\perp} =7.8
Absorption Coefficient	$10^4 \ (cm^{-1})$
Refractive Index at 560 nm	1.8-1.9
Refractive index at 590 nm	2.013-2.029
Exciton binding Energy	60 (meV)
Transmittance	> 90%

The optical transparency of ZnO in the visible and near-infrared regions of the solar spectrum is a consequence of its large bandgap (Eg = 3.3 eV), with the fundamental absorption threshold of ZnO being in the ultraviolet [6].

I.3.3.1.4. Mechanical properties

ZnO is a relatively soft material with an approximate hardness of 4.5 on the Mohs scale. Its elastic constants are smaller than those of relevant III-V semiconductors, such as GaN. The heat capacity, high thermal conductivity, low thermal expansion, and high melting point of ZnO are beneficial for ceramics. Among tetrahedral-bonded semiconductors, it has been indicated that ZnO

has the highest piezoelectric tensor comparable to that of GaN and AlN. This property makes it an important material for numerous piezoelectric applications, which require a high electromechanical coupling [17].

I.3.3.1.5. The piezoelectric effect

ZnO exhibits the highest piezoelectric effect of all semiconductors (relative dielectric constant equal to 8.75) [34]. This effect is closely related to its crystalline structure, because, as we have seen previously, the oxygen and zinc atoms form non-centrosymmetric tetrahedral, which causes a shift in the center of charge during deformations induced by external forces such as pressures. This imbalance results in the appearance of dipole moments [6].

I.3.3.1.6. Magnetic properties

The transition metals are the main dopants that can enhance ZnO's magnetic properties. It has been demonstrated that the majority of transition metals can be incorporated into the ZnO matrix with significant teneurs (5% to 40% after the ion is inserted).

For instance, using an ablation laser to incorporate cobalt (Co) into the ZnO matrix, has demonstrated a weak ferromagnetic coupling with a Curie temperature close to ambient, but for magnesium (Mn)-doped sofas, a strong antiferromagnetic coupling has been demonstrated [35].

I.3.3.2. Chemical Properties

ZnO has the following chemical properties [36].

- Large Tano can be found as zinc white, a white powder, or as the mineral zincate. Because of the manganese impurity, it is typically orange or red.
- Thermochromic crystalline zinc oxide turns from white to yellow when heated and back to white when cooled. At high temperatures, a very small loss of oxygen is what causes this hue shift.
- Zinc oxide is amphoteric, that reacts with both acids and alkalis. With acid, it reacts to form familiar compounds, such as zinc sulfate. With alkali forms zincates.

$$ZnO+2HCl \rightarrow ZnCl_2 + H_2O$$

 $ZnO+2NaOH+H_2O \rightarrow Na2(Zn(OH)_4)$

Large Table 2 Large 4 Large 2 Large 4 stability. Heating with carbon converts ZnO into Zn, which is more volatile.

$$ZnO+C \rightarrow Zn+CO$$

The following reaction is extremely important in zinc pyrometallurgy.

$$ZnO+CO \rightarrow Zn+CO_2$$

- Commercial zinc oxide has a water solubility of 0.005 g/L, which is detectable but low.
- ♣ When zinc oxide is exposed to air, it absorbs carbon dioxide and water vapor. As a consequence, basic zinc carbonate is created.

I.3.4. Applications of Zinc Oxide

Zinc oxide's exceptional physical qualities make it suitable for use in a broad range of applications, including electronics, optics, mechanics, cosmetics (sunscreen), and so on [18].

- 1) **Electronic applications**: ZnO's broad band-gap makes it suitable for laser diodes and lightemitting diodes (LEDs). ZnO may be used to create transparent thin-film transistors (TFTs). Nano rod sensors, made of ZnO, are devices that detect fluctuations in electric current passing through the wires due to the adsorption of gas molecules. Moreover, the Nano rods can be made partial towards H_2 gas by sputtering Pd clusters on the surface, which helps in dissociating the H_2 molecules thereby boosting the sensitivity of the nanorods [37].
- 2) **Photo-catalysis applications:** In recent years, intensive scientific work has taken place on photo-catalysis. Through oxidation or reduction events occurring on the catalyst's surface, an electron-hole pair is created in this process that occurs below the intensity of light. An organic pollutant can undergo direct oxidation by a photo-generated hole or indirect oxidation by an interaction with distinctive reactive groups (ROS) when a photo-catalyst is present, for example, the hydroxyl radical OH, produced in solution [38].
- 3) **Medical uses:** Calamine, which is used to make Calamine lotions, is a ZnO combination that contains 0.5% Fe₂O₃. Because of its antimicrobial and deodorizing properties, fine ZnO particles are employed in packaging. These qualities, as well as its capacity to neutralize acids, making it perfect for use in antibacterial, therapeutic, and other creams. Furthermore, they are a necessary part of dental prosthesis and toothpaste. ZnO is used in sunscreens and sunblock to avoid sunburns because of its capacity to absorb UV radiation. The ZnO is also used in the production of cigarette filters as it is helpful in removing harmful substances like H_2S and HCN without affecting the flavor [37].
- **Rubber manufacture**: Around half of the ZnO produced worldwide is used by the rubber 4) sector. ZnO and stearic acid are essential for starting the vulcanization process in the production of

rubber. Rubber curing becomes faster and more controlled when a combination of these two substances is utilized. It is also a crucial additive in car tires. It helps increase their thermal conductivity, which extends the tires' lifespan by facilitating rapid heat dissipation while they are moving [37].

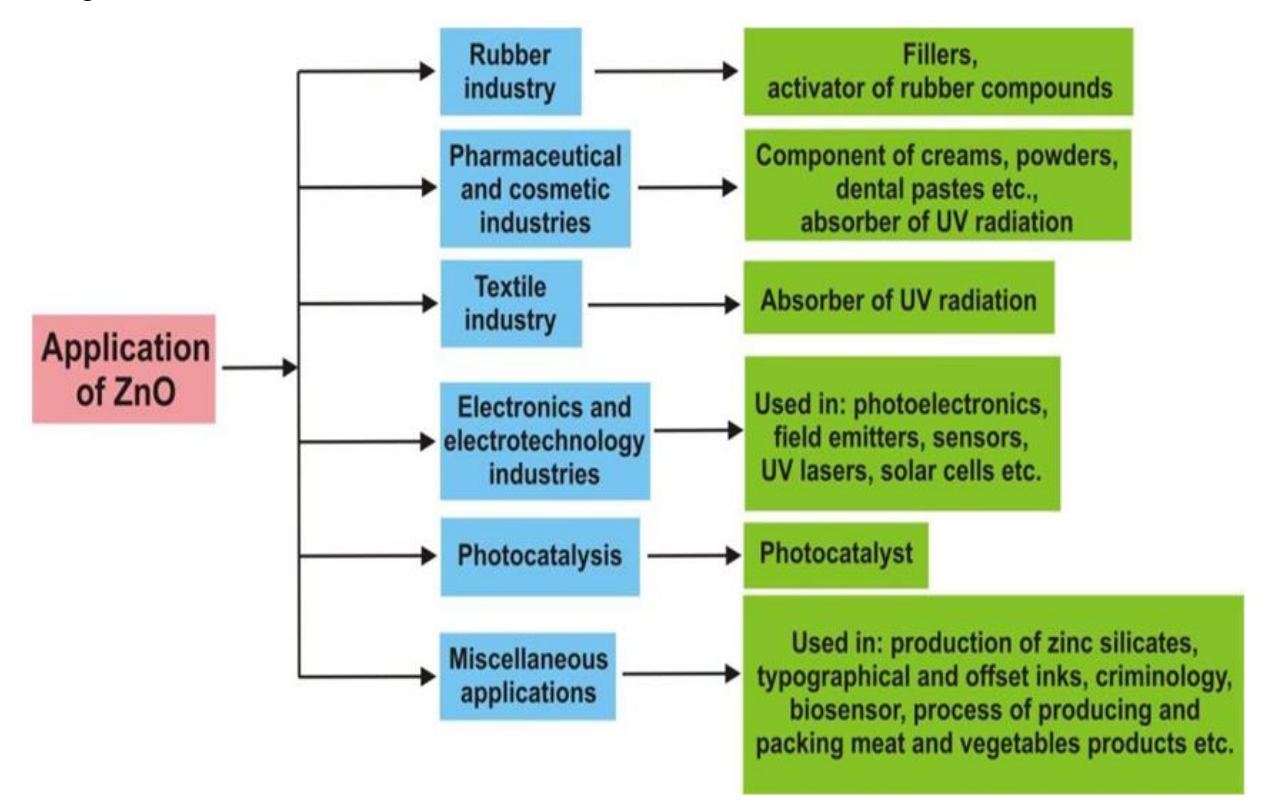


Figure I-9: schematic representations of all the application of ZnO [39].

I.4. Nanotechnologies

Nanotechnology - the ability to engineer matter at the atomic, molecular, and supramolecular level - is the creation and utilization of materials, devices, and systems through the control of matter on the nanometer-length scale, it is the generation of larger structures with fundamentally new molecular organizations. Starting from the premise that properties can dramatically change when dimension is reduced to the nanometer range, the manipulation of a material at the atomic and molecular scale to create new functionality and properties is a deep, scientific, productive, and modern concept. Considering the nanometer scale, the surface-to-volume ratios of materials become large and their electronic energy states become discrete, leading to unique electronic, optical, magnetic, and mechanical properties of the nanomaterials [40].

The first work on nanotechnology in textiles was undertaken by Nano-Tax [41]. And later, progressively, textile companies started to develop nanotechnologies modifying the surface of polymeric matrices using nanostructured materials.

The nanotechnology's use in textiles can be subdivided as follows:

- Fabrication of nanofibers and nanoparticle composite fibers.
- Surface modification of fibers and fibrous matrices for the purpose of upgrading existing functions and performance of textile materials and developing intelligent textiles with completely new characteristics and functions.

I.4.1. Materials at the nanoscale

Synthesis of nanostructured materials is performed by two ways: the top-down approach and the bottom-up approach. Generally, the classification schemes for nanostructured materials are based on different criteria: their chemical composition, the technique for their manufacture, and their dimensionality. For the classification, the most relevant criterion is the dimension of the array of constituents that form the nanostructured zero-dimensional (0D), one-dimensional (1D), twodimensional (2D), and three-dimensional (3D) nanomaterials [42].

The Nano material crystallizes and aggregates at temperature around 450 C° through Van der vales forces, forming spherical Zinc Oxide nanoparticles. The figure I-10 shows the crystallization diagram [43].

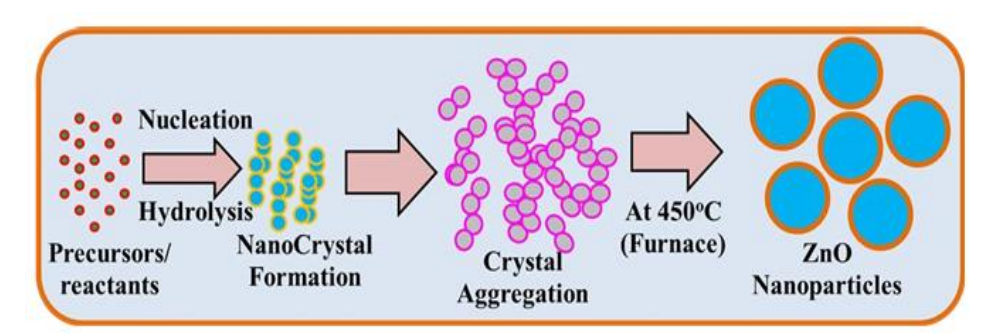


Figure I-10: Schematic representation of the growth mechanism of ZnO NPs by wet chemical methods [43].

Zero-dimensional nanomaterials include uniform particle arrays (quantum dots), heterogeneous particle arrays, core-shell quantum dots, onions, hollow spheres Nano lenses, nanocluster materials, and Nano dispersions in which nanoparticles are isolated from each other.

Ideal systems for exploring a large number of novel phenomena at the nanoscale are one-dimensional nanostructured materials, such as nanowires, nanorods, nanotubes, Nano belts, nanoribbons, and hierarchical nanomaterials [44].

Two-dimensional nanomaterials are films (coatings) with nanometer thickness. Structural elements in 0D, 1D and 2D nanomaterials can be distributed in a liquid or solid macroscopic matrix or be applied on a substrate.

Powders, fibrous, multilayer and polycrystalline materials in which the 0D, 1D and 2D structural elements in close contact with each other form interfaces belong to the fourth type, meaning three-dimensional nanomaterials [44]. By comparison with natural organic structures, nanoparticles are mainly in the size range corresponding to proteins (Figure I-11) [45].

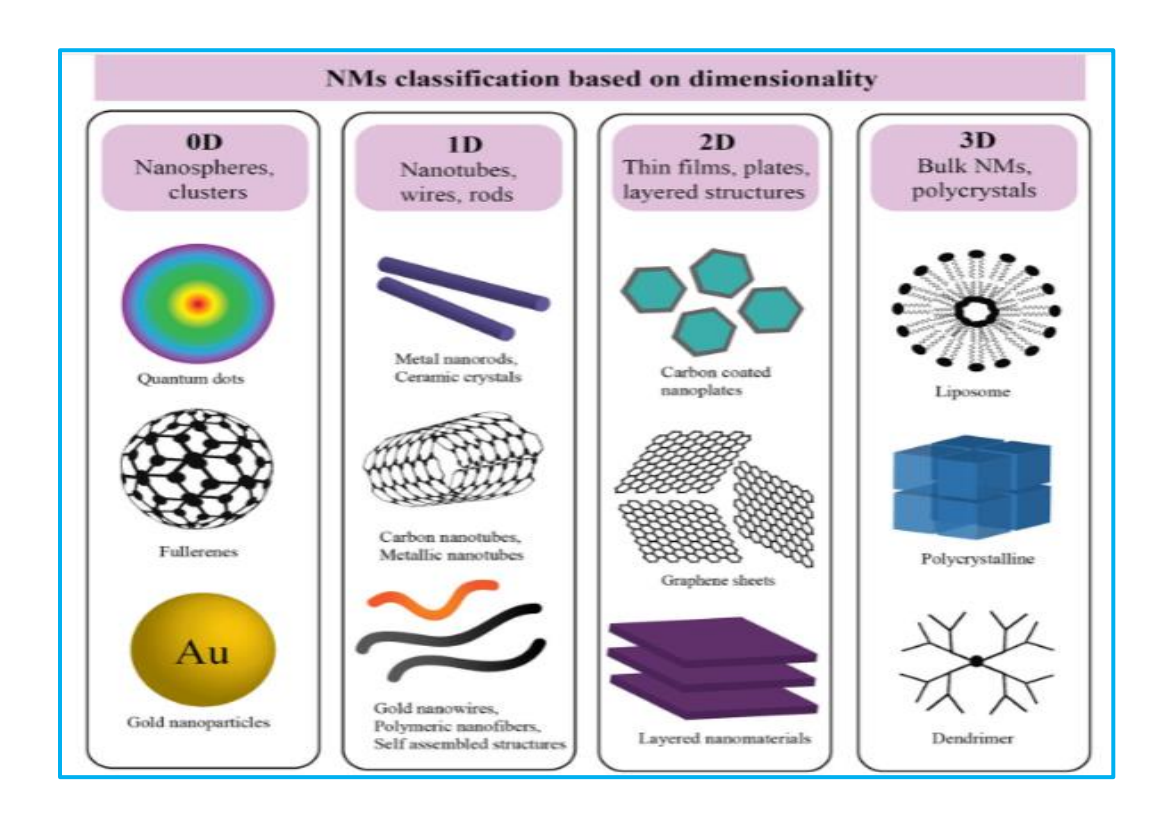


Figure I-11: Schematic illustrating the relative dimensions of nanoparticles [46].

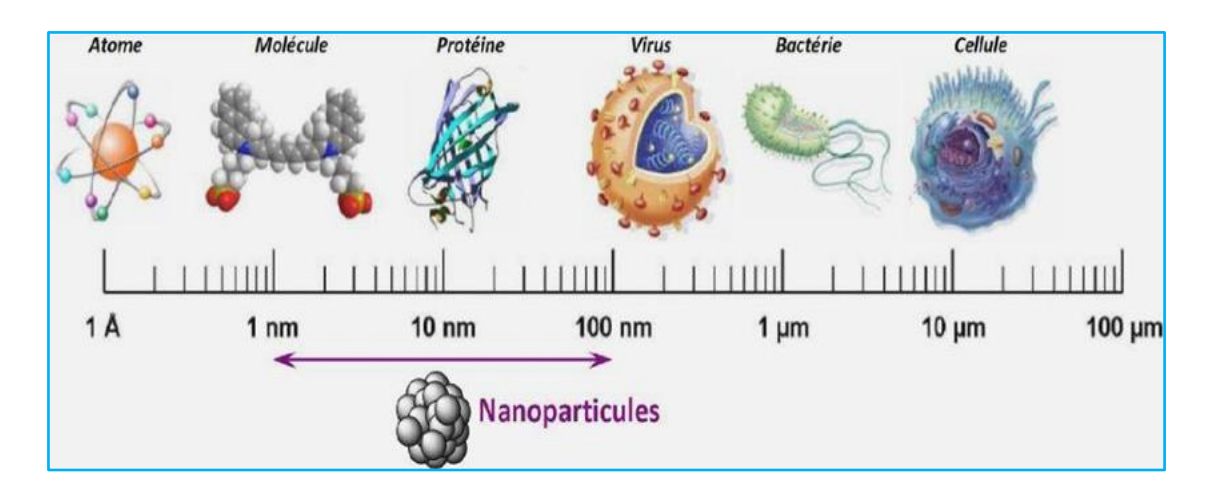


Figure I-12: Size range of nanoparticles compared to that of major chemical and biological structures [45].

I.4.2. ZnO nanoparticles

ZnO nanomaterial has been a subject of focused research nowadays due to its unique properties that are significantly different from those of bulk counterpart. It has various morphologies which can be synthesized by different simple and low cost growth methods.

I.4.3. Morphology Controlled

of all the known materials, ZnO offers a wide variety of particle structures: Onedimensional (1-D), two-dimensional (2-D), and three-dimensional (3-D). One-dimensional nanostructures, including nanorods, needles, rings, ribbons, tubes, belts, wires, and combs, are more numerous and make up the biggest category of all. Two-dimensional forms of zinc oxide include Nano plates, Nano sheets, and Nano pellets.

ZnO, even in its non-nanostructured form, is a very attractive material thanks to its features, like wide band gap, large exciton binding energy, chemical stability, biocompatibility, piezoelectricity, nonlinear optical effects, radiation hardness. Moreover, when passing from bulk material to nanostructures, the interest becomes strongly enhanced, since the properties deriving from the reduced dimensionality of nanostructures add to the intrinsic ZnO properties. Furthermore, the intense studies in this research field are promoted by the possibility to realize a very broad variety of ZnO nanostructures, such as dots, wires, rods, tetra pods, belts, combs, tubes, needles, hierarchical structures and so on. Some examples of ZnO nanostructures are displayed in (Figure I-13) [47].

ZnO, as bulk material or film, is very appealing for electronic and opto electronic devices, such as Ohmic contacts, Schottky contacts, LEDs, LASERs, transparent FETs, photodetectors and solar cells. Dealing with ZnO nanostructures, a lot of different possible electronic and optoelectronic applications have been explored. The possibility to realize Ohmic or Schottky metal Nano-contacts onto ZnO nanostructures has been reported. Electroluminescence for LED applications has been extensively studied with devices based both on ZnO nanorod arrays and on single ZnO nanorod [47].

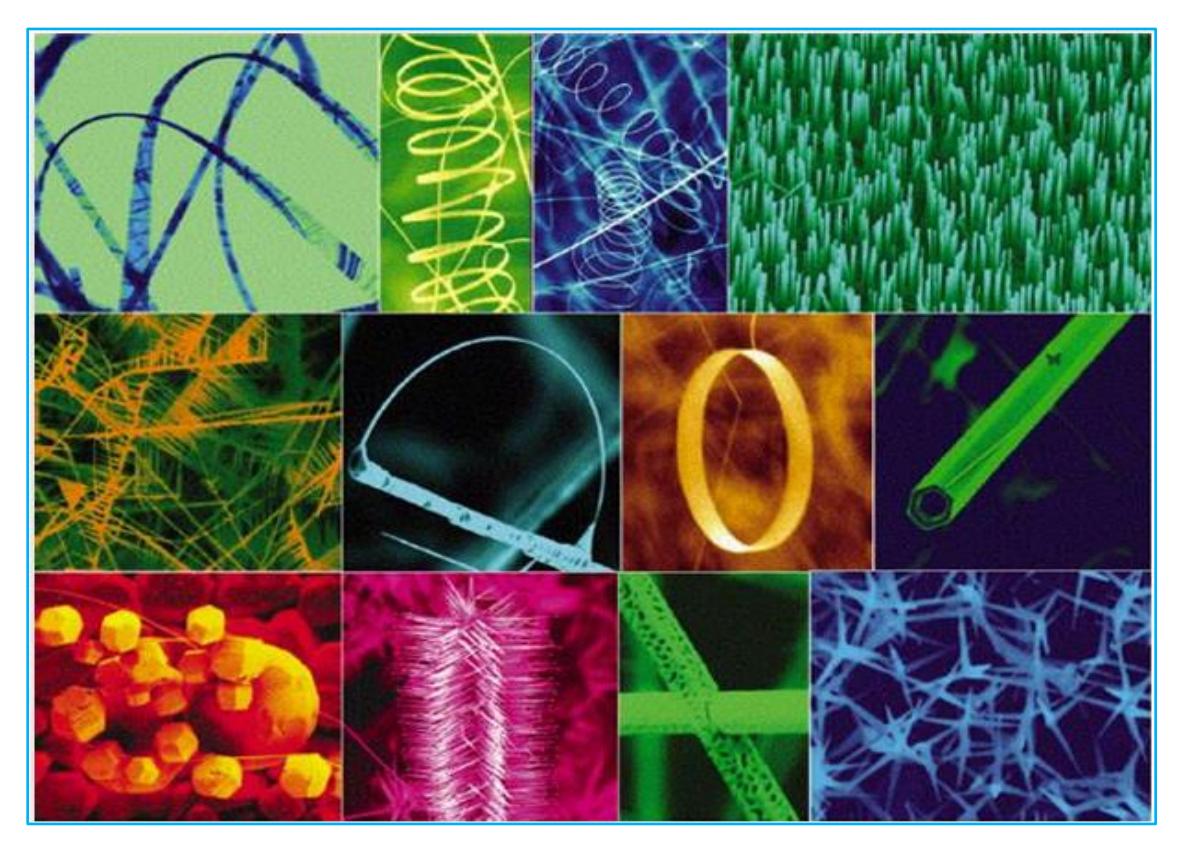


Figure I-13: Various nanostructures of Zinc Oxide (ZnO) [48].

I.4.4. Properties of Zinc Oxide Nanostructures

I.4.4.1. Electronic properties of nanomaterials

When a material's electron and hole cloud is compressed, one or more of its dimensions are reduced to the nanometric scale, which drastically alters the material's electrical characteristics. The electronic properties possessed by semiconductor nanocrystals are due to their very small size, which induces a confinement effect on optical excitations. The charge carriers generated during the absorption of an exciting light beam are free to move throughout the entire bulk semiconductor crystal [17].

I.4.4.2. Mechanical properties of nanomaterials

Several main and essential optical properties have been highlighted [16].

- Additional absorption is observed in the visible or near-infrared range associated with metallic particles.
- An abnormal absorption in the far infrared (possibility of a quantum effect).
- > Critical behavior of optical properties.
- A significant increase in the bandgap with a decrease in size is the result of confinement effects.

I.4.4.3. Piezoelectric properties of nanomaterials

The main advantages of the wurtzite structure of ZnO are the absence of a center of symmetry and the polarity of the surfaces. As a result, the surface of ZnO can be described by an alternation of planes composed of O²⁻ and Zn²⁺ ions along the C axis. The opposition of ionic charges produces polar surfaces positively charged (0001) of Zn and negatively charged (0001) of O. This is the origin of the creation of the dipole moment and spontaneous polarization along the C axis [49].

The piezoelectric property of ZnO nanocrystals has also been studied for their potential applications in Nano-electromechanical systems. The piezoelectric coefficient of ZnO nanocrystals was measured using AFM (Atomic Force Microscope). The piezoelectric coefficient of the (0001) surface of the nanocrystals is much greater than that of the (0001) surface in the bulk state [49, 50].

I.4.4.4. Optical properties of nanomaterials

The emission properties of ZnO nanoparticles strongly depend on the synthesis method employed. Because these properties are associated with surface defects. The quantum effect's dependency of optical characteristics on semiconductor nanoparticle size is among its most striking features. The bandgap widens as a result of the absorption edge shifting towards shorter wavelengths as these nanoparticles get smaller. If the forbidden band is within the visible range,

the particles will change color as the size of the particles decreases. Same for fluorescence if the particles fluoresce in the visible range [51].

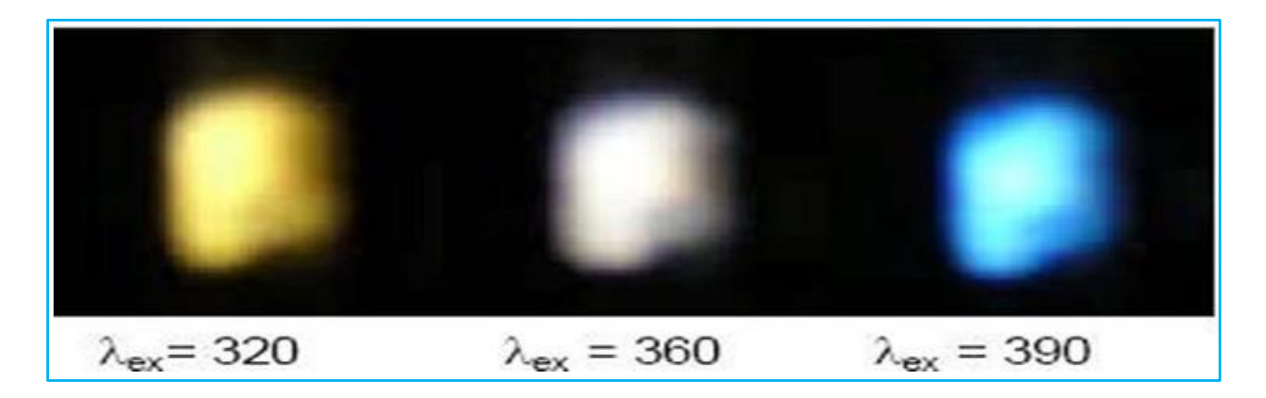


Figure I-14: Variation of emission as a function of excitation wavelength [27].

Two different emissions were observed at 580 and 440 nm associated with the presence of surface defects in the nanoparticles. The first emission at 580 nm corresponds to the yellow emission with a lifetime of 1850 ns for 4.0 nm particles. The second at 440 nm is observed only when amine ligands are present [51]. The figure I-14 illustrates the optical properties of nanomaterials.

I.5. Brief history

Thin films have been used for a long time in various fields such as optics, mechanics, electronics, etc. These served as reflective layers in the manufacturing of mirrors, anti-reflective layers in glassware, as abrasive or protective layers or even as conductive layers in electrical devices.

The advancement of electronics in the middle of the 20 th century opened up new possibilities and greatly increased interest in thin film technology. A staggering stride towards device downsizing was then taken with the introduction of integrated circuits, which employ thin-film materials rather than the typical bulk materials [52].

I.5.1 What is a thin film?

Any solid or liquid object with one of its dimensions very much less than that of the other two may be called a 'thin film'. Thin film devices would typically be about 5 to 50 µm thick in contrast to bulk devices, which are about 50 to 250 µm thick [53]. If the growth is atom by atom

or molecule by molecule, it is called the thin film, and if the growth is grain by grain, it is thick film. Although literature occasionally assigns an arbitrary value of 1 µm, the boundary between "thin" and "thick" films is often ill-defined. In general, a film is deemed "thin" if its characteristics differ considerably from those of the bulk [54].

The purpose of the thin layer is to impart specific properties to the surface of the part while benefiting from the bulk properties of the substrate (generally: mechanical strength), for example:

- electrical conductivity: surface metallization, for example, to observe an insulating sample under a scanning electron microscope
- optics: mirror backing, anti-reflective coating on camera lenses, nickel plating on firefighter helmets to reflect heat (infrared), gilding of their visors to avoid glare [55].
- **Economic:** development of electronic components with a few technological steps. The characteristics of the films are generally influenced by the preparation conditions, such as the deposition method, post-deposition annealing temperature, types of substrates, etc [55].

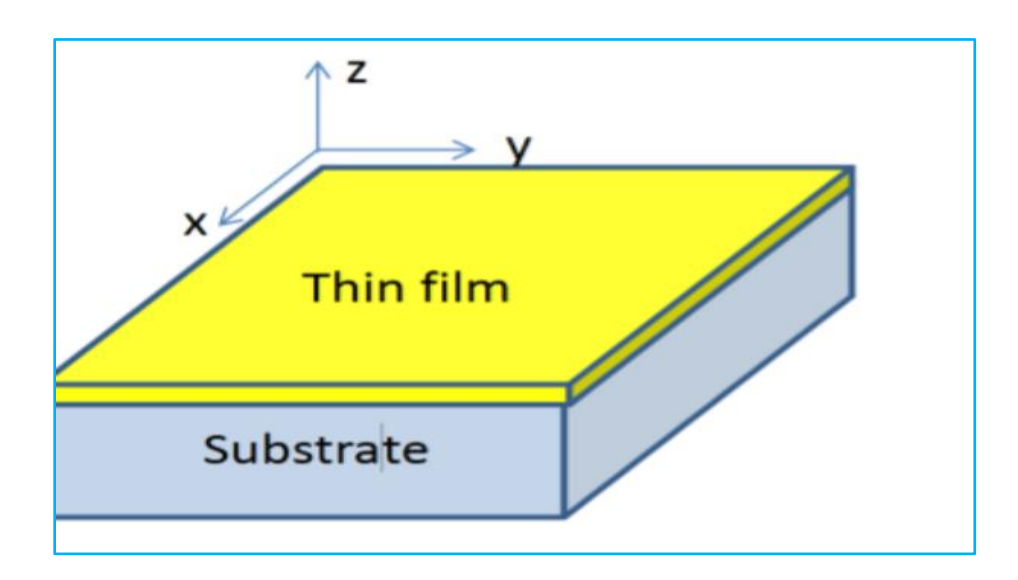


Figure I-15: Schematic of a typical thin film material on a substrate structure [56].

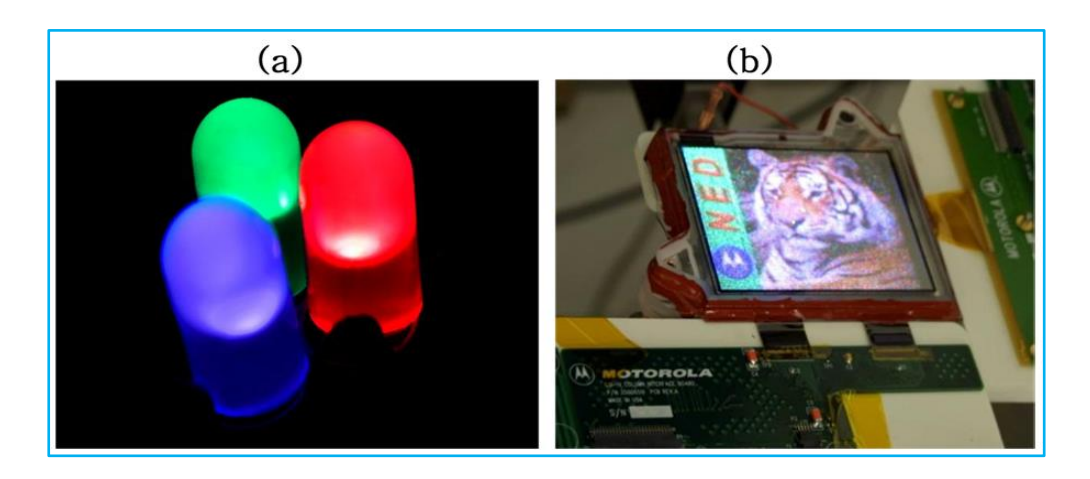
I.5.2. Applications of Zinc Oxide thin films

Zinc oxide in thin films has numerous applications due to its optical, semiconductor, piezoelectric, and catalytic properties, it is widely used in the electronics industry. Among the many uses of this material in optoelectronic devices, we can mention:

- ❖ Solar cells (transparent electrodes).
- ❖ Acousto-optic media and varistors.
- **Gas detectors (conductive gas sensors).**
- Pressure protector.
- Ultrasonic oscillators and piezoelectric transducers.
- Detectors in the (UV) laser and the photo detectors.
- * Transparent and anti-reflective layers.
- ❖ Photoelectrochemical cells and display devices [1].

I.5.3. Technological challenges of thin films

The semiconductor nanomaterials have attracted potential interest due to their unique properties and potential applications in all branches of science and technology. Semiconductor nanostructure materials have attracted an extensive attention owing to their unique properties and potential applications [57], which have been recognized as promising nanomaterials. It is exhibited a controlled morphology and composed of a number of irregular phases with geometricallycoordinated cooped metals and oxide atoms, which stacked alternately along the axes [58]. The Figure I-16 illustrates some applications of ZnO.



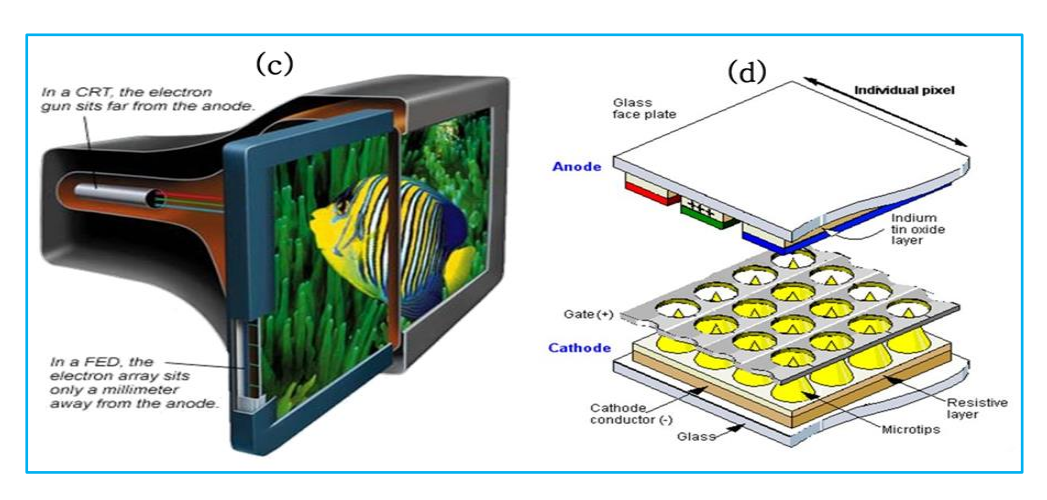
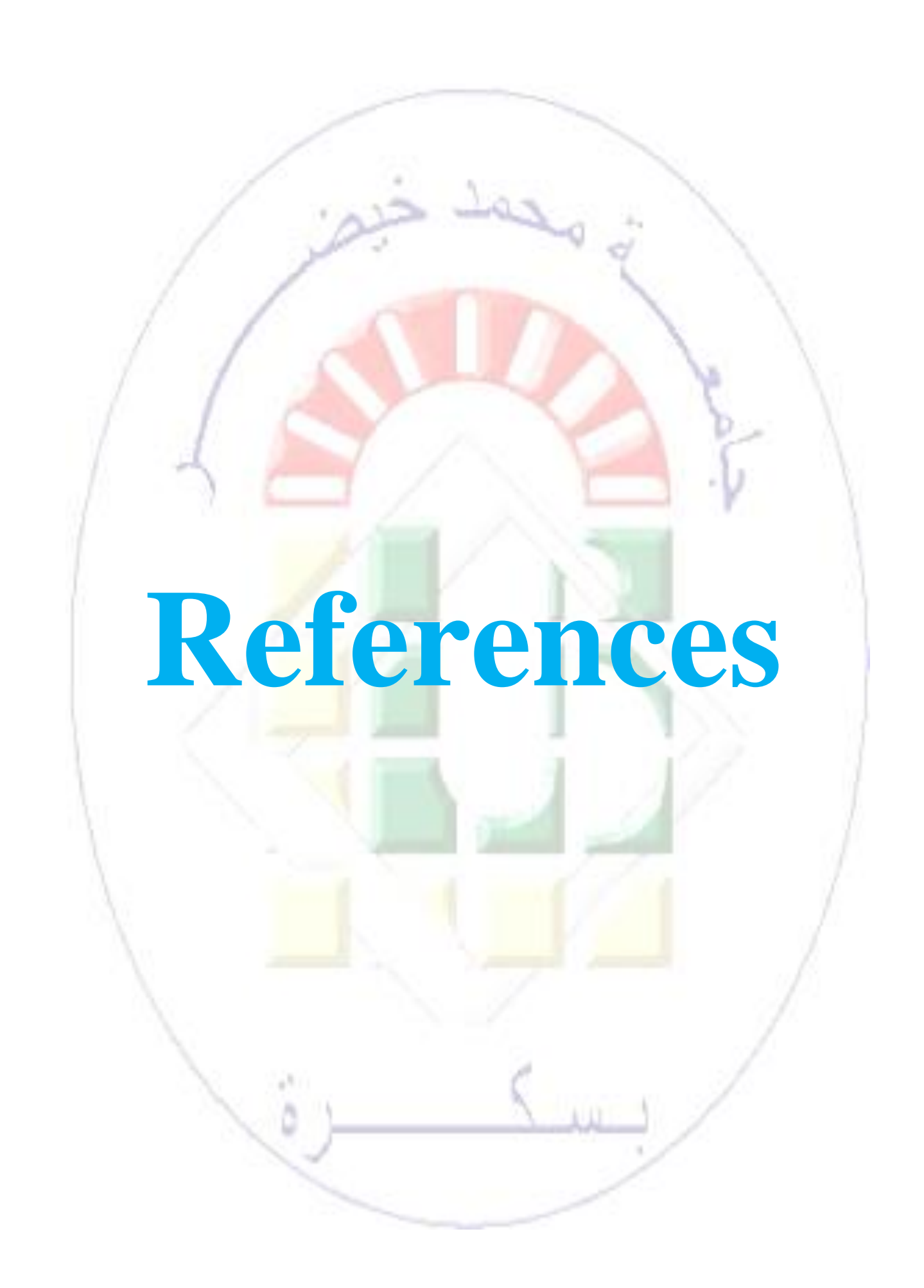


Figure I-16: Pictorials of some applications of ZnO (a) pure green and blue LEDs (b) TV (c) Cathode Ray Tube and (d) Solar cells [39].

For characteristic physical and chemical properties of nanomaterials, ZnO semiconductor has been also explored the significant attention due to their large-surface area and controlled sizes [59]. However, ZnO nanomaterials have also drawn an enormous interest towards itself owing to their extrinsic, remarkable and wonderful features in electrical, optical, thermal, and mechanical properties as compared to their un-doping materials. It is also essential for the facile synthesis of ZnO nanoparticles in order to achieve the exceptional quality of semiconductor structures. Advances in nanotechnology with innovative solid crystalline phases, semiconductor nanomaterial have been regulating a key-task in the fabrication and improvement of very precise, perceptive, accurate, sensitive, and stable crystalline adsorb.



References

- [1] A. Amri, "Development of ZnO-based thin films for thin-film transistors TFTs" Doctoral Thesis, Mohamed Khider University of Biskra-Algeria, 2024.
- [2] K. Baedeker, "Concerning the electricity conductibility and the thermoelectric energy of several heavy metal bonds" Annalen der Physic, vol. 22, p. 749, 1907.
- [3] K. Tonooka, H. Bando and Y. Aiura, "Thin Solid Films" p. 445, 2003.
- [4] G. Senadeera, K. Nakamura, K. Kitamura, Y. Wada and S. Yanagida, "Phys Appl" doi:10.1063/1.1633673, vol. 83, 2003.
- J. Stangl, V. Holy and G. Bauer, "Structural properties of self-organized semiconductor [5] nanostructures" p. 76, 2004.
- [6] N. Ben Amar, "Effect of catalyst concentration on the properties of ZnO thin films produced using the sol-gel method" Master dessertation, Mohemed Khider University of Biskra-Algeria, 2018.
- [7] F. Ynineb, "Study and realization of structures based on zinc Oxide", Doctoral Thesis, 2015.
- [8] S. Adachi, "Properties of group-IV, III-V and II-VI semiconductors" John Wiley Sons LTD, England, 2005.
- [9] N. Boubrik, "Comparison of the antireflective effects of SnO2 and ZnO used as antireflective layers on the properties of the homo-junction solar cell" Master dessertation, Mouloud Mammeri University of Tizi-Ouzou- Algeria, 2013.
- [10] A. Karroubi, "oxide structure intended to replace classical transparent conductive oxides in solar cells by photovoltaic effect" Master dessertation, Ahmed Ben Bella University of Oran- Algeria, 2012.
- [11] Z. Sofiani, "Contributions to the Study of Nonlinear Optical Properties of ZnO-Based Nanoparticles in Thin Films" Doctoral Thesis, University of Angers Ibn Tofail, 2007.

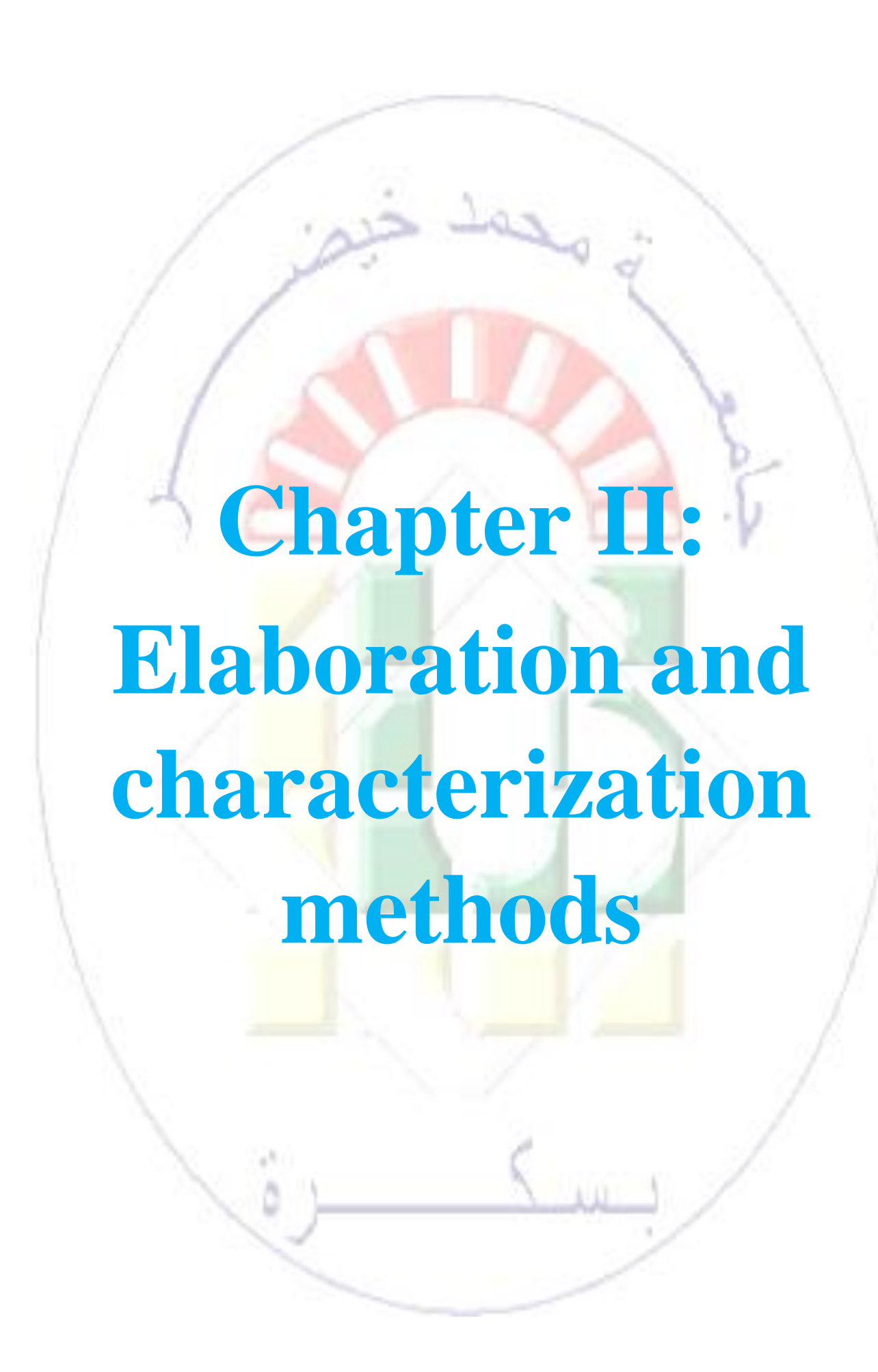
- [12] A. Valour, "Synthesis of Nitrogen-Doped Zinc Oxide in Powder and thin film Forms, Characterization of Conductivity Type", Doctoral thesis, University of Rennes, 2017.
- [13] C. Khelifi, "Tin dioxide (SnO2) thin films deposited by ultrasonic spray technique: Properties and applications" Doctoral Thesis, Mohamed Khider University of Biskra-Algeria, 2018.
- [14] M. Touatitliba, "Study of the optical and electronic properties of doped and undoped ZnO thin films, development and application", Doctoral Thesis ,Kasdi Merbah University of Ouargla-Algeria, 2019.
- [15] D. Tainoff, "Influence of defects on the optical and electronic properties of ZnO nanoparticles" Doctoral Thesis, University of Lyon- France, 2009.
- [16] L. Arab, "Elaboration by different methods and optical study of nanocrystal line powders of pure and doped ZnO with various oxides" Doctoral Thesis, University of Constantine-Algeria, 2012.
- [17] M. Mekhloul, "the electrical and optical properties of pure and Ga-doped ZnO nanopowders prepared using the Sol-gel method", Masters dessertation, 2021.
- [18] A. Latif, "Elaboration of pure and doped ZnO powders with the sol gel method" Doctoral Thesis, Mohamed Khider University of Biskra-Algeria, 2024.
- [19] P. Miller, "The electrical conductivity of zinc oxide", 1941.
- [20] C. Klingshirn, J. Fallert, H. Zhou, C. Sartor, F. Thiele, D. Thiel and Schneider et H. Kalt, "65 years of ZnO research - old and very recent results" pp. 22-27, 2010.
- [21] C. Klingshirn, "ZnO From basics towards applications", Physica status solidi, pp. 22-23, 2007.
- [22] M. Rebien, W. Henrion, M. Bär and C.-H. Fischer, "Optical properties of ZnO thin films" , lon layer gas reaction compared to sputter deposition, App. Phys, 2002.

- [23] B. Troudi, "Development and Characterization of Wide Bandgap Semiconductor Nanocrystals ZnO Dispersed in Two Matrices Polystyrene Polymer and SiO2 Silica", Doctoral Thesis, Mentouri University of Constantine-Algeria, 2006.
- [24] S. Guettaf Tamam and H. Hassine, "Effect of the number of depositions on the properties of ZnO thin films prepared by the sol-gel method", Master dessertation, Mohamed Khider University of Biskra-Algeria, 2019.
- [25] Z. Yao, "ZnO Nanoparticles as a Luminescent Down-Shifting Layer for Solar Cells", Doctorat Thesis, Ecole doctorale, Material of Lyon, 2015.
- [26] M. Othmane," Synthesis and characterization of Zinc Oxide (ZnO) Thin films deposited by spray pyrolysis for applying, electronics and photonics", Doctoral Thesis, Mohamed Khider University of Biskra-Algeria, 2018.
- [27] R. Boudiaf Yasmine, "Elaboration and Characterization of pure and Ga-doped ZnO nanopowders by the sol-gel method", Masters dessertation, Mohamed Khider University of Biskra-Algeria, 2020.
- [28] S. Desgreniers, "High-density phases of ZnO, Structural and compressive parameters", 1998.
- [29] U. Özgür, "General Properties of ZnO, in Zinc Oxide", Morkoç, Wiley-VCH Verlag GmbH Co, KGaA. pp. 1-76, 2009.
- [30] F. Ghomrani, "Elaboration and characterization of thin films of ZnO: Al and ZnO Al/TiO2", Doctoral thesis, Mohamed Bougara University of Boumerdes -Algeria, 2011.
- [31] F. Ynineb, "Contribution to the Development of Thin Films of Transparent Conducting Oxides (TCO)", Master dessertation, Mentouri University of Constantine -Algeria, 2010.
- [32] W. Xiao, Y. Liu, D. Zhao, J. Zhang, Y. Lu, D. Shen and X. Fan, "Ultraviolet photoconductive detector with high visible rejection and fast photoresponse based on ZnO thin film", 2007.

- [33] I. Deghiche, "Effect of solution concentration on the properties of ZnO thin films prepared by the sol-gel method", Master dessertation, Mohamed Khider University of Biskra-Algeria, 2018.
- [34] Handbook of Chemistry and Physics, Weast, CRS Press, 1975.
- [35] X. Zho, I. Yuri, X. Gan, I. Suzuki, G. Li and a. B. Biosensors, "Electrochemical study of the effect of nano-zinc oxide on microperoxidaseand its application to more sensitive hydrogen peroxide biosensor preparation" vol. 22, pp. 1600-1604, 2007.
- [36] O. Behera, "Synthesis and Characterization of ZnO Nanoparticles of Various Sizes and Applications in Biological Systems", Doctorat Thesis, Department of Computer Science and Engineering National Institute of Technology Rourkela Rourkela, Orissa-India.
- [37] R. N. E. H. Nezzal Hala," Elaboration of pure and Bi-doped ZnO nano-powders with the sol-gel method", Master dessertation, Mohamed Khider University of Biskra-Algeria, 2022.
- [38] Y. Ben Kheta, "Elaboration and characterization of thin layers of zinc oxide (ZnO) deposited by ultrasonic spray for photovoltaic and optoelectronic applications", Doctoral thesis, Mohamed Khider University of Biskra-Algeria, 2019.
- [39] U. Jatani," Growth and characterization of ZnO nanoparticles by sol-gel process", Doctoral Thesis, Department of Physics, University of Free State, 2015.
- [40] P. Jongnavakit, P. Amornpitoksuk, S. Suwanboon and T. Ratana, "Surface and photocatalytic properties of ZnO thin film prepared by sol-gel method" Thin Solid Films , p. 5561–5567, 2012.
- [41] S. Samal, P. Jeyaraman and V. Vishwakarma, "Journal of Minerals Materials Characterization Engineering", P.519-525, 2010.
- [42] A. Popescu, L. Duta and G. Dorcioman, "Radical modification of the wetting behavior of textiles coated with ZnO thin films and nanoparticles when changing the ambient pressure in the pulsed laserdeposition process", Appl Phys, 2011.

- [43] M. Maribor Rahman "ZnO Nanstructures Advances in researchand Applications" in Nanotechnology science and technology, Doctoral Thesis , Dana crawford, Nova Science Publishers Ney York, P. 59, 2020.
- [44] V. Narcisa and M. Petruta Suchea, "Novel Approach of Added Value Zeinc Oxide Powders for Polymeric Fibrous Matrices With Engineered Architectures for Highperformance Textiles", Nova Science Publishers, Inc, 2024.
- [45] M. Goutayer, "Nano-emulsions for the vectorisation of therapeutic and diagnostics agents Study of biodistribution by in vivo fluorescence imaginng", Doctoral Thesis, University Pierre of Marie Curie, 2008.
- [46] T. Yeow Poh, N.tikah, A. Binte Mohamed, M. Mac Aogain, M. Hussain Kathawala, M. Inggrid Setyawati, K Woei Ng and S. Haresh Chotirmall, "Content courtesy of Springer Nature, terms of use apply. Rights reserved" in Inhaled nanomaterials and the respiratory microbiome: clinical, immunological and toxicological perspectives, doi: 10.1186/s12989-018-0282, November, pp. 3-16, 2018.
- [47] D. Valerini, A. creti, A. caricato, M. Lomascolo , R. Rella and M. Martino, "Nanotechnology science and technology" in ZNO Nanstructures Deposited by laser ablation, Nova Science Publishers, Inc. New York, P.2, 2010.
- [48] B. Ghata, "Synthesis of Zinc Oxide Nanoparticles Through Various MethodsIts Its Characterization And Applications", Gujarat Technological University of Ahmed Ben bela, 2017.
- [49] Zhong Lin Wang, "ZnO nanowire and nanobelt platform for nanotechnology", Materials Science and Engineering, 2009.
- [50] M. Goutayer, "Nano-emulsions for the vectorization of diagnostic therapeutic agents; study of biodistribution by in vivo fluorescence imaging", Doctoral Thesis, Pierre and Marie Curie University, 2008.
- [51] O. Bouchoul," Nanostructured gas sensor", Science and Technology Mohamed Boudiaf University of Oran-Algeria, 2012.

- [52] P. Weimer, "The TFT A New Thin-Film Transistor" pp. 1462-1469, 1962.
- [53] A. Aldrin, "Preparation and characterization of certain II-VI, I-III-VI2 semiconductor thin films and transparent conducting oxides", Doctoral Thesis ,Cochin University of Science and Technology Kerala, India, 2004.
- [54] M. Dahnoons," Preparation and characterization of Titanium dioxide and Zinc oxide thin films via Sol-Gel (spin coating) technique for optoelectronic applications", Doctoral Thesis, Mohamed Khider University of Biskra-Algria, 2020.
- [55] S. Benramache," Elaboration and characterization of thin layers of ZnO doped with cobalt and indium", Doctoral Thesis, Mohamed Khider University of Biskra-Algeria, 2012.
- [56] T. Azzouni, "The Analytical study of The Laser Flash Method", Internship Report 10.13140/RG.2.2.10051.43048, 2020.
- [57] A. Umar, M. Rahman, S. Kim and Y. Hahn, "Zinc oxide nanonail based chemical sensor for hydrazine detection", Chem. Commun, vol. 166, 2008.
- [58] B. Willner, "Biomolecule-based nanomaterials and Nanostructures" Nano let, vol. 3805, 2010.
- [59] K. Ghosh, M. Kanapathipillai, N. Korin, J. McCarthy and D. Ingber, "Polymeric Nanomaterials for Islet targeting and Immunotherapeutic deliver" Nano Lett, vol. 203, 2012.



II.1. Introduction

The chapter consists of two sections. The first presents some methods for producing nanomaterials. The sol-gel process is one of Among these methods which is adopted in our study to prepare thin films of zinc oxide. The second section outlines the techniques used to characterize the elaborated zinc oxide thin films.

II .2. Thin Film Deposition Methods

Thin films are essential in many applications such as electronics, optics, and material science. Thin film deposition methods are broadly categorized into chemical deposition and physical deposition methods:

- 1) Chemical Deposition Methods: These techniques involve chemical reactions to form thin films. can be further divided into gas phase and solution-based methods [1].
- Chemical vapor deposition (CVD): It uses volatile precursors that react on the substrate to form a thin film. It includes: plasma enhanced CVD (PECVD), and Metal-Organic CVD (MOCVD).
- Atomic Layer Epitaxy(ALE): Specialized CVD process that deposits thin films with atomic precision through sequential self-limiting reactions.
- Spray pyrolysis: A precursor is sprayed onto a heated substrate, where it decomposes to form a thin film.
- Sol-Gel process: A colloidal solution (Sol) undergoes gelation, followed by heat treatment to form a thin film.
- **2) Physical deposition Methods:** These techniques rely on physical processes such as evaporation or sputtering to deposit thin films [1].
- Physical Vapor deposition (PVD): Encompasses techniques where the material is vaporized and condensed on a substrate. (Thermal Evaporation) and (Electron Beam Evaporation).
- Sputtering: DC Sputtering and RF Sputtering.
- Laser Ablation (pulsed Laser Deposition (PLD)): A high-energy laser beam vaporizes the target material, which then deposits as a thin film. Several considerations must be respected while choosing the deposit method:
 - ❖ Characteristics of the surface on which the film will be deposited.
 - Material to be deposited.

- * The required film thickness.
- ❖ The expected structure of the film.
- ❖ Application of the thin film.

The careful selection of the appropriate deposition technique is essential for controlling the properties of the resulting films; the following figure summarizes the different methods of depositing of thin films [1].

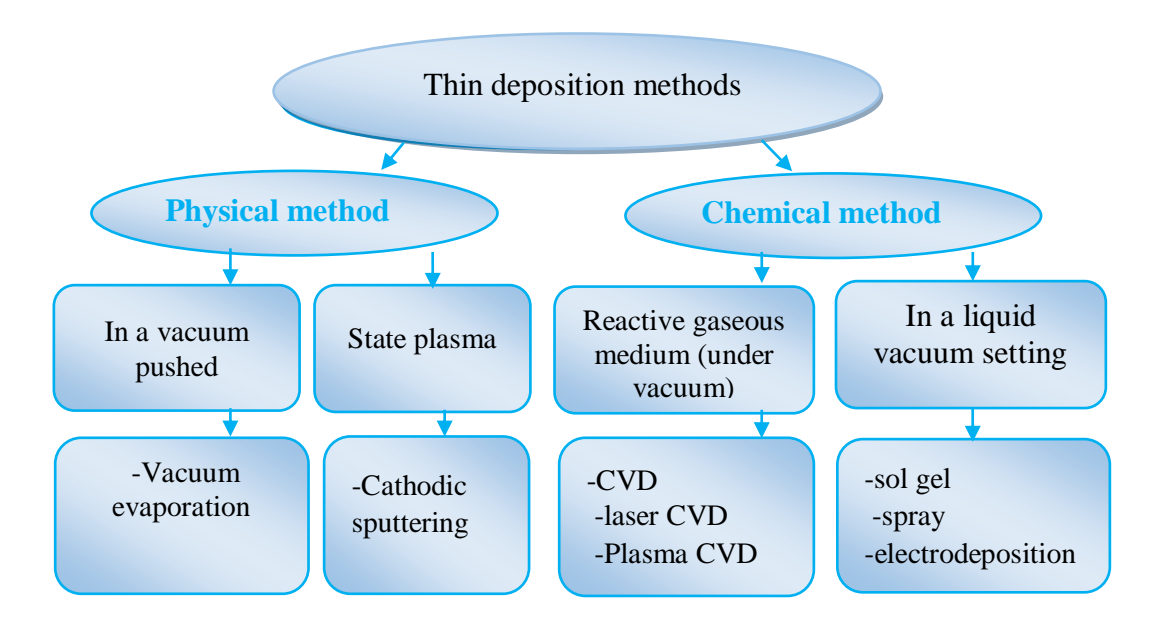


Figure II-1: General methods for depositing a thin films [2].

II .3. Sol-gel method

II .3.1. History of the sol-gel method

In 1939, the company Schott Glaswerke filed the first patent for the deposition of thin films on glass by dip coating. In contrast to huge gels known as xerogels, the industry started to produce this type of material in thin layers, which are easier to shape and have a rapid drying period. This form helps prevent the traditional issues of gel breaking during drying. Thus, the German business Scott Genossen produced silica coatings by applying colloidal silicic acid solutions to a glass plate, many ceramic materials based on aluminum oxides, silica, titanium, or zirconium that were impossible to produce using conventional ceramic fabrication techniques were synthesized in the 1950s and 1960s thanks to the sol-gel process. It has been gaining popularity for over 20 years because it allows the creation of unique materials with a large range of shape possibilities by managing the various phases from precursor to substance. Thus, the uses of the sol-gel technique can produce dense thin films, fibers, or monoliths [3].

II .3.2. Definition of the sol-gel

The property of the sol-gel process is a chemical method known as soft chemistry. The term "sol-gel" is an acronym for "solution-gelation," in which the precursors are in the liquid phase at the start of the process and the solution turns into a gel at room temperature via a sequence of chemical reactions of the polymerization type. Numerous organic, inorganic hybrid compounds may be created with this method in a broad range of forms, including thin films, optical fibers, monolithic glasses, and calibrated Nano-powders and nanoparticles. The advantages of Sol-gel include its application to technical domains such as biometrics, electronics, etc [4].

II.3.3. The Sol-gel process

The sol-gel method is started by establishing a stable suspension (Sol) based on chemical precursors in the solution. As a result of interactions between the suspended specie the solvent, the "sols" will change during the gelation process creating a solid, three-dimensional network, that spreads across the sol, the system is in a "Gel" state. These "humid" gels are then turned into dry amorphous material by either evaporating the solvents (which yields an aerogel) or by simply evaporating at atmospheric pressure (xerogel) [5].

- Sol: It is an abbreviation for the word solution and refers to a colloidal suspension (the term colloidal indicates that particle size ranges from 1to1000 nm). The solution typically consists of a primary substance and a solvent (usually alcohol), and sometimes a catalyst (acid or base) and water. The dosage of each component is determined with high precision because the characteristics of the product depend on it. The nature of the desired material determines the choice of solvent and catalyst, based on the chemical properties of the dissolved substance, which is the main compound of the prepared solution [6].
- ■Gel: A gel is defined as a three-dimensional structure that contains a solvent, such that macroscopically the system appears as a single phase. This state results from the aggregation of particles and their collisions driven by Brownian motion. The resulting aggregates entrap the solvent within a three- dimensional network [6].

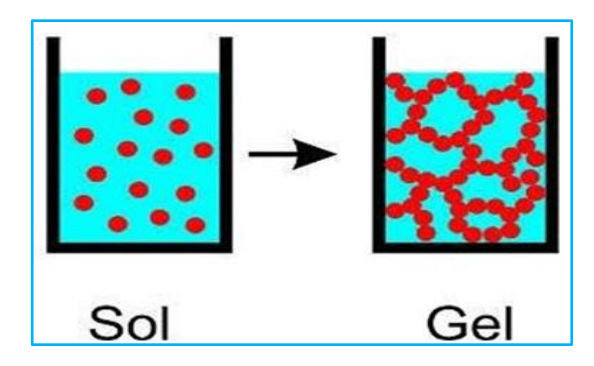


Figure II-2: Sol-gel synthesis [6].

The time required for the "sol" to transform into "gel" is called the gelation time or gel point. There are two sol-gel synthesis routes, which are:

- Colloidal route: It is obtained from metal salts in an aqueous solution. This method is less costly route but more difficult to control. It relies on the formation of a sol (a stable colloidal suspension) and its subsequent transformation into a gel (a three-dimensional network). Therefore, it is still rarely used, however, it remains the preferred method for obtaining ceramic materials.
- ➤ **Polymeric route**: is obtained from metal alkoxides in organic solutions. This route is relatively expensive but allows, for fairly, easy control of the particle size [6].

II.3.3.1. The sol-gel transition

Polymeric clusters whose size increases over time are formed during the polymerization process. When one of these clusters reaches an infinite dimension, essentially the container's size, the viscosity becomes infinite. This is known as the sol-gel transition point. This point is illustrated in (figure II-3). From then on, the cluster continues evolving by incorporating smaller polymeric groups. Once all the bonds have been utilized, the gel is formed [7].

The time required to obtain the gel after adding water is known as the gelling time (**tg**) [6]. Like any chemical reaction, the Sol-gel transition is sensitive to its surroundings, such as temperature and humidity, which may alter its chemistry [8].

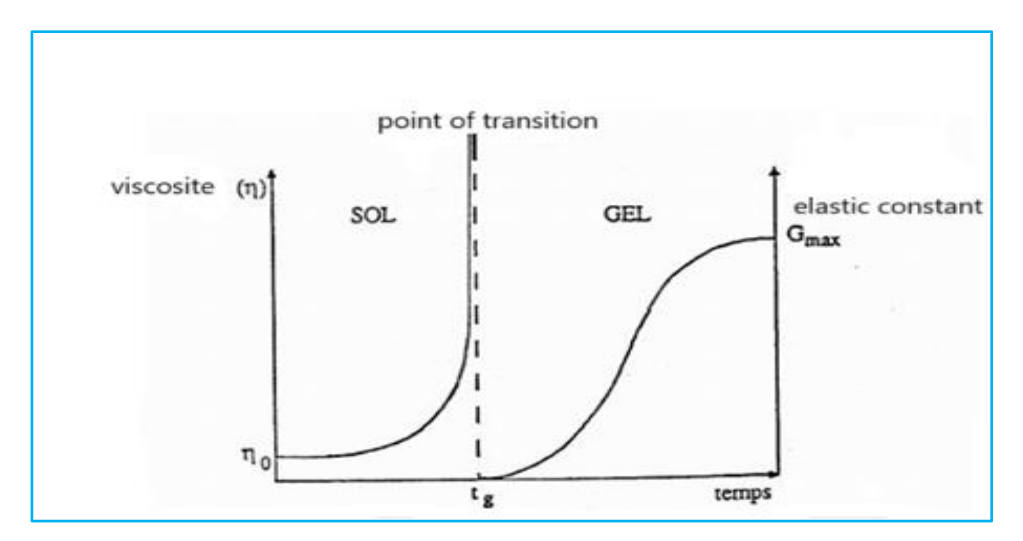


Figure II-3: Macroscopic characterizations of the peaks of the Sol-Gel transition [8].

II .3.3.2. Reaction mechanisms

Understanding the various phases of oxide production will allow one to comprehend the function of each component produced in the solutions. The chemical transformation mechanism is divided into two steps [8].

II .3.3.2. a. Hydrolysis reaction

During the hydrolysis reaction, the alkoxide groups (OR) are replaced with hydroxyl group (OH) through the addition of water as shown in the equation below [8].

$$M(OR)_n + H_2O \rightarrow M(HO)_n - (OR)_{n-1} + {}_nR-OH$$
 (II.1)

Although hydrolysis can occur without additional catalyst, it has been observed that with the help of acid or base catalyst the speed and extent of the hydrolysis reaction can be enhanced [9].

II .3.3.2. b. Condensation reaction

The groups $(HO-M (-OR)_{n-1})$ generated during the hydrolysis react either with each other to give a molecule of water (Oxolation) or with a molecule M of the alkoxy (-OR) to give an alcohol molecule (Alcoxolation) and leading to the creation of the or each flight MOM oxygen atom becomes a bridge connecting two atoms of the metal M. This leads to the formation of a gel whose viscosity, increases over time; this gel contains solvents and precursors which have not yet reacted [10].

II.3.3.3.Gelation

The most comprehensive description of gel formation is that clusters grow by polymer condensation or particle aggregation through collisions, forming physical bonds such as hydrogen bonds between clusters to produce a single large cluster known as a gel. This gel extends throughout the container holding it, so that the liquid can no longer flow when the container is tilted. At the moment of gel formation, many clusters are present in the aqueous phase and are entangled, but they are not yet fully connected to the spanning cluster. Over time, they gradually become linked to the network, and the gel becomes increasingly rigid [10].

II.3.3.4. Ageing

After gelation, the continuing chemical and physical changes during aging are extremely significant. During this process, further cross-links continuous continuously, the gel shrinks as the covalent links replace non-bonded contacts and both the pore sizes and pore wall strengths change as the gel's structure evolves [10].

II.3.3.5. Drying

The gel has three-dimensional linked pores and a high water ratio inside the structure. Because the liquid trapped in the linked pores must be eliminated before the pore is closed during the densification process, drying is a necessary step. However, because of inhomogeneous shrinkage, removing the liquid from the microscopic holes results in substantial tension. Because of the high load in the structure, cracking became the primary problem that needed to be resolved. No extra attention is required to prevent cracking for sol-gel structures with small cross-sections, such as powder, coating, or fiber because the drying stress is minimal and can be handled by the materials. For monolithic objects greater than 1 cm drying stress developed in the ambient atmosphere can introduce catastrophic cracking, consequently, control of the chemistry of each processing step is crucial to prevent cracking during drying [10].

II.3.4. parameters influencing the reaction rate

The speed of sol-gel reactions depends on several parameters that must be taken into account during the implementation of the process:

- ❖ The temperature: is the first parameter in the setting, which interacts with all chemical reactions. the augmentation of the temperature increases the hydrolysis and condensation reactions, but this also affects the structure of the material forms [8].
 - ❖ The type and concentration of alkoxide: This selection is made based on the interaction of alcohol and the type of wax it will work on, as well as the degree of sunlight concentration, which is very important during condensation. In fact, it is something impossible, in addition to the molecules being capable of separating from each other, which delays the reactions [8].
 - ❖ The solvent: The choice of solvent is also dictated by process imperatives (ease of drying, integrity of the final material), potential toxicity, or environmental constraints (emission of volatile organic compounds) [8].
 - **♦ The pH (catalyst selection)**: Because of the mechanisms involved in gelation, pH plays an important role in the evolution of the reactions: H⁺ ions do not have the same influence on the two reaction types. The H⁺ cation, through oxygen, facilitates the substitution of OR groups and therefore hydrolysis, while the electronegative M metal favors the formation of gelling bonds. The pH will play an important role in the evolution of the reactions: H₃O⁺ ions influence both reaction types.

Therefore, Catalysis directly affects the shape of the developed material. This factor will also significantly affect the porosity of the final material, which will partially determine its physical properties [8].

II.3.5. Gel Drying:

Once the solution is gelled, the gel undergoes drying due to capillary forces in the pores, and this drying leads to volume shrinkage. The drying process required to obtain the sol-gel material necessitates that the alcohol or water escape while the gel solidifies. The sol-gel material's pores and channels allow the evaporation process to occur [11]. Several types of drying allow for the production of different materials types.

➤ **Xerogel:** conventional drying, or regular evaporation, it reduces volume by 5–10%. When the solvent evaporates, a xerogel is created, which may then be heated to a moderate temperature to densify the substance. The drying of the gel is a delicate step because the kind of material and

Chapter II......Elaboration and characterization methods

the required qualities have a significant impact on the densification temperatures. Therefore the solvent must be evaporated very slowly to avoid the fragmentation of the xerogel [11].

Aerogel: drying in a high-pressure autoclave under critical conditions causes minimal to no volume shrinkage. An aerogel that has not undergone densification, is created when the solvent is removed under supercritical circumstances. As a result, we get a very porous substance with remarkable insulating qualities. In addition, the change from a sol to a gel, whose viscosity is controllable, makes it possible to dip or spray fibers and films onto a variety of surfaces. Xerogels are generally denser than aerogels [11].

II.3.6. Sol-gel deposition techniques

Two techniques can be utilized for the deposition of thin films on a specific substrate: "spin-coating" and "dip-coating". Each one has unique properties, and the size or shape of the substrate influences the choice of deposition technique, as shown in the figure below [12].

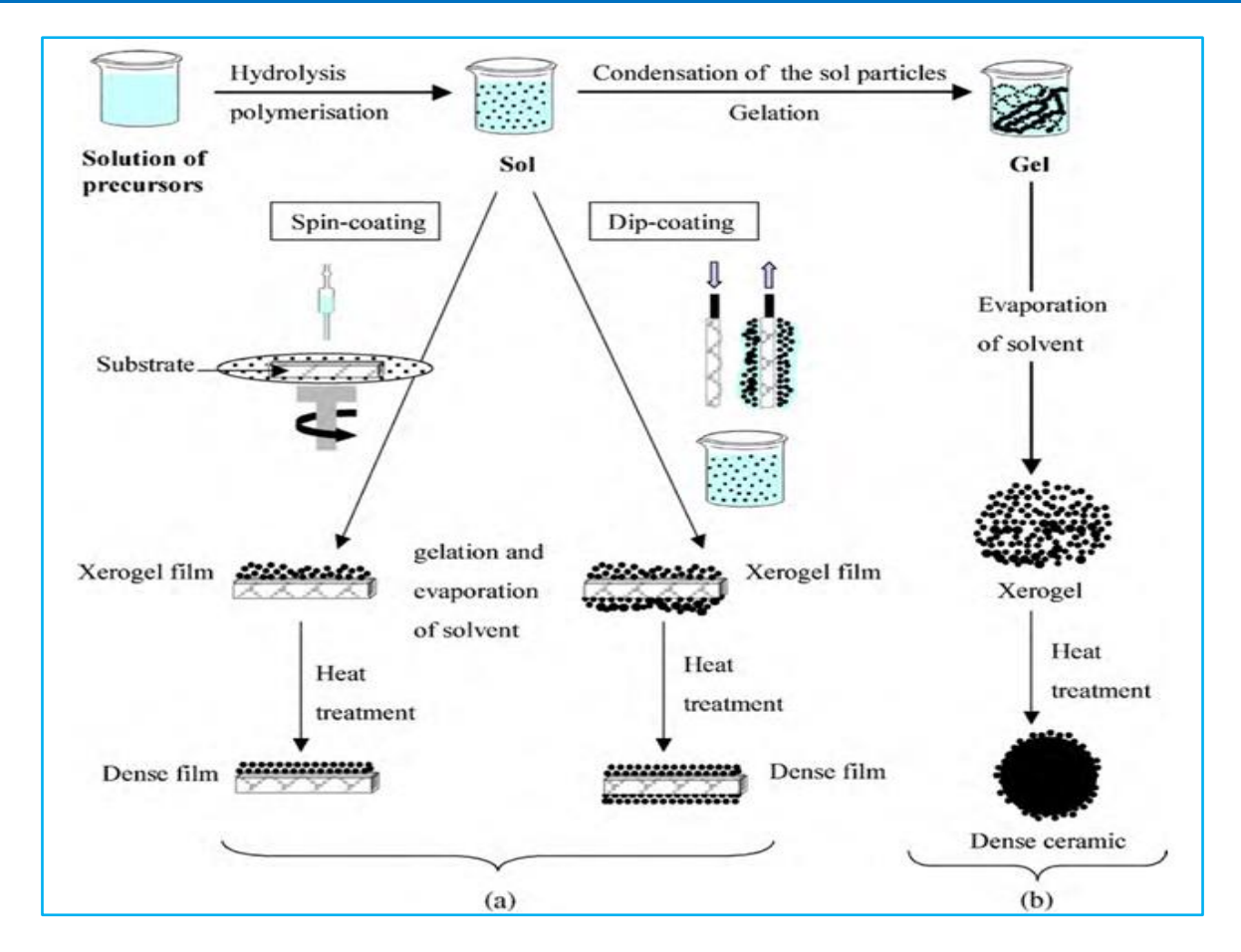


Figure II-4: The main steps of preparation and deposition of thin films and powder by the sol-gel process [13].

II.3.6.1. Spin-coating

The spin-coating deposition technique is one of the most used methods for thin film fabrication on flat substrates making use of the centrifugal force of the spinning substrate to spread and uniformly coat its surface. The coating material is dissolved in a volatile solvent that evaporation during the baking process. Attending to the viscosity, concentration and rotation speed, it is possible to precisely control the thickness of the thin films, with increasing angular speed leading to thinner films [14]. This process is widely used for photoresist deposition on flat substrates for microfabrication through photolithography processes. It is also used for metal oxide layers deposition using sol-gel precursors [15]. Figure II-5 represents the typical spin-coating deposition process. Which is done in four main steps.

- The deposition of the solution.
- The start of rotation: The acceleration step causes the fluid to flow out of the substrate.

- * Rotating at a constant speed allows the ejection of excess liquid in the form of droplets and the reduction of the thickness of the film uniformly.
- * Evaporation of the more volatile solvent which increases the reduction of the thickness of the deposited film. Final film thickness and other properties depend on the parameters chosen for the spin process [16].

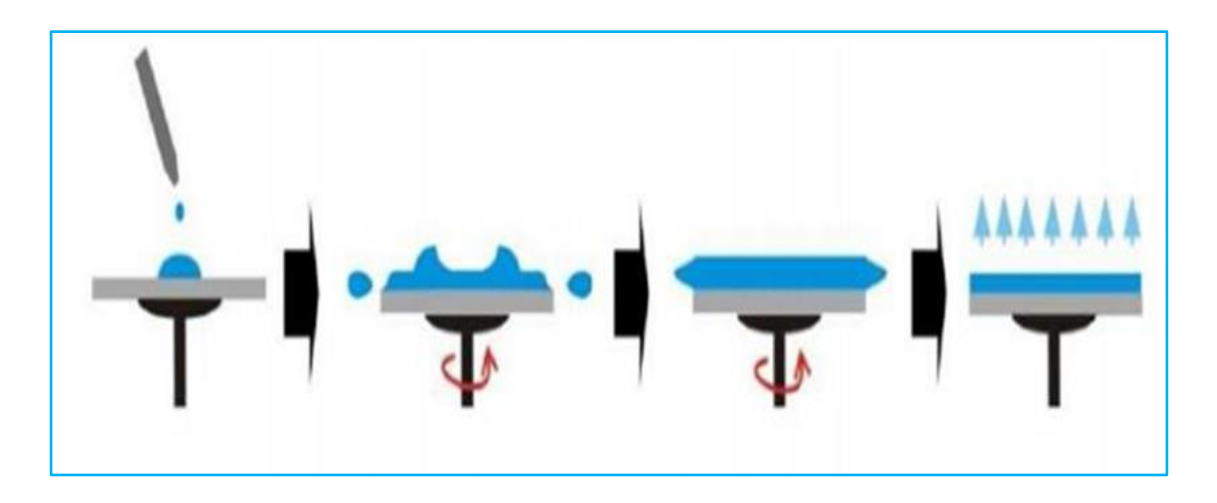


Figure II-5: The four steps of spin coating [17].

We can measure the film thickness by the equation (II-2), which shows how some parameters affect thickness [16].

$$d = (1 - \rho_A/\rho_{A0}) \cdot (3\eta \cdot m/2\rho_{A0} \cdot \omega^2)^{1/3}$$
 (II-2)

d: thickness.

 ρ_A : density of volatile liquid (ρ_{A0} represents the initial mass of solvent over solution volume).

 η : viscosity of solution.

m: rate of evaporation.

 ω : rotational speed.

Due to the increased rotational speed, the film's size decreases, and a simpler equation like the following is suggested [16].

$$d = \alpha \omega^{-2/3} \tag{II-3}$$

 α is a constant parameter calculated experimentally.

II.3.6.2. Dip-coating

The coating technique by immersion is a film deposition process in which the object to be coated is submerged in a liquid and then emerged at a predetermined speed under temperature and atmospheric control figure II-6 [16]. The dip-coating technique is particularly well-suited for producing thin layers as it allows for the deposition of very homogeneous films on large substrates. Additionally, it provides the ability to manage the thickness of the deposits as well as their microstructure (porosity, crystallinity) [2].

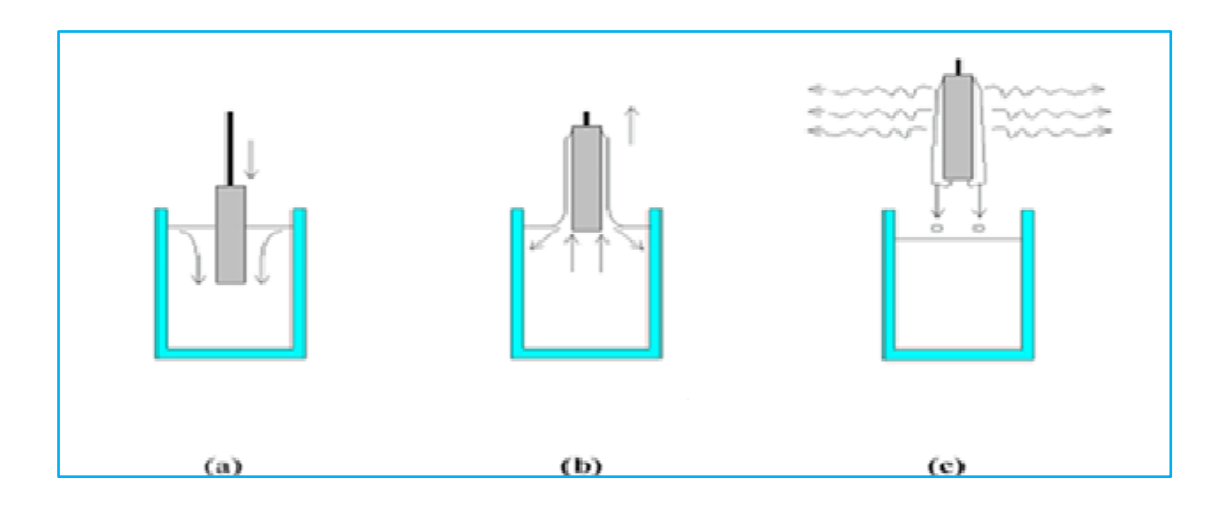


Figure II-6: Stages of the dip-coating process; a) dipping of the substrate into the coating solution; b) wet layer formation by withdrawing the substrate; c) gelation of the layer by solvent evaporation [14].

II.3.7. Application of the Sol-Gel method

The sol-gel process is incredibly effective for creating a variety of factional materials. Effective implementations have been made, which may be summed up in Figure II-7. Where examples of materials used in high-temperature technologies, electronics, optics, photonics, chemical technologies, biochemistry, and medicine are provided [10].

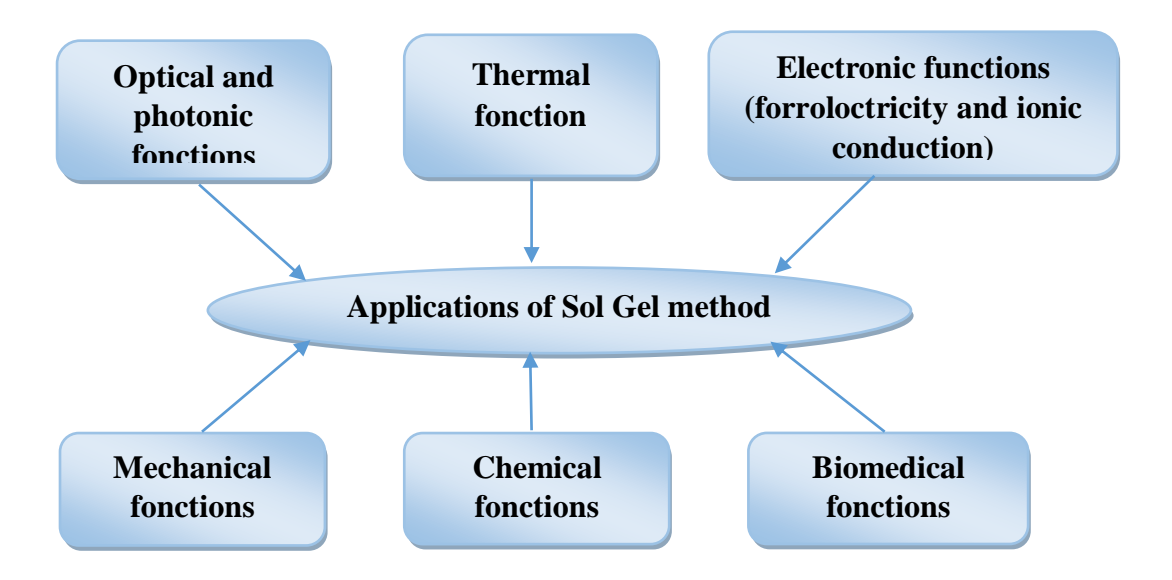


Figure II-7: Application of the sol-gel method [10].

II.3.8. Advantages of the sol-gel method

- ➤ **Versatile:** Sol-gel has better control of the structure, including porosity and particle size, and the potential for adding organic compounds and nanoparticles to oxides made via solgel.
- > Extended composition ranges: it permits the production of some non-oxides as well as any oxide composition. It also creates novel organic-inorganic hybrid materials that are not found in nature.
- > Improved homogeneity: It has excellent purity as a result of molecular mixing.
- Less energy: is used since the network structure may be formed at relatively low temperatures close to Tg, negating the requirement to attain the melting point.
- ➤ No expensive or specialized equipment is required [7].

II.3.9. Drawbacks of the sol-gel method

- Precursor costs.
- A wet gel's shrinkage after drying frequently results in fracture because it creates large capillary strains, making it challenging to achieve massive monolithic chunks.
- A specific oxide's preferential precipitation during sol formation (in multicomponent glasses) as a result of the alkoxide precursors' varying reactivity.
- ➤ Difficult to avoid residual porosity and OH groups [7].

II.4. Characterization techniques

Several characterization methods were employed during this study. Each method has been examined, by briefly recalling the underlying theoretical concepts, the advantages they offer, and the data they allow to be obtained regarding the characterization of samples [2].

II.4.1. X-ray Diffraction

In materials science, X-ray diffraction (XRD) is a method used to ascertain the atomic and molecular structure of the material. This is accomplished by exposing a material sample to incident X-ray radiation. Then the intensities and angles of X-ray scattering are measured as the material disperses them and the intensity of the dispersed X-rays is plotted against the scattering angle Beyon calculating the atoms' average locations inside the crystal, it is possible to ascertain how the real structure differs from the ideal structure, for instance, due to internal tension or flaws [7].

In addition to measuring the crystallite size, lattice parameter, and dislocation density, this study attempts to clarify the structure of the ZnO samples.

II.4.1.a. Apparatus

The measurements are made in 2.5×10^{-3} degree increments using a goniometer θ - 2θ (Rigaku Mini Flex 600). The K α line from a copper anticathode (Cu K α = 1.541838 Å) is the X-ray radiation that is used. The apparatus setup is shown in (figure II-8).



Figure II-8: Rigaku Mini Flex 600 type diffractometer (LPCMA).

II.4.1.b. The X-ray diffraction measurement principle

The Bragg-Brentano goniometer method is used to conduct X-ray diffraction on a crystal. The intensity of lines as a function of the detecting angle 2θ is then represented as a diffraction pattern.

Preferred crystal orientations are highlighted and interlinear distances are easily accessible using the measurement of the diffraction angles (Figure II-9) [18].

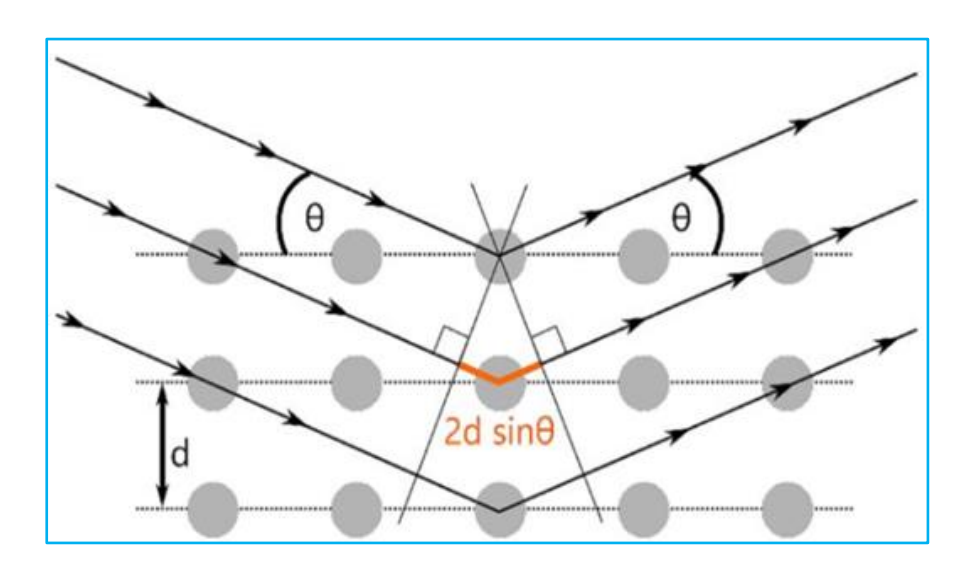


Figure II-9: Schematic of X-ray diffraction [7].

II. 4.1. c. Determination of interatomic distances and lattice parameters

The Scherrer Method

It is possible for a spot to appear in a position corresponding to reflection in any set of planes having integral indices (hkl). In an actual pattern obtained by allowing the diffracted X-ray to fall on a photographic plate, since there is not an infinite number of spots, only a selection of the planes can be operative [19]. Bragg law is used to determine the interplanar distances between various (hkl) planes:

$$2d_{hkl}\sin\theta_{hkl} = n\lambda \tag{II-4}$$

where n is the diffraction order and λ is the wavelength of the diffracted photon. where θ_{hkl} is the diffraction angle and d_{hkl} is the interplanar spacing of the corresponding crystallographic plane. Lattice parameters are found by comparing a diffract gram with JCPDS data base. Concerning ZnO (hexagonal lattice), the correlation between crystallographic parameters and the interplanar spacings of the (**hkl**) planes is given by the following equation [7].

$$\mathbf{d_{hkl}} = \frac{a}{\sqrt{\frac{4}{3}(h^2 + k^2 + hk) + l^2 \frac{a^2}{c^2}}}$$
(II-5)

 \boldsymbol{a} and \boldsymbol{c} are the lattice parameters.

Parameters **a** and **c** can be obtained using the pics (002) and (100) respectively. The comparison of these experimental lattice parameters with the theoretical values referenced in the [JCPDS] data ($a_0 = 3.249 \text{ Å}$ and $c_0 = 5.206 \text{ Å}$), We can learn more about the state of the tensions in the layer in question [20].

II.4.1. d. Determination of grain size and stresses

The size of the gains of the different samples was first deduced from the X-ray diffraction spectra using the Scherrer equation [21].

$$\mathbf{D} = \frac{0.89.\lambda}{\beta_{hkl} \cos \theta_{hkl}} \tag{II-6}$$

With:

D: crystalline size.

 λ : the wavelength of the X-ray beam.

 $oldsymbol{eta}_{hkl}$: the width at mid-height expressed in radians.

 θ_{hkl} : he angles of diffraction.

Figure II-10 shows the half-width β_{hkl} of the peak at the position $2\theta_{hkl}$.

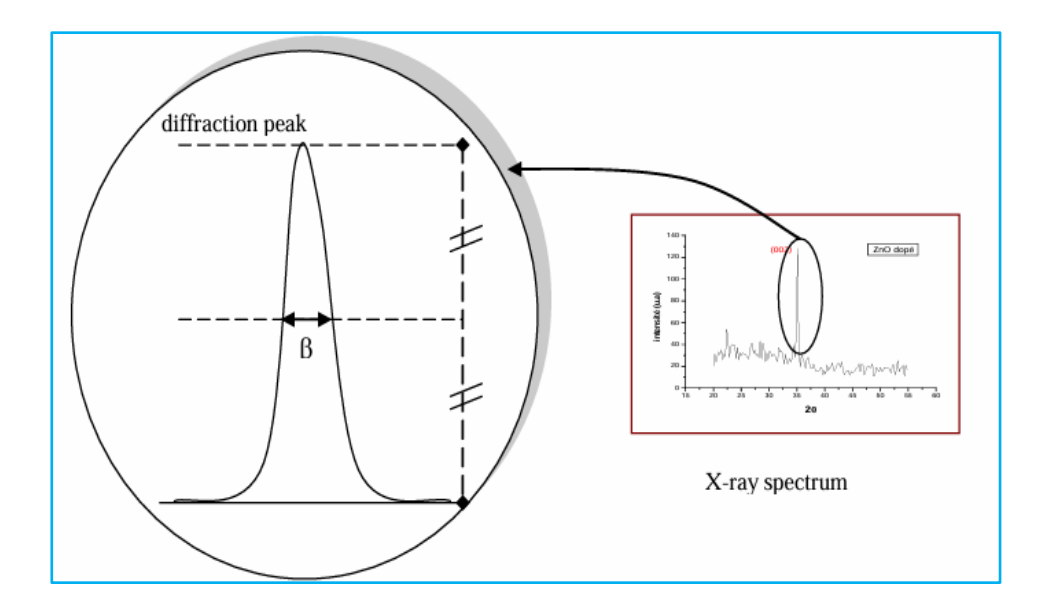


Figure II-10: The extraction of the full width at half maximum (β) from X-ray diffraction **peak** [1].

The Williamson -Hall Method

The strain induced in powders due to crystal imperfection and distortion was calculated using the formula:

$$\varepsilon = \frac{\beta_{hkl}}{4\tan\theta_{hkl}} \tag{II-7}$$

While the original Scherrer equation encounters limitations due to uncertainties in the crystallite shape factor (K), researchers have developed a modified version to estimate the sizes of Nano crystallites more accurately [22].

The standard method was developed in 1953. which is the Williamson-Hall method, through the past five decades. W-H plots emphasized the plots caused by strain. The peak's width derived from crystallite size differs from $(1/\cos\theta)$ while the strain differs from $(\tan\theta)$. This behavioral difference as a function of 2θ helps us differentiate between the strain's effects and the size of the peak expansion. Williamson-Hall's research simplified integral breadth approaches by deconvoluted sizes and strain-induced development when the width of peaks is the function of 2θ [23, 24].

The significance of the broadening of peaks evidences grain refinement and the large strain associated with the powder. The instrumental broadening (β_{hkl}) was corrected, corresponding to each diffraction peak of ZnO material using the relation:

$$\boldsymbol{\beta}_{hkl} = [((\boldsymbol{\beta}_{hkl})^2) \text{ Measured} - ((\boldsymbol{\beta}_{hkl})^2) \text{ Instrumental}]^{1/2}$$
 (II-8)

From Equations 7 and 8, it was confirmed that the peak width from crystallite size varies as $1 \cos\theta$ strain varies as $tan\theta$. Assuming that the particle size and strain contributions to line broadening are independent of each other and both have a Cauchy-like profile, the observed line breadth is simply the sum of equations II-6 and II-7.

$$\beta_{hkl} = \frac{K.\lambda}{D.\cos\theta_{hkl}} + 4 \varepsilon.\sin\theta_{hkl}$$
 (II-9)

II.4.2. Optical characterization

The optical characterization has been studied using the spectrophotometer. The interaction between the sample to be and the light emitted in the range of visible and ultraviolet forms the basis of this technique. The sample will either transmit or absorb a portion of the incoming light beam [2].

The optical characteristics of the material to be examined, including light absorption and transmission, the optical gap, and the Urbach energy, are revealed using spectrophotometry. In some circumstances, it is also feasible to determine the film's thickness and refractive index [25].

When a substance absorbs light in the ultraviolet and visible range, this causes changes in the ions' electrical configuration, electrons to leap from a lower energy level to a higher one in molecules or atoms. These electronic transitions occur in the visible range, between 350 and 800 nm, as well as in the ultraviolet, between 200 and 350 nm [26].

Figure II-11 illustrates the principle of ultraviolet-visible spectrometers schematically.

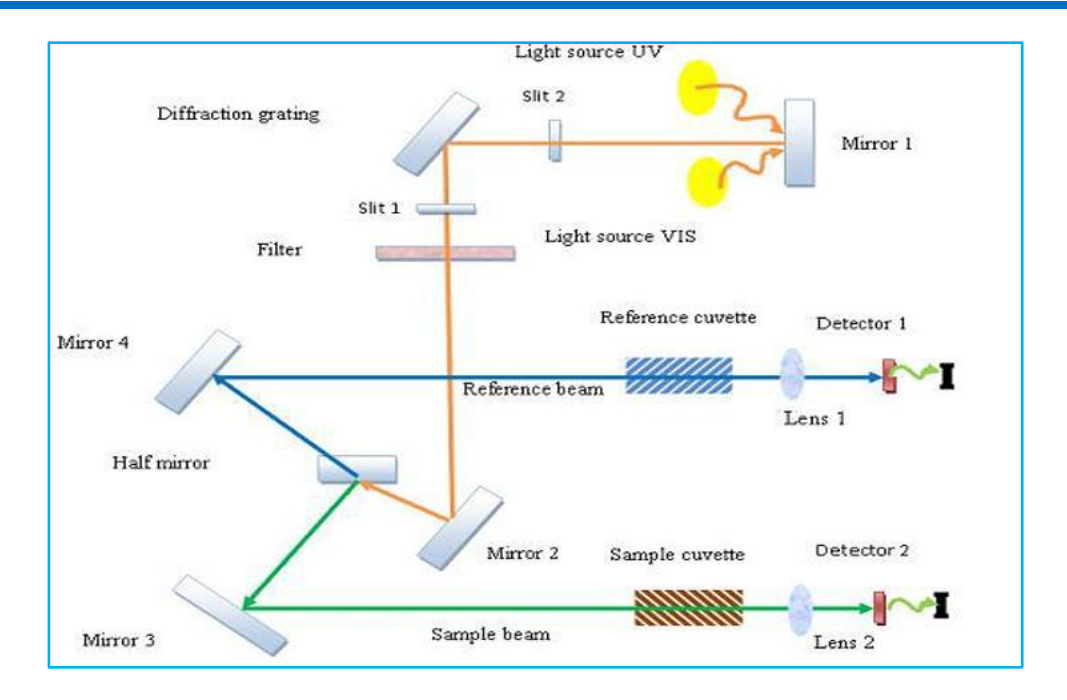


Figure II-11: The principle of operation of UV-Visible [27].

The spectral results show the variation of transmittance, expressed as a percentage T(%)in relation to the wavelength λ (nm).

Using the physical characteristics specified in Figure II-11 and the interference fringes that emerge in the transmission spectrum, we can calculate the thin layer's thickness using the following relation:

The thickness of the film d the thickness can be determined using the method proposed by Swanepoel [2].

$$d = \frac{\lambda_1 \cdot \lambda_2}{2[(\lambda_1 \cdot n_2) - (\lambda_2 \cdot n_1)]}$$
 (II-10)

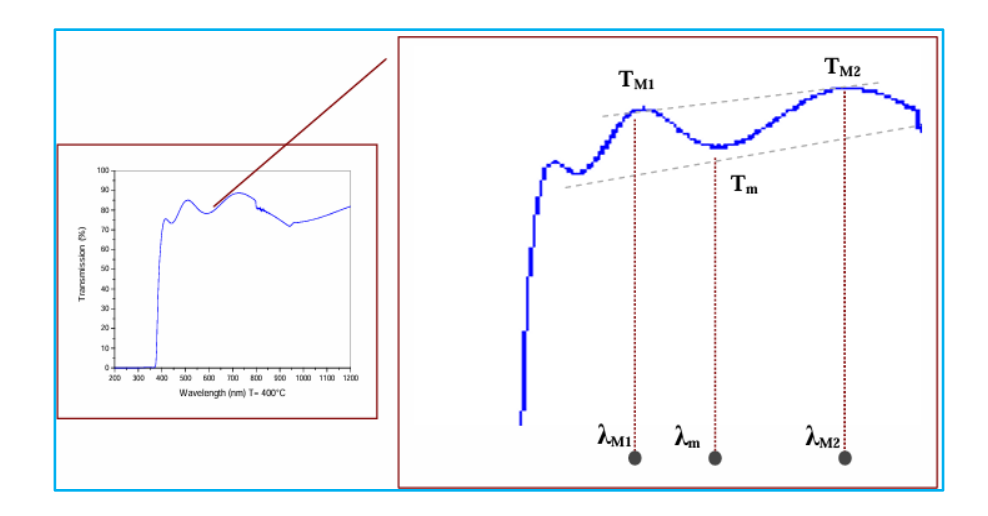


Figure II-12: determination of thickness using optical interference curves [1].

Determination of the refractive index: Where: n_1 and n_2 are the refractive indices of the film for the wavelengths λ_1 and λ_2 respectively, we can calculate n_1 and n_2 from the following relation:

$$\mathbf{n}_{1,2} = [\mathbf{N}_{1,2} + (\mathbf{N}_{1,2}^2 - \mathbf{S}^2)^{1/2}]^{1/2}$$
 (II-11)

Where: S is the refractive index of the substrate and $N_{1,2}$ can be obtained using this relation [2].

$$N_{1,2} = \frac{2.S.(T_{M1,2} - T_m)}{(T_{M1,2} - T_m)} + \frac{(S^2 + 1)}{2}$$
 (II-12)

With: $T_{M1,2}$ is the minimum transmission corresponding to $\lambda_1\lambda_2$ and T_m is the maximum transmission confined between $T_{M1,2}$ and T_m

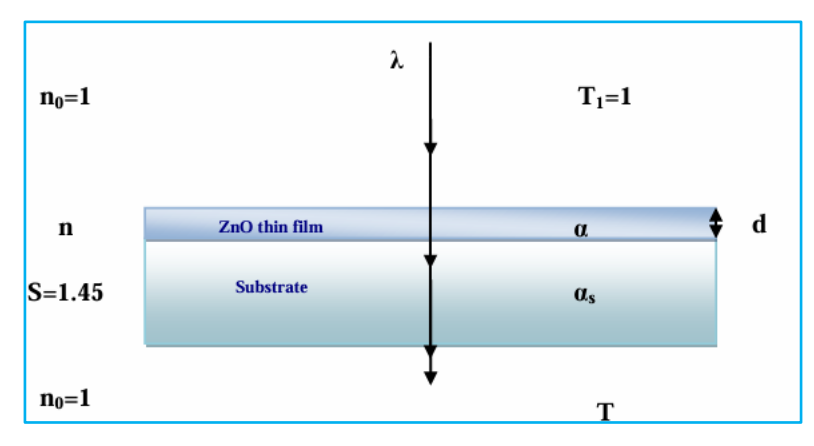


Figure II-13: Appearing from of radiation passes through the sample on a glass substrate [1].

Figure II-13 shows that **T** is the transmission, α is the film's absorption coefficient, and λ is the incoming light's wavelength [1].

II.4.2.1 absorption spectra

We may calculate the absorption coefficient for any transmission value T in (%) that corresponds to energy using the Beer-Lambert law [10].

$$T = \frac{I}{I_0} x 100 \tag{II-13}$$

 I_0 is the incidental light intensity, I the transmitted light intensity, α coefficient of absorption and d the thickness of the cell. This relation can be written [10].

$$\alpha = \frac{1}{d} \ln(\frac{I_0}{I}) \tag{II-14}$$

When T (λ) is expressed in (%), the above expression becomes

$$\alpha(cm^{-1}) = \frac{1}{d} ln(\frac{100}{T})$$
 (II-15)

II.4.2.2. Optical band gap (Eg)

The optical gap may be rapidly ascertained from the UV-Visible transmittance spectrum. Absorption occurs at high energies due to electronic transitions between broad states of the band. It is often described by tauc law [28].

$$(\alpha h \upsilon) = A(h \upsilon - Eg)^{m}$$
 (II-16)

Where:

Eg is the optical gap, m and A are constants, and hv is the photon energy. The optical type of transition is indicated by m, which can be either ½ for permitted direct transitions or 2 for permitted indirect transitions [10]. We will trace the curves $(\alpha hv) = f(hv)$ in order to ascertain the nature of the transition based on the films produced in this study. We can determine the value of Eg as shown in figure (II-14).

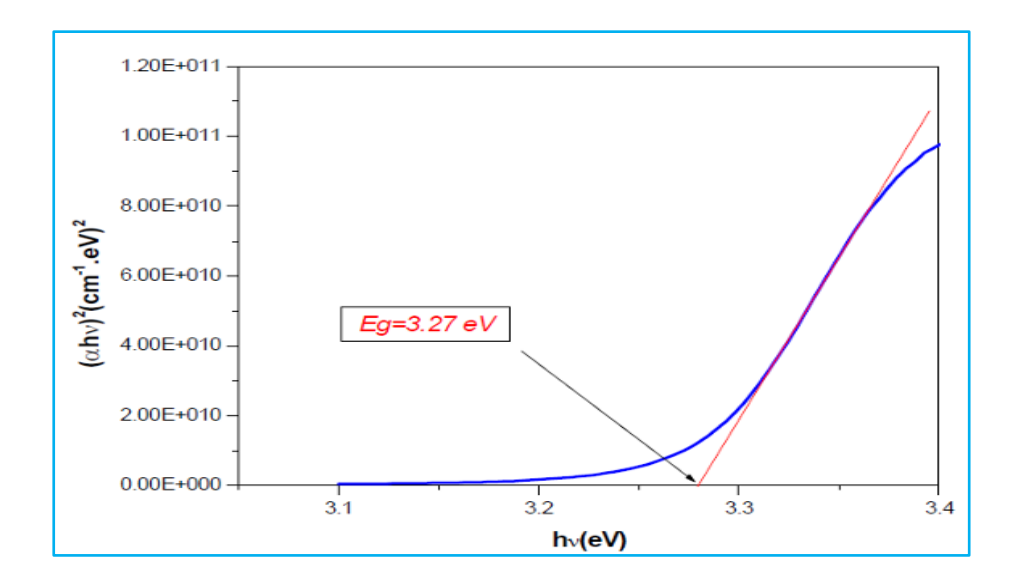


Figure II-14: Determination of the optical gap according to the Tauc method [29].

II.4.2.3. Determination of the Urbach energy

The Urbach energy is another crucial metric that describes the material's disorder. The absorption coefficient may be expressed using the Urbach law as follows [6].

$$\alpha = \alpha_0 \exp(\frac{h\upsilon}{E_0}) \tag{II-17}$$

The Urbach energy E_0 may be calculated by graphing $ln(\alpha)$ against hv.

$$\ln(\alpha) = \ln\alpha_0 + (\frac{\hbar\nu}{E_0})$$
 (II-18)

II.4.3. Electrical characterization

II.4.3.1. Four probes technique

The method is used when the sample is in the shape of a parallelogram for a delicate object, such as a thin semiconductor material deposited on a glass substrate. The sample is millimeters in size and has a thickness (w). In a straight line, the four probes are placed at the same distance (S) from each other.

Four contacts that are evenly spaced and aligned make up the probes. The voltage V is monitored across the two internal tips, and a source applies a current I through the exterior terminals. Parasitic contact resistance between the tips and the substance can be overcome using this technique. Using this method, it is demonstrated that for small sofas, the square resistance (\mathbf{R}_{Shit}) and the resistivity ($\boldsymbol{\rho}$), which are expressed in Ω and Ω .cm, respectively, are determined by the following relations [30]. For thin samples, the resistivity ($\boldsymbol{\rho}$) can be calculated using the equation:

$$R_{shit} = \frac{\pi}{\ln 2} \cdot \frac{V}{I} \tag{II-19}$$

$$\rho = \left(\frac{\pi}{\ln 2} \cdot \frac{V}{I}\right) \cdot d = R_S \cdot d \tag{II-20}$$

Where:

V:is the measured voltage between the inner probes.

I:is the applied current through the outer probes.

S:is the spacing between adjacent probes.

the four-point method is a fast and very advantageous measurement technique.

The measurement principle is schematized in Figure (II-15).

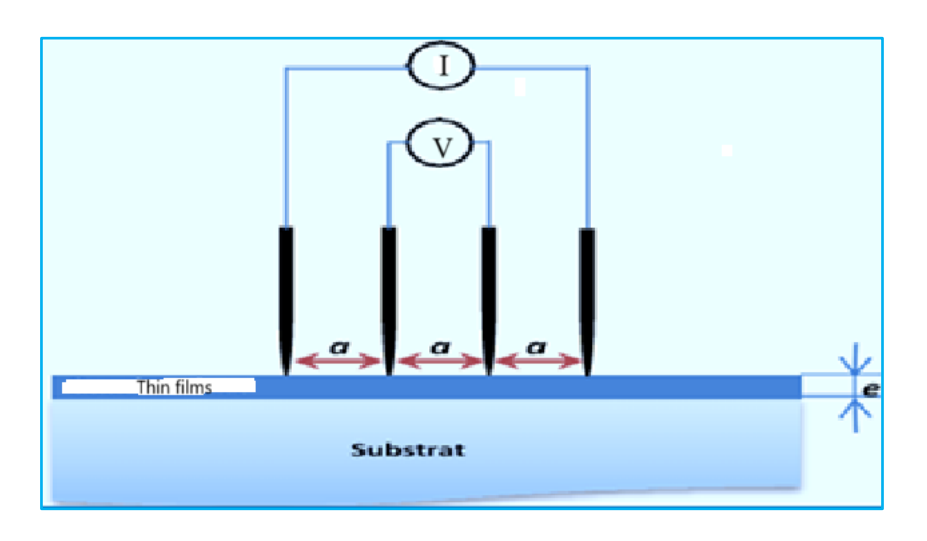


Figure II-15: Representative diagram of the principle of the four-point method [4].

The benefit of this setup over two probe studies is that it eliminates the impact of any contact resistance between the probes and the sample. These tests are likely to produce findings

Chapter IIElal	boration and chara	cterization method	ds
----------------	--------------------	--------------------	----

that are more indicative of the film's surface than its bulk because of the electrical connections that are made to the film's surface.



References

- [1] M. Othmane," Synthesis and characterization of Zinc Oxide (ZnO) Thin films deposited by spray pyrolysis for applying electronics and photonics" Doctoral Thesis, Mohamed Khider University of Biskra-Algeria, 2018.
- [2] A. Amri, "Development of ZnO-based thin films for thin-film transistors TFTs" Doctoral Thesis, Mohamed Khider University of Biskra-Algeria, 2024.
- [3] J. Phalippou," Comptes Rendus Chimie" 855–863, 2002.
- [4] M. Mekhloul, "The electrical properties and optics of ZnO nanopoudres purified and applied in Ga élaborés with the solution gel method" Mohamed Khider Univarsity of Biskra, 2021.
- [5] I. Deghiche, "Effect of solution concentration on the properties of ZnO thin films produced using the sol-gel method" Master dessertation, Mohamed Khider University of Biskra-Algeria, 2018.
- [6] R. Boudiaf, "Development and Characterization of Pure and Ga-Doped ZnO Nanopowders by Sol-Gel Method", 2019.
- [7] A. Latif, "Elaboration of pure and doped ZnO powders with the sol gel method" Doctoral Thesis, Mohamed Khider University of Biskra-Algeria, 2024.
- [8] N. Ben Amar, "Effect of catalyst concentration on the properties of ZnO thin films prepared by the sol-gel method, Masters dissertation" Mohamed Khider University of Biskra-Algeria, 2018.
- [9] L. Yang," Fabrication and characterization of microlasers by the Sol-Gel method", California institute of technology, Pasadena, California, Doctorat Thesis, USA, 2005.
- [10] H. Nezzal et N. Redjouh, "Elaboration of pure and Bi-doped ZnO nano-powders with the solgel method" Master dessertation, Mohamed Khider University of Biskra,, 2022.
- [11] Y. Bouachiba, "Contribution to the development of titanium oxide by the sol-gel process Effect of doping and experimental conditions" Doctoral thesis, 2014.

- [12] S. Guettaf Tamam et H. Hassine, "Effet number of positions on small beds of ZnO production with the sol-gel method" Mohamed Khider University of Biskra-Algeria, 2019.
- [13] L. Znaidi, "Sol-gel-deposited ZnO thin films" Materials Scienceand Engineering, vol. 174,P. 18-30, October, 2010.
- [14] L. Scriven, "Physics and Applications of Dip Coating and Spin Coating" MRS Proceedings 121, 717, 1998.
- [15] D. Hanaor,, G. Triani et C. Sorrell, "Morphology and photocatalytic activity of highly oriented mixed phase titanium dioxide thin films" Surface and Coatings Technology, vol. 205, p. 3658, 2011.
- [16] M. Dahnoun," Preparation and characterization of Titanium dioxide and Zinc oxide thin films via Sol-Gel (spin coating) technique for optoelectronic applications" Doctoral Thesis Mohamed Khider University of Biskra-Algeria, 2002.
- [17] N. Nadar, "Functionalized surfaces based on metallic nanoparticles for optics and photonics" Doctorat thesis, Jean Monnet University, Saint-Etienne, France, 2011.
- [18] A. Moustaghfir, "Development and characterization of thin zinc oxide layers. Application to the photoprotection of polycarbonate", [Online]: Available:https://tel.archives-ouvertes.fr/tel-00012168.
- [19] W. Bragg, "The structure of some crystals as indicated by their diffraction of X-rays", Series A, Containing papers of a mathematical and physical character. Proceedings of the Royal Society of London.P. 248-277, 1913.
- [20] Y. Larbah, "Elaboration and characterization of conductive and transparent thin films for TCO/ZnS/CIS type solar cells" Doctorat thesis, University of Oran-Algeria, 2011.
- [21] P. Scherrer, "Nachr Gottinger Gesell" 98, 1918.
- [22] T. Sakae, O. Hiroyuki, H. Nakada, H. Ogawa, T. Tsukioka et T. Kaneda, "X-ray micro diffraction analysis revealed the crystallite size variation in the neighboring regio small bone mass "J Hard Tissue Biol, vol. 26, n.11, p. 103-107, doi: 10.2485/jhtb.26.103, 2017.

- [23] J. Gubicza, G. Ribarik, A. Borbély et T. Ungar, "Crystallite size distribution and dislocation structure determined by diffraction profile analysis principles and practical application to cubic and hexagonal crystals research papers Crystallite size distribution and dislocation structure determined by J Appl Crystallogr, p. 298–310, 2001.
- [24] V. Mote, Y. Purushotham et B. Dole, "Williamson-Hall analysis in estimation of lattice strain in nanometer-sized ZnO particles" Journal of Theoretical and Applied Physics, vol. 6, n.11, p. 2–9, doi: 10.1186/2251-7235-6-6, 2012.
- [25] M. Touati liba, "Study of the optical and electronic properties of doped and undoped ZnO thin films development and application" Doctoral Thesis, Kasdi Merbah University of Ouargla-Algeria, 2019.
- [26] D. Mencanaglia, "Influence of hydrogen on electronic transport properties, the density and kinetics of deep states in amorphous silicon prepared by sputtering cathodic" Doctorat Thesis, Paris-France, 1987.
- [27] S. Benramache, "Elaboration and characterization of thin layers of ZnO doped with cobalt and indium" Doctorat Thesis, Mohamed Khieder University of Biskra-Algeria, 2012.
- [28] j. Tauc, "Grigorovici and A. Vancu, Phys. Status Solidi", 15, P. 627–637, 1966
- [29] H. Belkacemi, Deposition and Characterization of ZnO Thin Films with Different Zinc Sources, Doctoral Thesis, Mohamed Khider University of Biskra-Algeria, 2011.
- [30] P. Somani et S. Radhakrishnan, "Electrochromic materials and devices", Present and future, Materials Chemistry and Physics, 77. P.117-133, 2003.

Chapter: III Results and discussions

III.1. Introduction

This chapter is dedicated to the synthesis and analysis of ZnO thin films prepared on different substrates using the sol-gel method. It included the different experimental steps followed and the selection of the substrates, which play a crucial role in this experimental work. The films were deposited using the spin-coating technique. All experiments were conducted at the Laboratory of Metallic and Semiconductor Materials (LMSM) at the University of Biskra, Algeria.

The samples were characterized using X-ray diffraction (XRD) to determine the structural properties, ultraviolet-visible spectrophotometer (UV-Vis) to determine optical properties, and the four-point probe technique (I-V) for electrical properties.

III.2. Used apparatus (Spin coating)

The figure below shows an image of the spin coating device, it used for depositing thin films of pure Zinc Oxide (ZnO) on different substrates. The device is manufactured in the (MSML) Laboratory at the University of Biskra.



Figure III-1: Spin coating.

III. 3. Experimental details

III.3.1. Choice of deposition substrates

The choice of substrate type in the thin film deposition process is very important, as it affects the results and the thin film applications. This is the objective of our experimental study. Therefore, we have selected three types of substrates, including:

- Glass substrate: it is insulating, ensuring that they do not affect electrical conductivity measurements. Additionally, their high transparency is well-suited for the optical characterization of thin films in the UV-Visible spectrum. Moreover, their thermal compatibility with the deposited ZnO material, estimated at ($\alpha_{glass} = 3.3 \times 10^{-6} K^{-1}$), helps reduce stress at the films/substrate interface [1].
- Monocrystalline silicon substrate: It is a semiconductor and the most commonly used as a light-sensitive material in photovoltaic solar cell systems. It is characterized by a high industrial quality, low slip density, and thermal conductivity. Additionally, thin layers of Zinc Oxide (ZnO) can enhance the mechanical stability of porous silicon [2].
- Tin-doped indium oxide (ITO): It is the third substrate choice. It exhibits very high electrical conductivity (similar to a metal) and high optical transparency (> 80 %) in the visible region [3], and high reflectivity in the infrared region. Thanks to this unusual combination of optical and electrical properties, this material is widely used in optoelectronic devices. These properties are combined in a single material, which explains its wide range of applications and diverse production methods [4].

III.3.2. Cleaning of the substrate

The adherence and the quality of the deposit are based on the purity and state of the substrate; thus, the cleaning of the substrate is one of the most important steps. The cleaning protocol is as follows [1].

- The substrates are cut using a pen with a diamond point.
- Cleaning with the soap solution.
- > Rinsing with the water distilled.
- > Rinsing with acetone for 5 min.
- ➤ Rinsing with distilled water.
- Rising with Ethanol during 5 min at ambient temperature.
- Cleaning in the water-distilled bath.

Finally, the substrates are dried using a dryer.

The different steps of cleaning are realized in an ultrasonic bath with different solution.

III.3.3. Preparation of Zinc Oxide

Zinc acetate dehydrate (Zn, (CH₃COO)₂, 2H₂O), Ethanol (C₂H₅OH) 10 ml and Diethanolamine (NH (CH₂CH₂OH)₂) were used as precursor, solvent, and stabilizer, respectively. Zinc acetate was first dissolved in Ethanol, and the two compounds were mixed for 10 min. When the solution turned milky, Diethanolamine was added, and then the resulting mixture was stirred at 60°C for tg time: 30 and 60 min to yield a clear and homogeneous solution. The molar ratio of DEA to Zinc acetate was fixed at 0,5 M. The solution is used after aging at room temperature for more than 24 hours.

The films were deposited on different substrates by spin coating at room temperature with a rate of 1000 rpm for 30 s. After each deposition, the deposited layers were dried in ambient atmosphere at 500°C in a furnace for 30 min to evaporate the solvent and remove the organic component in the film.

The coating and drying procedures were repeated seven times to increase the film thickness.

Finally, the film were annealed in ambient atmosphere at 500°C because there is a risk of a possible thermal fusion. The figure III-3 shows the process for preparing ZnO sol-gel and thin film.

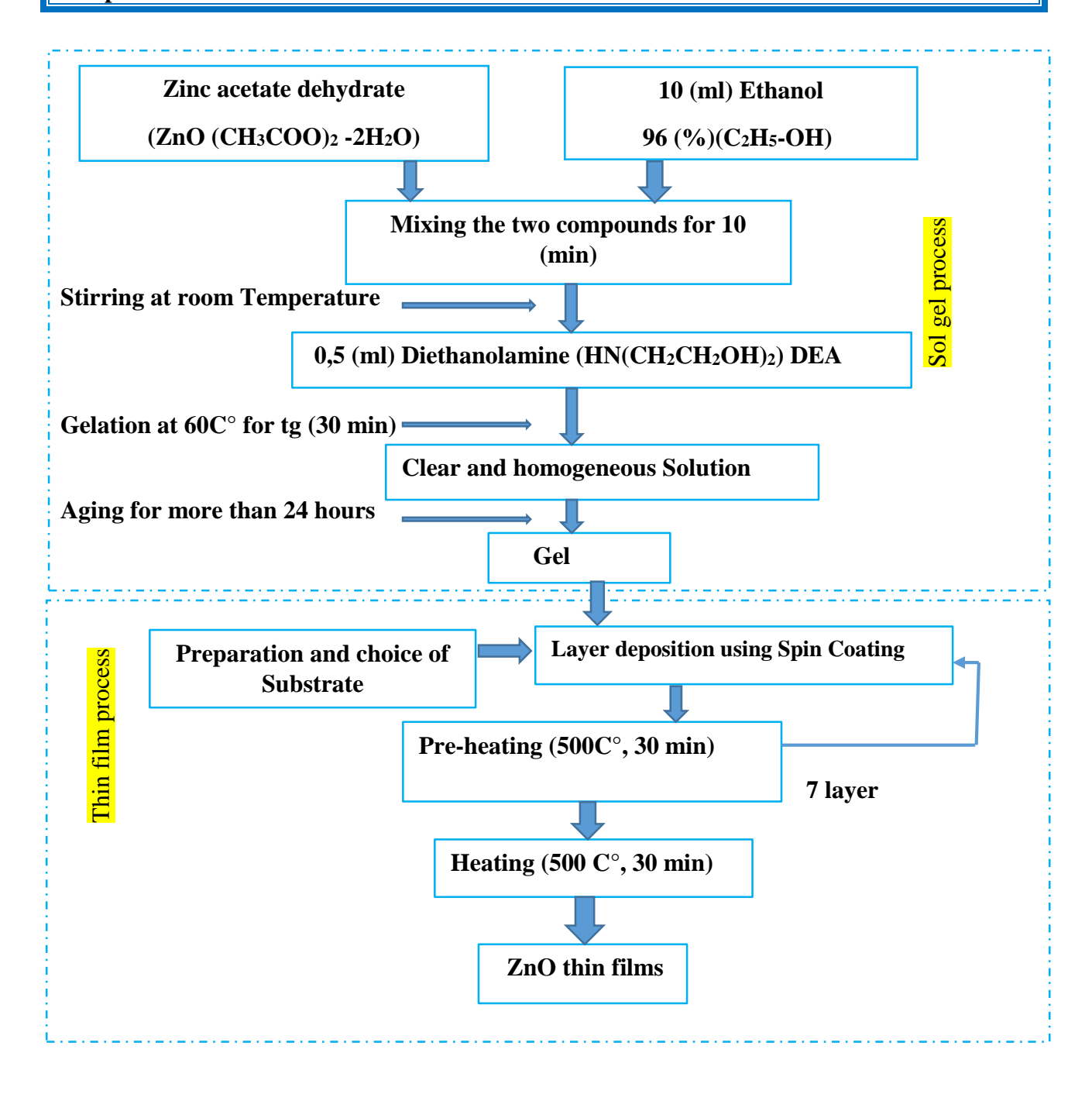


Figure III-2: Flow chart of sol-gel method for preparation of ZnO thin films.

III.3.4. Drying and heat treatment of Thin Films

After the deposition process, drying and heat treatment stages were followed to densify the thin films. These two stages are essential to achieving high-quality results [5].

Thin films are typically semi-crystalline after the drying process. Therefore, they must undergo a subsequent thermal treatment in a high-temperature furnace to promote crystallization, figure III-3 as all applications of these materials depend on their crystalline properties.

During the experimental work, thin films have been dried in the same furnace used for thermal treatment after each deposited layer for 30 min at a temperature of 500°C to evaporate all solvents. Finally, the films, all the layers deposited, have undergone annealing treatment for 30 min at a constant temperature of 500 °C to obtain a crystalline material suitable for characterization.



Figure III-3: Furnace for Heat Treatment.

III.3.5. Adhesion quality test

The term adhesion refers to the interaction between closely adjacent surfaces of neighboring objects, such as films and a substrate. According to the American Society for Testing and Materials (ASTM), adhesion is defined as the state in which two surfaces are held together by valence forces, mechanical interlocking, or both. Adhesion to the substrate is undoubtedly the primary characteristic that a thin film must possess before any of its other properties can be utilized.

To test the adhesion of the films or coating to the substrate, a tape is applied to the film's surface and then pulled back. This test is subjective and depends on the type, the pulling speed, and the pulling angle [6]. Figure III-4 illustrates the method for testing adhesion quality.

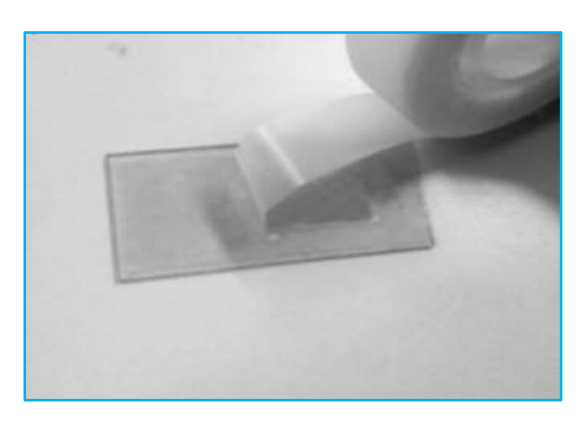


Figure III-4: Adhesion force test.

The test results on the prepared ZnO thin layers showed good adhesion strength to all types of substrates.

III.4. Results and discussion

III.4.1. Structural characterization

III.4.1.1. X-ray diffraction

The XRD diffractograms were obtained using a Rigaku diffractometer with $Cuk\alpha 1$ radiation ($\lambda = 1.5405$ Å) was used over a 20 range from 25° to 80. The information that can be drawn from them, are presented below. Indeed, and as already mentioned in (chapter II), the diffractograms allow us to determine the reticular planes and the structure of the coating as well as the crystal lattice of the grains of the coating formed and this for the different experimental conditions considered for this, the calculations are carried out using equations (II-6, II-7, II-9) [7].

III.4.1.2. Analysis of X-ray spectra

From the X-ray spectra, the state of the films can be determined. These spectra show that the samples are polycrystalline with different orientations. The comparison of the diffraction measurements (XRD) with the ASTM data sheet (American Society for Testing and Materials) provides information about the sample nature, crystal quality, crystalline parameters, and orientation (Figure III-5).

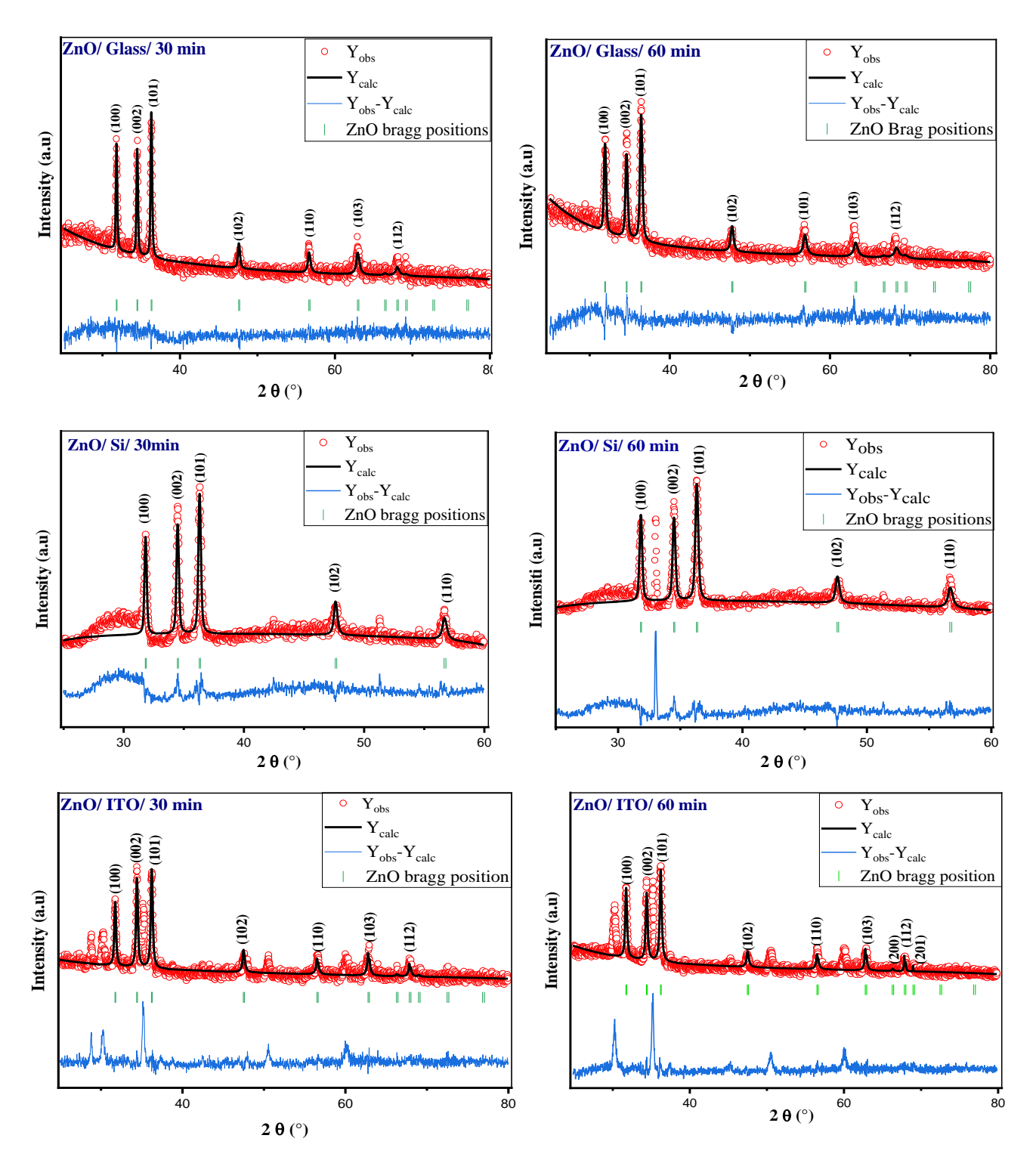


Figure III-5: X-ray diffraction ZnO elaborate on different substrates for tg of 30 and 60 min

This paragraph presents the influence of the substrate on the pure ZnO films. X-ray diffraction patterns were recorded for annealed ZnO thin films deposited [8]. On different substrates: glass, p-type silicon, and ITO.

The comparison of the X-ray diffraction patterns with the JCPDS data [98-006-5119] confirms that all samples grown on three substrates and elaborated with the Sol-Gel method are ZnO crystal crystallized in a hexagonal wurtzite structure [9].

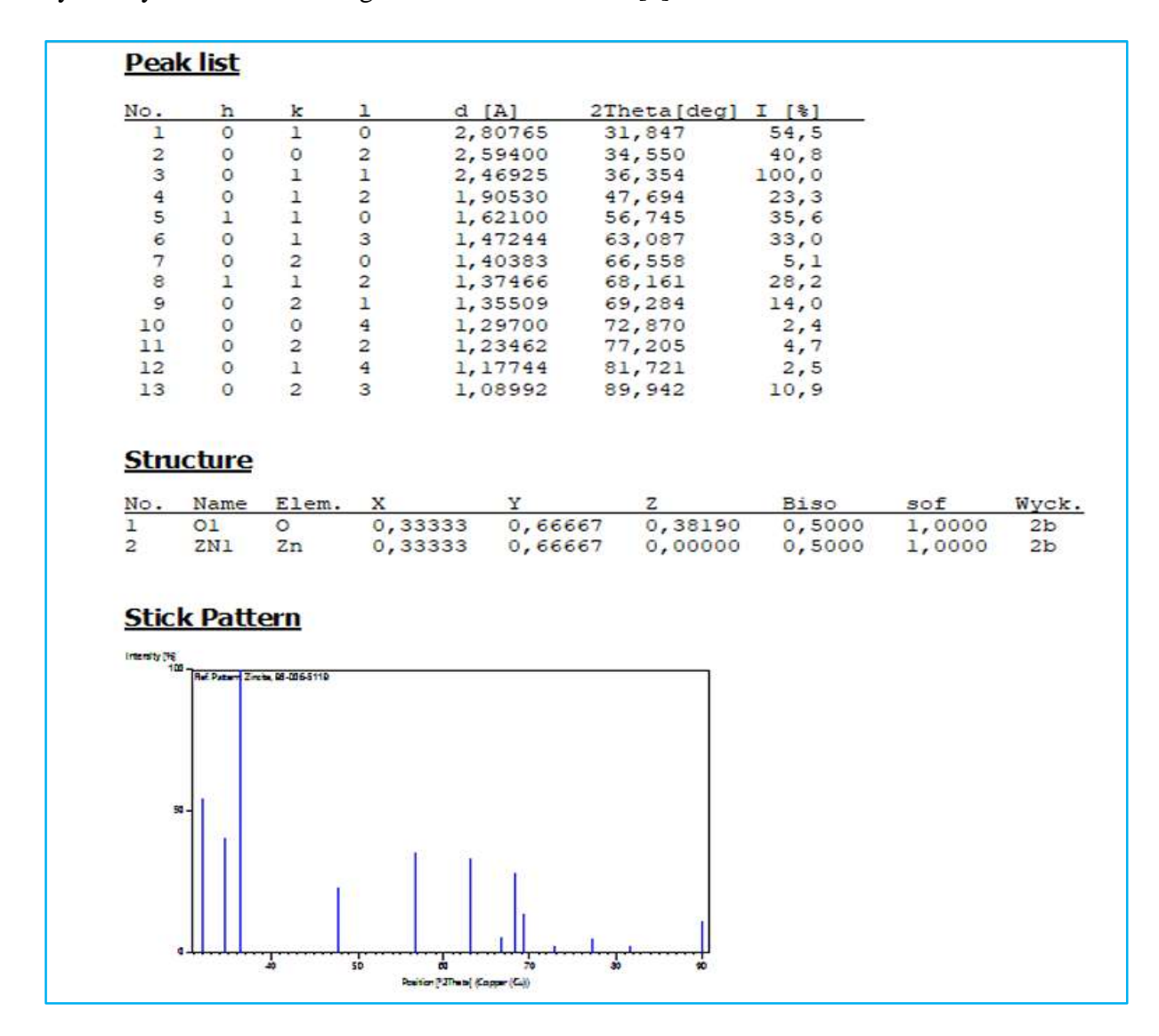


Figure III-6: X-ray diffractograms of ZnO [98-006-5119] from the FASTM file.

All sample patterns on different substrates have been recorded three main crystalline orientations (100), (002), and (101). These three main orientation have been found in previous studies [10, 11].

The crystallinity of ZnO films was determined from the Full width at Half Maximum (FWHM) values of the diffraction peaks corresponding to the (100), (002), and (101) planes, which are highly intense peaks.

The diffraction peaks observed (100), (101), (002), (102) and (110) are characteristic of a polycrystalline ZnO hexagonal wurtzite structure. The dominant growth plane for all samples is (002). This later confirm that the preferential orientation is along the c-axis. The results align with previous studies [12].

In addition, weak intensity peaks corresponding to (102), (110), (103) and (112) planes are observed for the samples elaborated on glass and p-type Si substrates. For the ITO substrates, weak intensity peaks have been recorded just for (103) and (112). These results confirm a relative variation between the substrates on which the films are deposited.

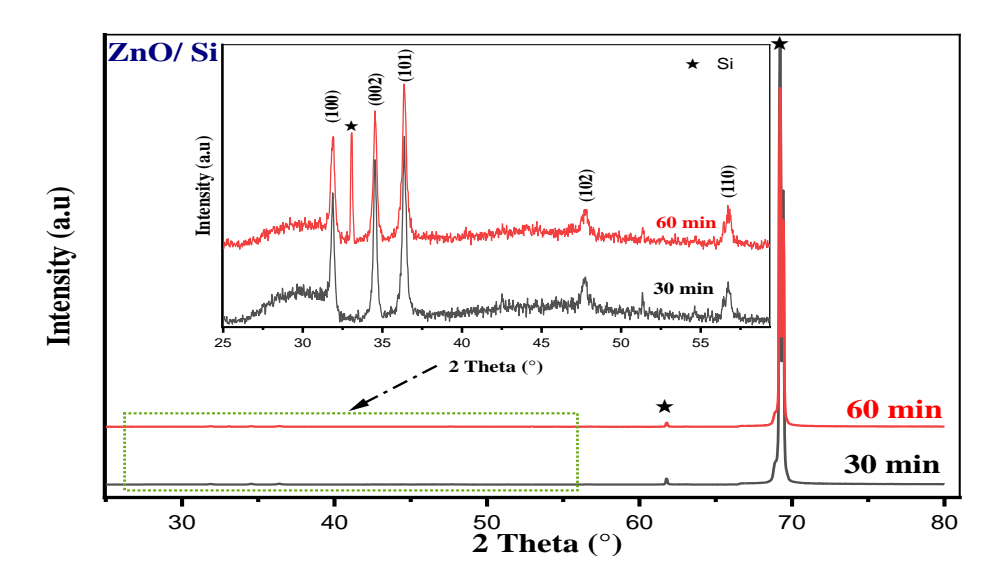


Figure III-7: X-ray diffraction patterns of ZnO thin films grown on p-type silicon substrate.

In the case of silicon substrate, it has been recorded a high peak noticed by (*) in the figure III-7, this later is the peak (400) of silicon structure as shown by Haneen D. Jabbar [13].

The zoom figure shows the spectra of ZnO thin films grown on Si substrate for time of gelation 30 and 60 min. Also, it remarked a peak designed by (*), it is also another (200) peak of p-type Si.

As it has been said above, the silicon substrates show a high crystallinity quality along the orientations (001), (002) and (111).

The swing curve profiles of the silicon P-type substrate crystal planes were presented with a diffraction resolution of approximately 0.003° . By rotating the Si (001) sample in its plane, it was possible to suppress the symmetric (θ , 2 θ) scans, which could have partially overlap with the ZnO (002) reflections and complicate the pattern analysis [2].

The preferential orientation of ZnO thin films deposited on substrates of different natures is influenced by the chemistry of the precursor material, thermal treatment procedures, and the preparation time of the deposited solutions. These factors strongly affected the preferred orientation of pure ZnO films in the present work. The experimental conditions appear to be more favorable for high growth along the C-axis direction on the P-type silicon substrate, compared to glass and ITO substrates.

Rietveld refinement was performed using the Full-prof program for undoped zinc oxide samples, using different substrates including glass, p-type silicon, and indium tin oxide (ITO) substrates. The small red cycles and the black straight lines show experimental and calculated levels of data, respectively. The profile graph shows the difference between the actual and predicted levels. Every design has its Bragg position shown above it. The results revealed that the actual and estimated standards were very similar, which means the structures and the starting factors are right.

The Rietveld XRD analysis of the (ZnO) sample confirms that it has a hexagonal wurtzite structure and is in the P63mc. The figure III-8 illustrates the three-dimensional hexagonal crystal structure of ZnO realized through Vesta software.

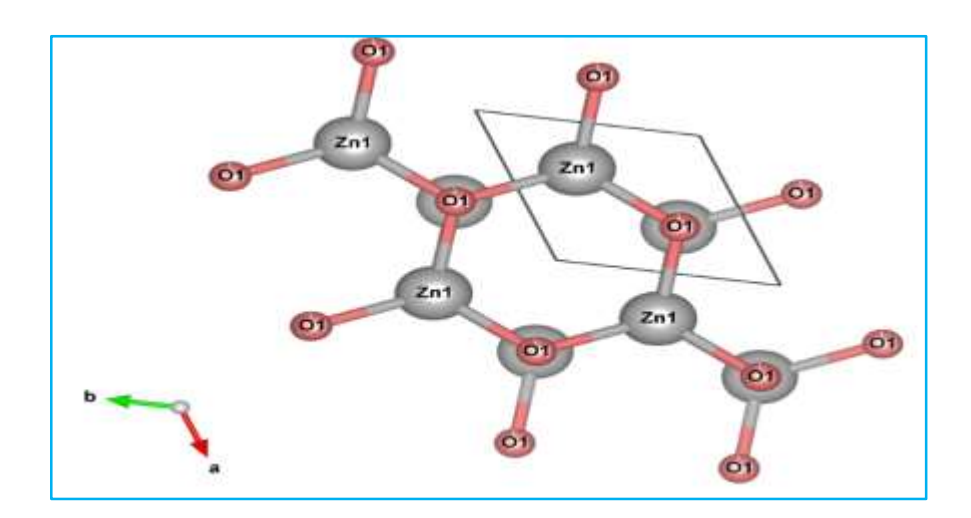


Figure III-8: Hexagonal crystal Structure of ZnO.

III.4.1.3. Determination of grain size

Williamson-Hall plots are used to analyze X-ray diffraction (XRD) data to determine both internal strain and crystalline grain size (**D**) in nanomaterials and crystalline substances. This type of analysis is useful in studying the effects of heat treatment, deformation, or crystal size reduction

on the material. The method is based on the relationship between the full width at half maximum (**FWHM**) and the reflection angle (θ), combining the effects of size and strain [14].

By rearranging the above equation, we get.

$$\beta_{hkl}\cos\theta_{hkl} = \frac{K.\lambda}{D} + 4\varepsilon\sin\theta_{hkl}$$
 (III-1)

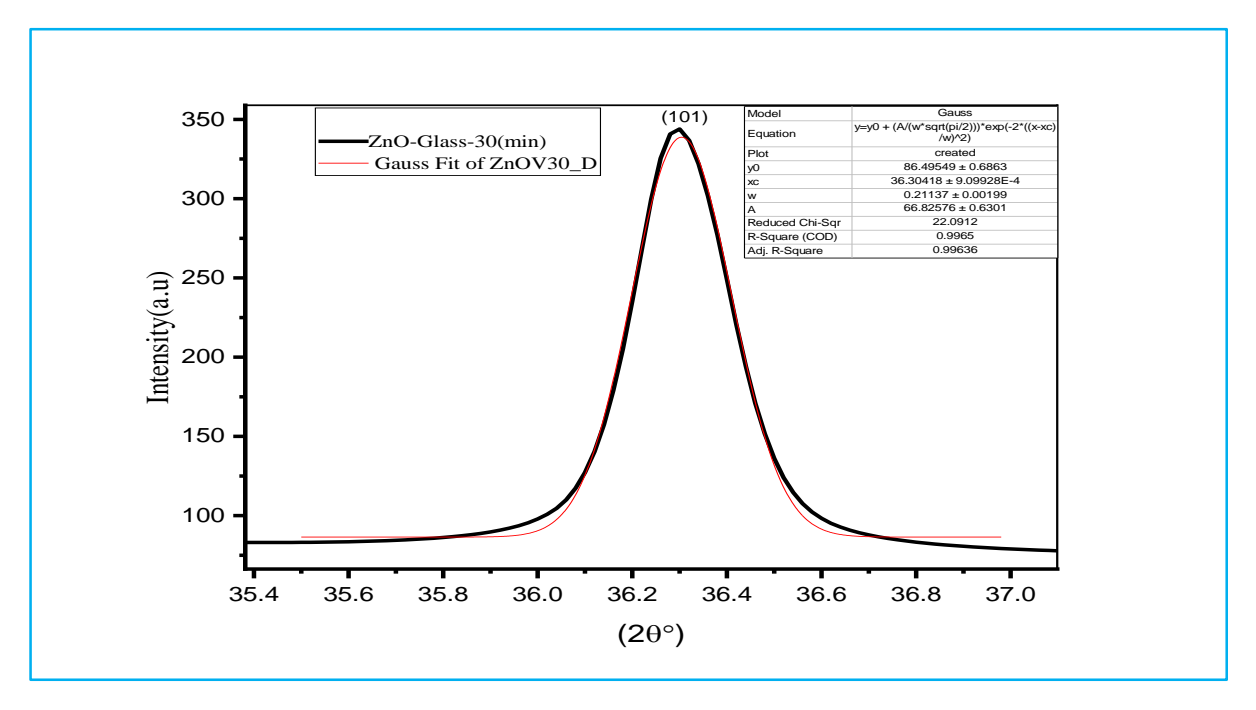


Figure III-9: Gaussian extrapolation of the (101) peak shows the full width at half maximum and the position of the peak.

The half-width β and the peak position (20) are determined using the 'Origin 2018-64 bit' software by applying Gaussian extrapolation to the curve as shown in the figure below.

Based on the figure III-9, we have:

$$2\theta$$
 (101) = X_c = 36,30418°.

$$\beta_{hkl} = FWHM = 0.21137^{\circ}$$
.

The above equations are W-H equations. A plot is drawn with 4 sin θ along the x-axis and β_{hkl} cos θ along the y-axis for as-prepared ZnO nanoparticles.

From the linear fit to the data, the crystalline size was estimated from the y intercept, and the strain (ε) from the slope of the fit, where the strain was assumed to be uniform in all crystallographic directions, thus considering the isotropic nature of the crystal, where the material properties are independent of the direction along which they are measured [15]. The Williamson-Hall plot for ZnO nanoparticles is shown in (figure III-10).

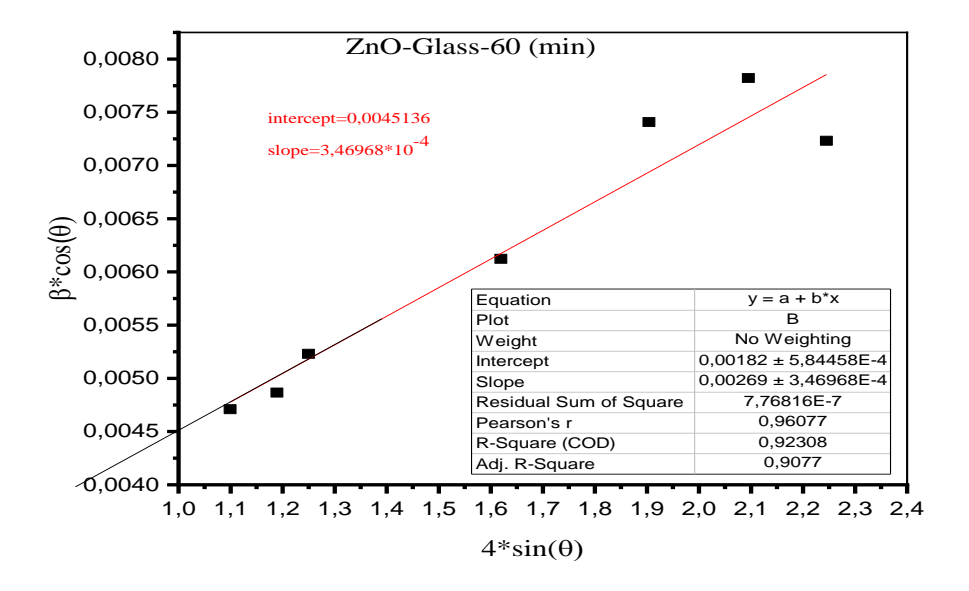


Figure III-10: Williamson-Hall plot for thin films of Zinc Oxide.

The samples are exposed to X-ray emitted by Copper $K\alpha$ radiation with a wavelength λ =1.5406 A° By recording the diffraction intensity as a function of the incident angle, we can determine whether the material is crystalline or amorphous [16]. It is possible, based on the diffraction spectra, to measure the full width at half maximum of the diffraction peaks to determine the grain size [17].

By applying Williamson-Hall equation to all the observed peaks, the grain size is found 30,3656 nm. To calculate the average crystallite size of thin films deposited on different substrates using the Scherrer equation II-8 [9].

A dislocation is known as a crystallographic defect or irregularity in a crystal structure. Its presence inside the crystallite structure strongly affects many of the properties of materials. Using the values of grain size, the dislocation density (δ) is defined as the number of dislocation lines per unit volume of the crystal, and it has been calculated depending on the Williamson and Stallman's.

$$\delta = \frac{1}{D^2} \tag{III-2}$$

The values of dislocations and strains within the crystal structure of ZnO thin films vary with the substrates grown on, where they are subjected to stresses due to differences in lattice constants or thermal expansion coefficients that change depending on the type of substrate.

A decrease in these values indicates a more ordered and purer crystal structure, which is important for electronic and optical applications.

III.4.1.3.1. Effect of substrates on Zinc Oxide thin films.

III.4.1.3.1.a. Variation of crystallin parameters with substrates grown on

Table III-1 shows the results of variation of crystallin parameters \mathbf{a} , \mathbf{c} , and the volume V for thin films deposited on glass, p-type silicon and ITO substrates grown for gelation time tg = 60min [18].

The Pseudo-Voigt peak function was utilized to refine various parameters. The obtained refined parameters, such as three lattice parameters (**a**, **b**, and **c**), and the unit cell volume, as shown in the table III-1, We observe that the lattice parameters (**a**, **b**, and **c**) of all the produced samples closely match the standard values for ZnO [JCPDS data: 98-006-5119].

The results show a variation of crystallin parameters with substrates grown on. The p-type silicon substrate appears to have values nearest to those of ZnO FASTM. This result can be explaining by the crystallin properties of p-type Si. As a consequence, the p-type silicone is the more stable substrate for growing the ZnO thin films.

Table III-1: Structural parameters values of ZnO thin films grown on different substrates with gelation time tg = 60min.

Sample	Gelification Time	a=b (Å)	c (Å)	V (Å) ³	c/a
ZnO-Glass	60 (min)	3,2373	5,1839	47,0492	1,6013
ZnO-Silicon	60 (min)	3,2460	5,2000	47, 4494	1,6019
ZnO-ITO	60 (min)	3,2550	5,2131	47, 8331	1,6015
ZnO (ASTM)		3,2420	5,1880	47,22	1,6002

The Table III-1 presents the lattice parameters of ZnO thin films. It is evident that the values of **a**, **c**, and the unit cell volume vary from the values of ZnO of FASTM. For the ZnO films grown on glass, the parameters **a** and **c** show a little decrease compared to ZnO FASTM, that means

there is a compression of the unit cell. This result is obtained by D. Aryanto et al [24]. However, the films grown on ITO substrates, present an increase in these parameters, which means there is a stretched of the unit cell.

On the other hand, we observed a similarity between the lattice parameters of zinc oxide grown on P-Si substrates and those reported in the FASTM, which leads to a reduction in the level of lattice strain and the defects resulting from the significant mismatch in lattice parameters. This confirms that the materials used as substrates for zinc oxide thin films play a crucial role in the deposition process. Figure III-11 illustrates the differences in the lattice parameters of zinc oxide with substrates grown on, and a comparison with the ZnO FASTM data [98-006-5119].

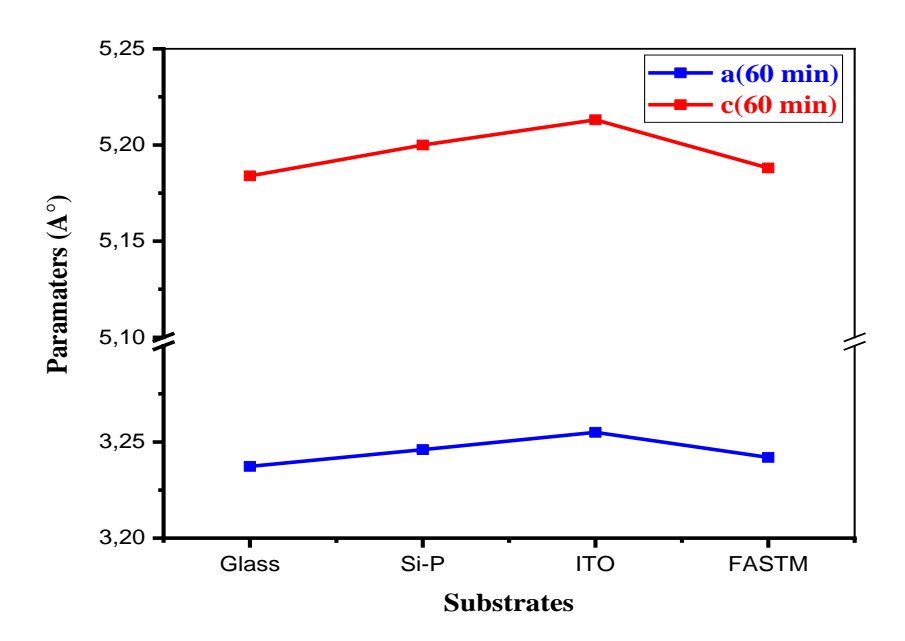


Figure III-11: Changes in the values of a and c as a function of substrates and FASTM.

III.4.1.3.1.b Variation of grain size with substrates grown on

Table III-2 shows the variation of grain size, micro strains (ϵ), and dislocation densities (δ) for ZnO thin films deposited on different substrates, with gelation time tg = 60 min [18]. A little grain size has been recorded for ZnO thin films grown on glass substrate (30,3656 nm). The same value has been found in literature [10]. A little value of strain has been recorded for ZnO thin films grown on p-type silicon substrate, which enhanced the result above and confirms that p-type silicon substrate is more suitable for ZnO thin films grown.

Table III-2: Grain size, micro strains (ϵ), and dislocation densities (δ) of ZnO thin films grown on different substrates with gelation time tg = 60 min.

Sample	Gelification Time	D (nm)	ε (x 10 ⁻⁴)	δ x 10 ⁻⁴ (nm ⁻²)
ZnO-Glass	60 (min)	30,3656	3,4696	10,845
ZnO-Silicon	60 (min)	40,2738	1,1553	6,1652
ZnO-ITO	60 (min)	37,3596	6,7494	7,1646

The figure III-12 shows a variation in grain size (\mathbf{D}) and dislocation density($\mathbf{\delta}$) values. The smallest grain size of the deposited ZnO is observed on glass substrates, while the lowest dislocation density is recorded on Si-P substrates. This result confirms the lower strain in the films grown on p-type Si substrate, and indicates a lower density of crystal defects in the ZnO, as a result a high growth on this p-type Si substrate.

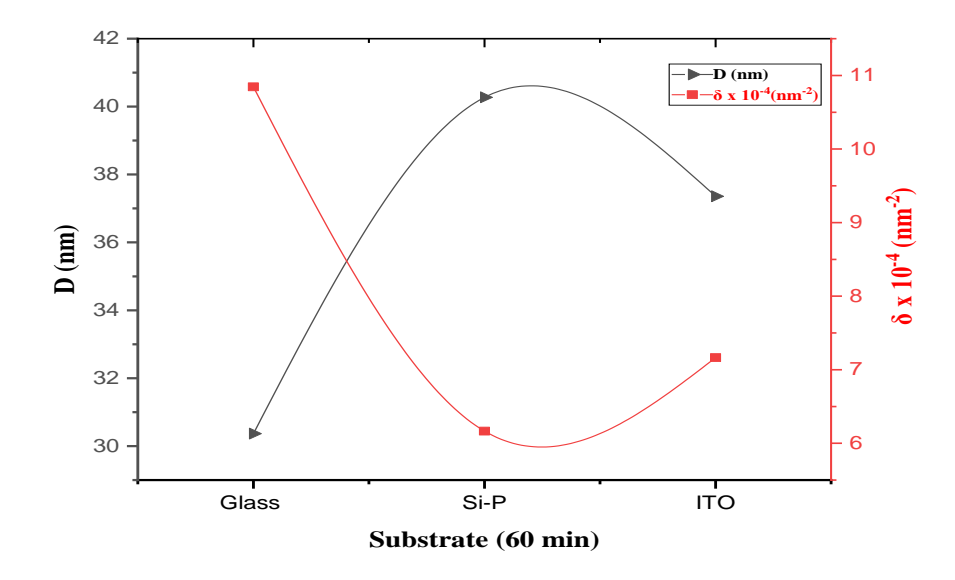


Figure III-12: Changes in grain size and dislocations as a function of Substrate.

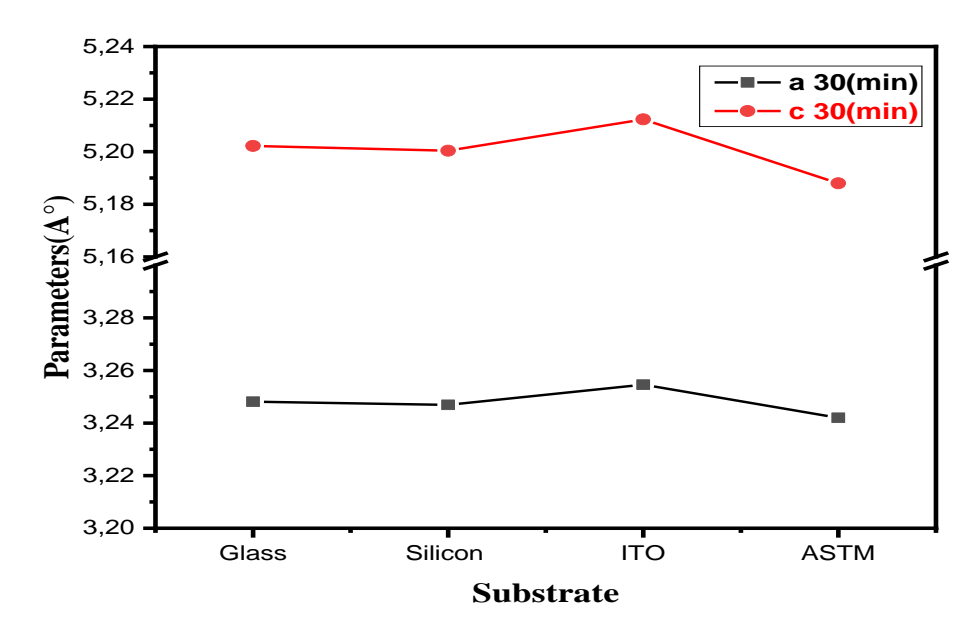
III.4.1.3.2. Effect of gelation time on Zinc Oxide thin films

Table III-3: Structural parameters values of ZnO thin films grown on different substrates with gelation time tg = 30 and 60 min.

Sample	Gelification Time	a=b (Å)	c (Å)	c/a	V (Å) ³
ZnO-Glass	30 (min)	3,2481	5,2022	1,6016	47,5309
	60 (min)	3,2373	5,1839	1,6013	47,0492
ZnO-Silicon	30 (min)	3,2469	5,2004	1,6016	47, 4794
	60 (min)	3,2460	5,2000	1,6019	47, 4494
ZnO-ITO	30 (min)	3,2546	5,2123	1,6015	47, 8140
	60 (min)	3,2550	5,2131	1,6015	47, 8331
ZnO ASTM		3,2420	5,1880	1,6002	47,22

Figure III-13 and Figure III-14 gives a clear image about the variation of **a** and **c** with gelation time (**tg**), this later affect especially the films elaborated on glass substrate, there is differences between film elaborated at 30 min and 60 min.

The comparison with the value of ZnO ASTM shows that films elaborated on Si-P at 60 min are more closes to the value of ZnO FASTM. It can be conclude this film are more stable which confirmed by the lower value of strain ($\varepsilon = 1,1553 \times 10^{-4}$).



FigureIII-13: Variation of parameters a and c with substrate at gelation time tg = 30 min.

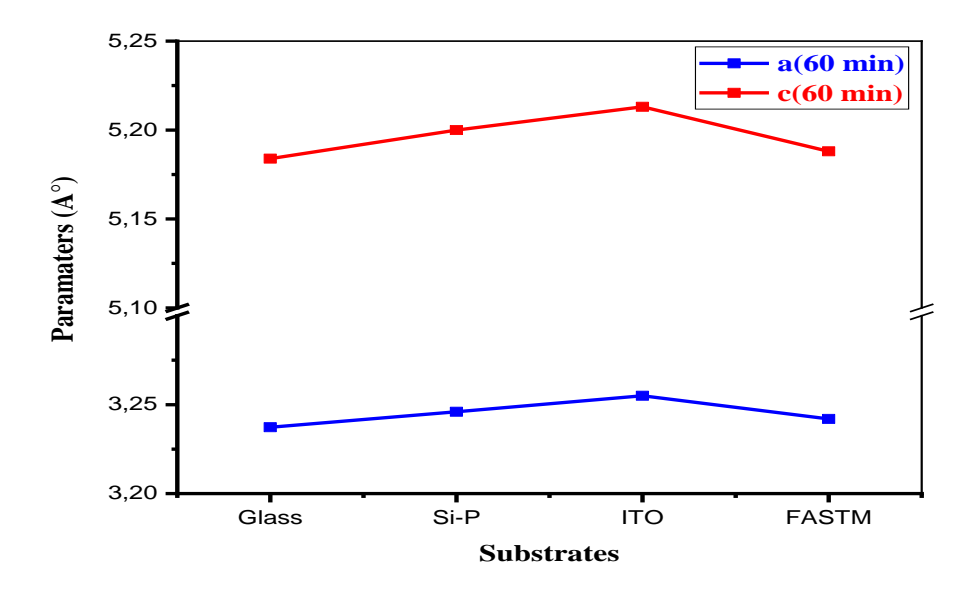


Figure III-14: Changes in the values of a and c as a function of substrates and FASTM at gelation time tg=60 min.

Table III-4: Structural parameters of ZnO thin films.

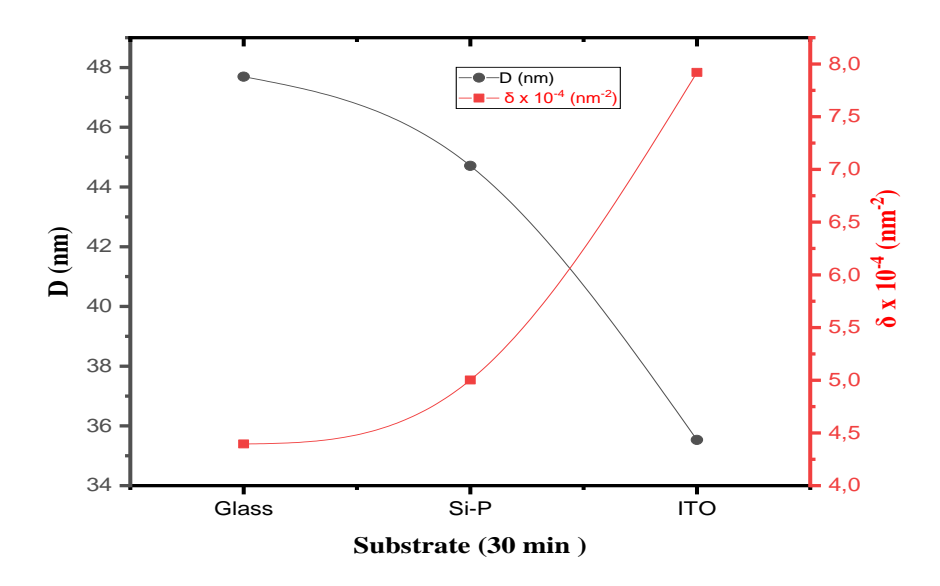
Sample	Gelification Time	D (nm)	ε (x 10 ⁻⁴)	δ x 10 ⁻⁴ (nm ⁻²)
ZnO-Glass	30 (min)	47,6956	2,7278	4,3958
Ziio-Giuss	60 (min)	30,3656	3,4696	10,845
ZnO-silicon	30 (min)	44,7091	1,1793	5,0027
	60 (min)	40,2738	1,1553	6,1652
ZnO-ITO	30 (min)	35,5314	2,3030	7,9209
	60 (min)	37,3596	6,7494	7,1646

The thin ZnO Oxide films deposited on Si-P substrates appear to be of higher quality and better adhesion to the substrates, this result is confirmed by the lower values of strain, as evidenced by the appearance of multiple crystal planes that indicate a good lattice match between the substrate and the ZnO thin films.

Unmodified Zinc Oxide nanoparticle samples were analyzed and showed a wurtzite structure with hexagonal shapes. The sample was crystallized in a furnace at a temperature of 500°C, confirming the formation of crystalline anaphases.

According to the X-ray diffraction (XRD) data, different grain sizes of zinc oxide grown on various substrates were observed. The values presented in the Table III-4 indicate that the smallest grain sizes were obtained on glass and ITO substrates, which leads to a significant increase in dislocation density. In contrast, larger grain sizes were observed on silicon substrates, resulting in a considerable reduction in both dislocation density and lattice strain.

The lattice strain and dislocation density varies with the substrate type. This leads to lattice parameters variation during the growth processing and reducing the driving force for growth. Moreover, lattice mismatch contributed to increased strain. The crystallite size of ZnO thin films decreases with changes in the substrate type, which may, be attributed to internal stresses and defects within the thin films layer, particularly dislocation density as shown in Figure III-15.



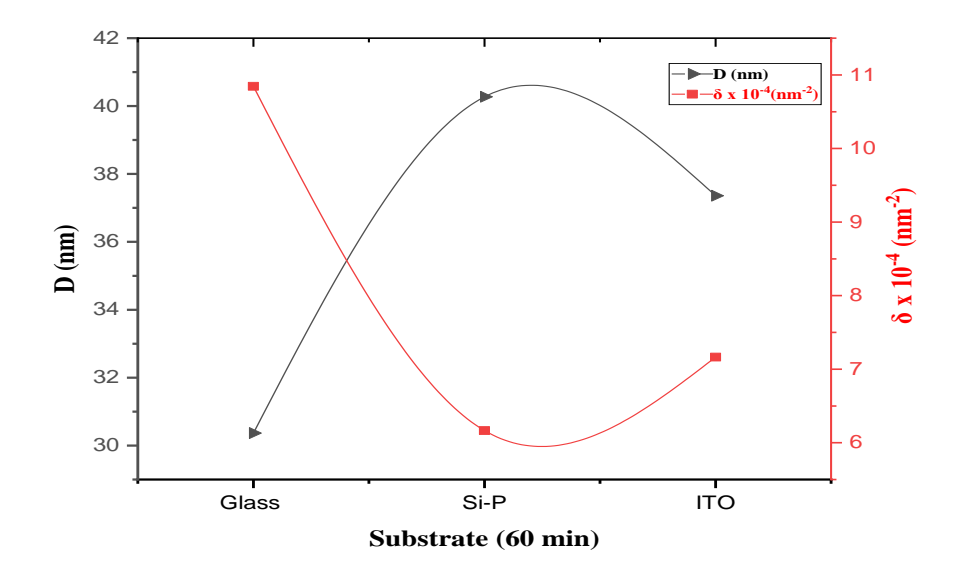


Figure III-15: Variations in grain size and dislocation values as a function of the substrates on which they are deposited.

As a conclusion, the substrates influence the size of ZnO thin films by causing either shrinkage or elongation of the grain size, which in turn affects the lattice dimensions of the undoped ZnO films. The figure III-15 illustrates the variations in grain size and dislocation density for all substrates on which the films were deposited at the gelation time of 30 and 60 min

III.4.2. Optical characterization

III.4.2.1. UV-visible

The optical characterization of pure ZnO thin films was carried out using ultraviolet-visible (UV-Vis) spectrophotometer (EVOLUTION 220), which covers a spectral range from 200 nm to 1100 nm, as shown in the (figure III-16) [5].



Figure III-16: UV-VIS Spectrophotometer (EVOLUTION 220)

III.4.2.1.1. Transmittance

The optical properties, such as transmittance, ware studied though the analysis of UV-Visible patterns for undoped Zinc Oxide (ZnO) thin films in the wavelength range of 350 to 800 nm, as shown in Figure III-16.

Transmission spectra were obtained for the ZnO films deposited on glass and ITO substrates. Results indicate that all films were highly transparent in the visible range (400-800 nm). The spectra were taken using an empty substrate as the optical reference. Figure III-17 shows the spectra of optical transmission (T%) of ZnO films grown on different substrates. The average transmittance for all films is ≥ 90 % in the visible range (400-800 nm). The spectra also appear that all films have fringes that appear as small curvature of the transmittance between on the absorption edge wavelength 290 nm to 350 nm. The appearance of this latter due to two or may be three phenomena [19].

- The thickness effects.
- The light scattering due to the difference of the quality of the layer surface.
- Grain size.

III.4.2.1.1.1. Effect of substrates on Zinc Oxide thin films

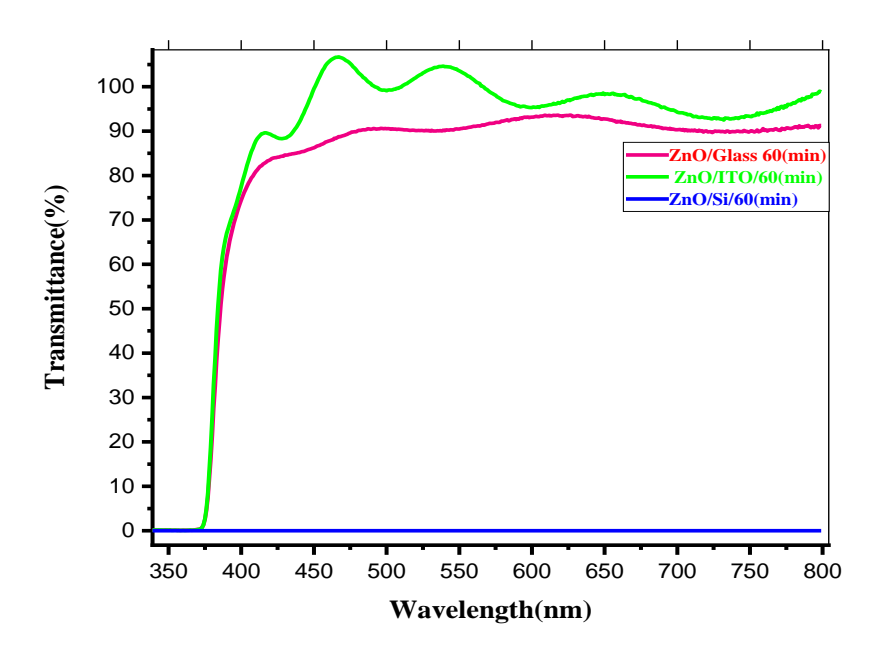


Figure III-17: Optical transmittance spectra of ZnO thin films prepared on glass and ITO and Si-P substrate.

Figure III-17 shows the variation of the transmittance of ZnO thin films elaborated on glass, ITO and p-type silicon substrates. High transmittance has been recorded for ITO substrate with the appearance of the fringes.

The ZnO thin films prepared on p-type silicon show a 0% optical transmission since the silicon substrate is opaque and does not transmit in the UV-Vis range.

III.4.2.1.1.2. The Effect of gelation time on ZnO thin films

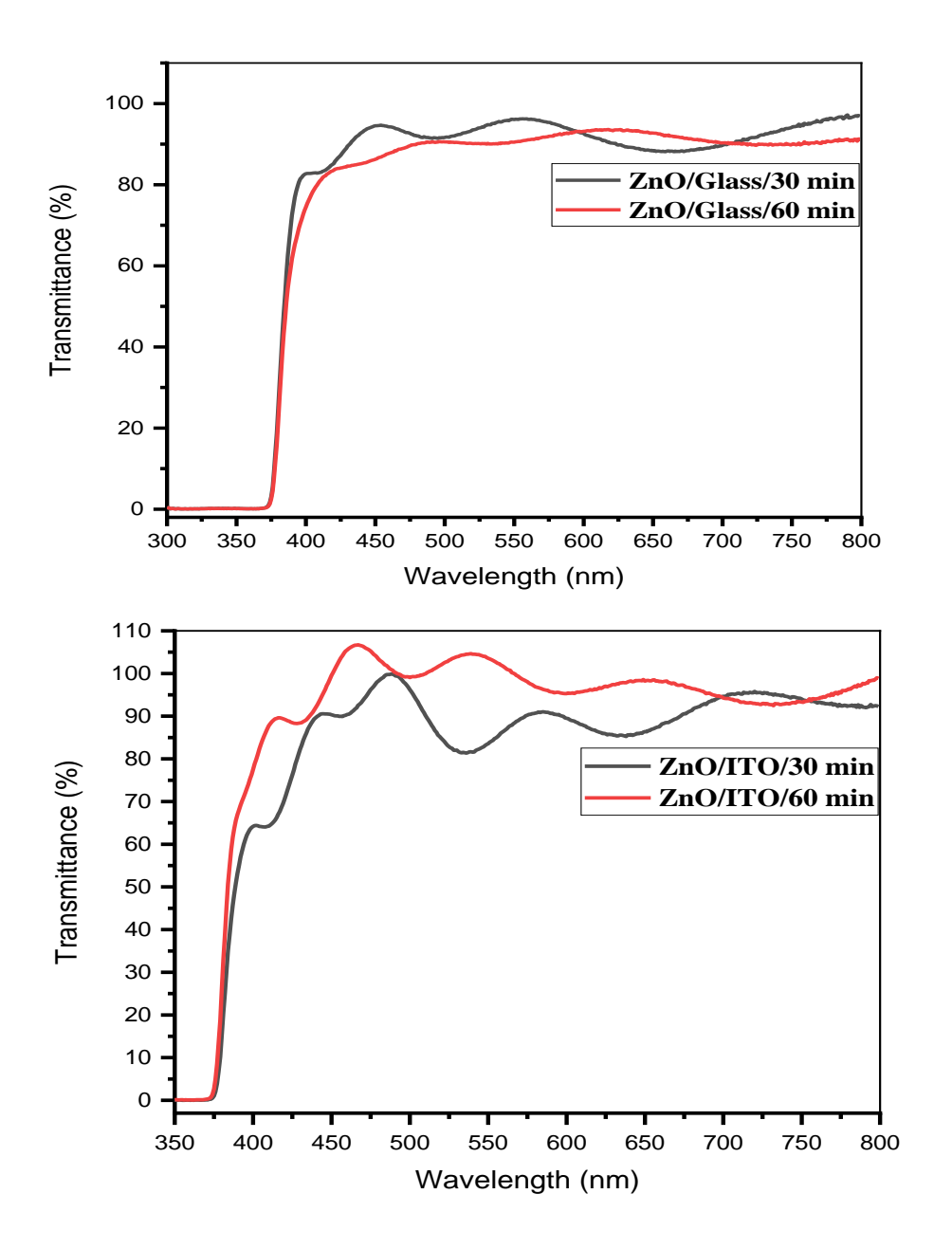


Figure III-18: Optical transmittance spectra of ZnO thin films prepared at tg=30 and 60 min.

Based on our observations regarding the effect of gelation time, the films prepared at 60 min show higher transmittance (>95%) compared to those prepared at 30 min (\approx 90%). This remark is really obvious for films deposited on ITO substrates (figure III-18).

III.4.2.1.1.3. Effect of rest time of the solution on ZnO thin films

During the experimental work, some solutions have been rested for more than 24 hours, almost 10 days. This solution has been used to study the effect of rest time (tr) on the optical properties of thin ZnO films. The figure below shows the variation of the transmittance using a solution has been left to rest of 10 days.

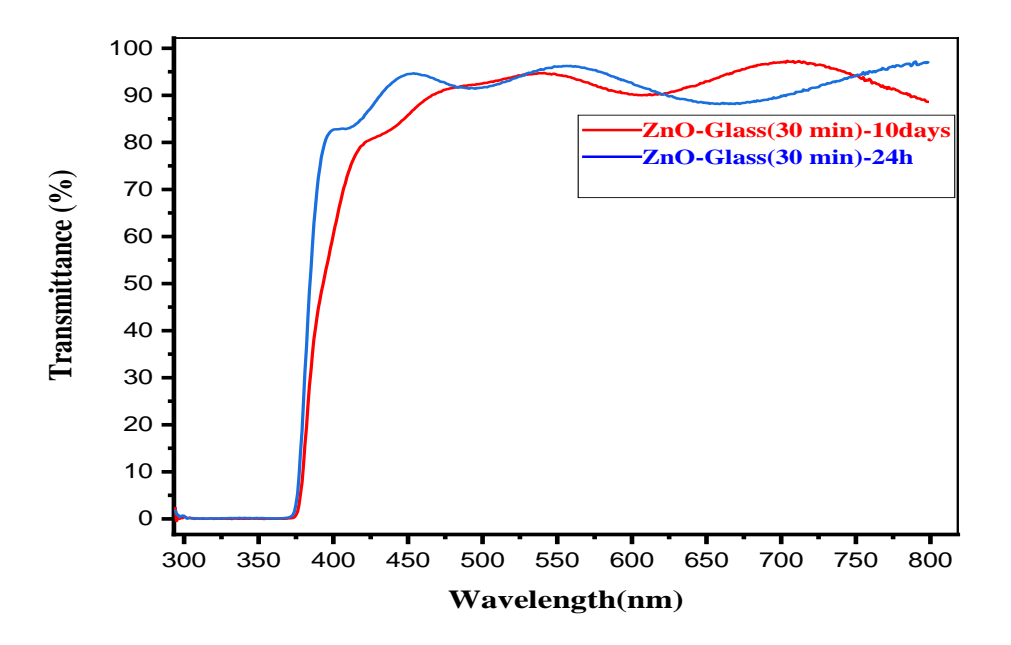


Figure III-19: Effect of rest time of the solution on ZnO thin films prepared on glass substrates.

The observation of the figure III-19 shows the transmittance of ZnO films using a solution that left to rest for 24 hours and for 10 days is almost the same rate of transmittance ($\approx 95\%$). But it has recorded some shift in absorption edge, which affect the gap energy as will be shown later.

III. 4.2.1.2. Optical band gap

From the transmittance spectra, we deduced the optical gap according to equations (II-6, II-7, and II-8 in chapter II).

We plotted the curves of the variation of $(\alpha h v)^2$ as a function of (h v) to determine the energy of the gap from took plan for direct transition. We previously saw that the energy of the forbidden band gap of a direct material can be obtained by extrapolating the $(\alpha h v)^2$ the linear part of the curve. The point of intersection with the horizontal axis indicates the value of the band gap (figure III-20) [20].

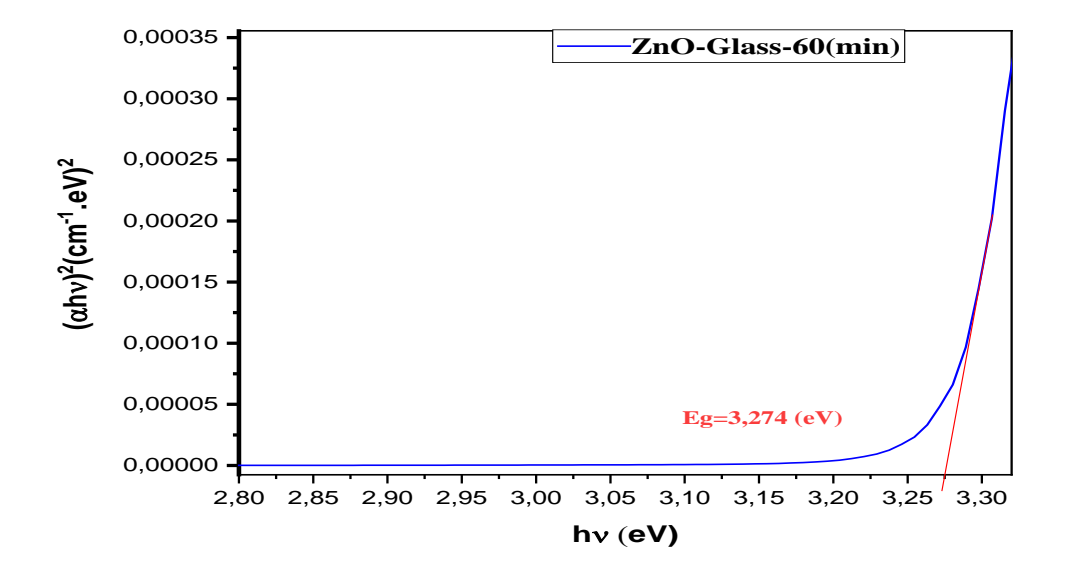


Figure III-20: Variation of $(\alpha hv)^2$ as a function of (hv) for ZnO thin films for tg =60min III.4.2.1.3. Urbach energy

The Urbach tail is a key parameter used to estimate structural defects or the degree of disorder in materials. This exponential tail appears in low-quality crystals, weak crystals, crystalline, and amorphous materials because these materials contain localized states extending into the energy gap [21].

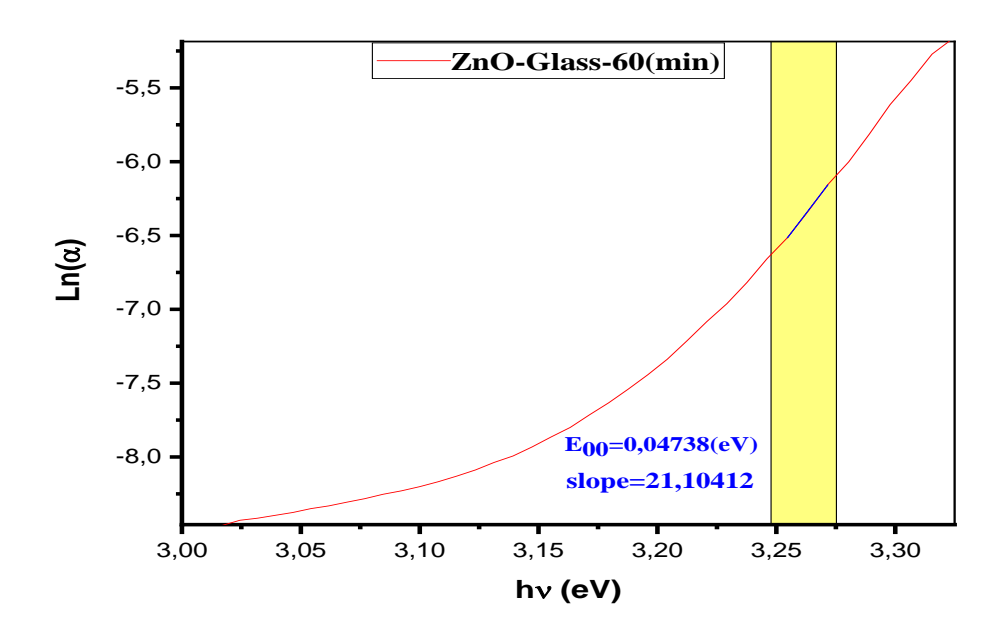


Figure III-21: Graph of (Lnα) as a function of (hv) for thin films of pure ZnO.

The figure shows $\mathbf{Ln}(\alpha)$ as a function of (hv) for thin films of pure ZnO. The Urbach energy is estimated from the graph of $\mathbf{Ln}(\alpha)$ Figure III-21 by taking the inverse of the slope of the linear region [21]. It is important to consider that the Urbach tail energy is closely related to the disorder in the thin film network. It can be seen that the minimum Urbach energy was obtained from glass substrates rather than ITO substrates. This result confirms the effect of substrate properties, as crystallin parameters and structure, on the quality of the structure. The substrate has a crystalline structure and parameters closest to those of the thin films deposited on it, the more these films have high quality and fewer defects. This result confirms the lower value of the strain for the films prepared on the glass substrate (Table III-5).

Also, in Table III-5, it is noticed that Urbach energy is lower for tg = 30 min in the case of the glass substrate. However, the lower value is recorded for tg = 60 min in the case of ITO substrate. **d** is the thickness of the films calculated using the equation II-10.

Table III-5: Variation of the optical parameters of ZnO thin films with elaboration conditions

Sample	Gelification Time	d (nm)	Eg (eV)	E ₀₀ (eV)	ε(%)	K
ZnO-Glass	30 (min)	806,3998	3,2888	0,0282	2,7278	7,7934
	60 (min)	808,4346	3,2744	0,0473	3,4696	7,3718
ZnO-ITO	30 (min)	618,1828	3,2745	0,0555	2,3030	11,8451
	60 (min)	896,5174	3,2855	0,0419	6,7494	7,7480
ZnO-Glass 10j	30 (min)	691,7972	3,2739	0,0559		10,5844

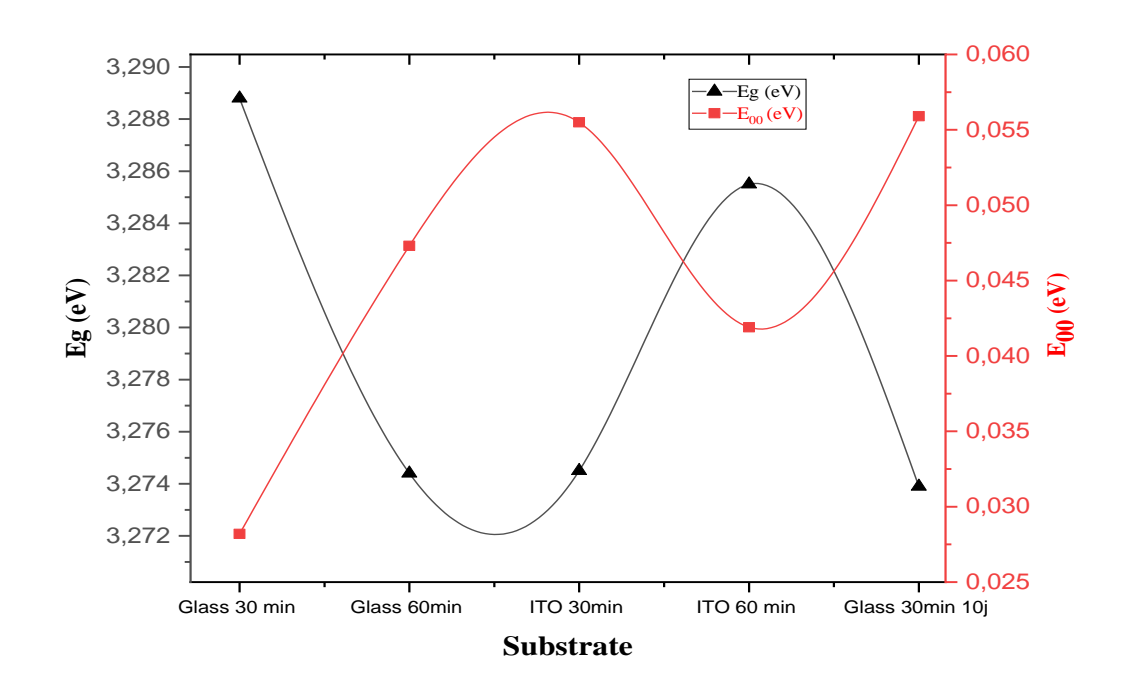


Figure III-22: Variation of Eg and E₀₀ for different Simple.

The variation of the gap energy and the extinction coefficient is well shown in Figure III-22. The values obtained for Eg are aligned with the published values of the band gap data in ZnO films [16]. The variation of Eg for each substrate is different. A minimum value of Eg was recorded for

tg = 60 min for the films developed on glass, however, the minimum value of Eg for ITO substrates is recorded for tg = 30 min. The lower value of Eg = 3,2739 eV is find for the thin films prepared with the solution left to rest for 10 days.

The relationship between the Eg and the Urbach energy is inverse. It can be explained by the Moss-Burstein effect, also known as the Burstein–Moss shift, which is the phenomenon in which the apparent band gap of a semiconductor is increased as the absorption edge is pushed to higher energies as a result of some states close to the conduction band being populated. This is observed for a degenerate electron distribution such as that found in some degenerate semiconductors and is known as a Moss–Burstein shift [22].

The difference in band gap energy between the various substrates affects the optical scattering between the grains that cluster together in the thin films. The variation in band gap energy for each substrate could be useful in many applications, such as sensors, solar cells, and various other applications [23].

The value of the extinction coefficient was calculated based on equation I-7, where we observed variations in the values, ranging between (7,3718 to 11,8451). This is attributed to the difference in substrate type and its effect on the growth of the film, the formation of grain boundaries or defects, as well as changes in the crystal structure, such as absorption centers within the energy gap. These factors lead to deviations from the ideal crystalline structure. All these reasons can result in changes in the absorption coefficient, reflecting the quality of the thin films and its crystallographic and optical properties.

It can be concluded that the structural and optical properties of the ZnO thin films were affected by the nature of the different substrates and the elaboration conditions.

III.4.3. Electrical characteristics

III.4.3.1. The four-point Technique

The electrical properties of pure ZnO thin films deposited on different types of substrates were studied using the four-point probe technique. This standard technique allows for determining the resistance sheet R_s of the thin films from the slope of the linear V(I) curve.

Figure III-23 presents the apparatus used KEYSIGHT B1500A Semiconductor Device Analyzer.



Figure III-23: KEYSIGHT B1500A Semiconductor Device Analyzer.

For our study the resistivity is calculated by the following equation:

$$\rho = R_{S}. d \tag{III-3}$$

Where is the resistivity, \mathbf{R}_s is the square resistance and \mathbf{d} the sample thickness.

The thickness of the films was calculated by weighting difference method using a sensitive microbalance according to relation:

$$\mathbf{d} = \frac{\Delta \mathbf{m}}{\rho \times \mathbf{A}} \tag{III-4}$$

Where $\Delta \mathbf{m}$ is mass of the deposited film, \mathbf{d} is density of ZnO, equal 5.72 g/cm³, for bulk ZnO cubic structure and \mathbf{A} = area of film [24].

It has observed a variation in the layer thickness even it has used the same number of layer and the same gelation time, which it permits to conclude that the nature of the substrates plays an important role in the films adherence on the substrates. The highest thickness values were recorded for the glass and silicon substrates. This is attributed to the solution being stored for 10 days, which led to an increase in the density of the solution compared to the solutions that were deposited after only one day. Consequently, thicker layers formed, resulting in an increase in the thickness of the thin films. The results are presented in (Table III-6).

Chapter III......Results and Discussion

Table III-6: Results of resistance and resistivity of ZnO thin films for different substrates used.

Sample	$ m R_{Shit}\left(\Omega ight)$	ρ (Ω.cm)	σ (Ω.cm) ⁻¹	d (cm)
ZnO-Glass 30 (min)	1,0301 x 10 ⁸	1700,4499	5,8807 x 10 ⁻⁴	165,0762 x10 ⁻⁷
ZnO-Glass 60 (min)	1,7153 x 10 ⁸	9442,6647	1,0163 x 10 ⁻⁴	550,4964 x10 ⁻⁷
ZnO-Glass 30 (min) 10 days	1,6335 x 10 ⁷	116124,6656	8,6114 x 10 ⁻⁶	710,8948 x10 ⁻⁵
ZnO-Silicon 30 (min)	$6,3936 \times 10^7$	2204,6590	4,5358 x 10 ⁻⁴	344,8228 x10 ⁻⁷
ZnO-Silicon 60 (min)	$4,4871 \times 10^3$	0,2470	4,0485	550,6544 x10 ⁻⁷
ZnO-Silicon 30 (min) 10 days	$1,8345 \times 10^7$	1503, 2103	6,6524 x 10 ⁻⁴	819,4115 x10 ⁻⁷

The electrical resistance measurements at room temperature show that the thin ZnO films on a silicon substrate for (60 min) have the lowest resistance value of (4,4871 x 10^3) ohms. This value represents the lowest resistance among undoped ZnO films. This result can be explained by the lower value of the strain ϵ in the films prepared on silicon at 30 min (ϵ =1,1553x10⁻⁴) as shown in Figure III-24. This result is particularly interesting as it indicates the possibility of obtaining a low-resistance polycrystalline Zinc Oxide thin film using a simple and cost-effective sol-gel coating technique [25].

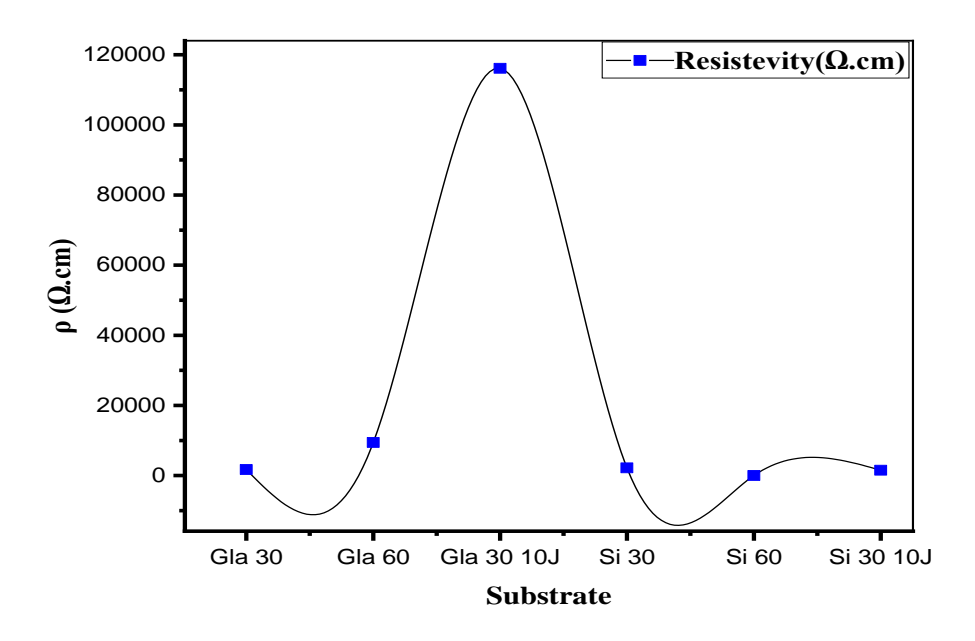


Figure III-24: Variation of Resistivity for different Simple.

The variations in the resistivity and conductivity of ZnO layers with respect to the types of substrates used for deposition are illustrated in figure III-24. We observed the effect of the substrates, tg, and tr on the resistivity of the ZnO thin films. This later shows a high resistivity especially for ZnO thin films deposited on glass for tr =10 days. However, the best values were obtained on silicon substrates deposited with solutions prepared for (60 min), indicating the success of this type of substrate.

The results obtained show that zinc oxide (ZnO) thin films grown on P-Si substrates exhibit a high electrical conductivity compared to films grown on glass substrates. This behavior can be explained by the high quality of the grown layers and the activation of acceptor as a defects located at deep level in the band gap. The acceptor atomes become active at elevated and annealed temperatures, which is around of $500 \, \text{C}^{\circ}$ [26].

It has been established that the growth dynamics of ZnO thin films on silicon substrates can be influenced by the surface composition, with the graded nature of the silicon surface playing a crucial role in the film growth process. In p-type silicon, boron (B) atom substitute silicon atoms just beneath the surface, which in turn affects the initial stages of ZnO films growth. The good conductivity of the ZnO thin films is attributed to the reduced concentration of intrinsic defects at

the substrate interface achieved through specific substrate growth conditions and its structural properties [26].

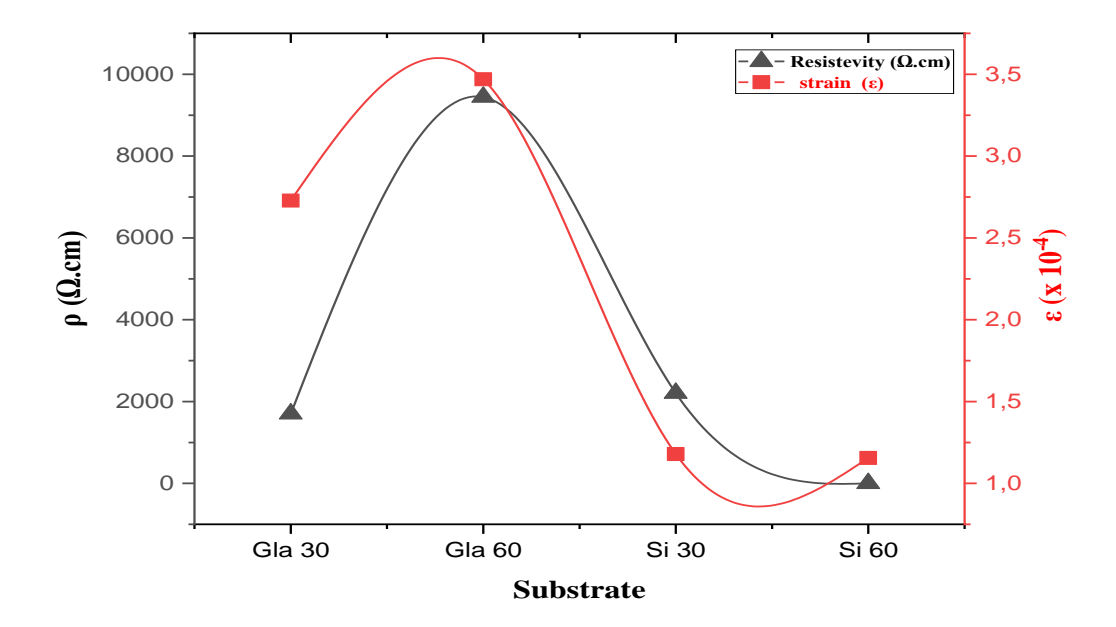
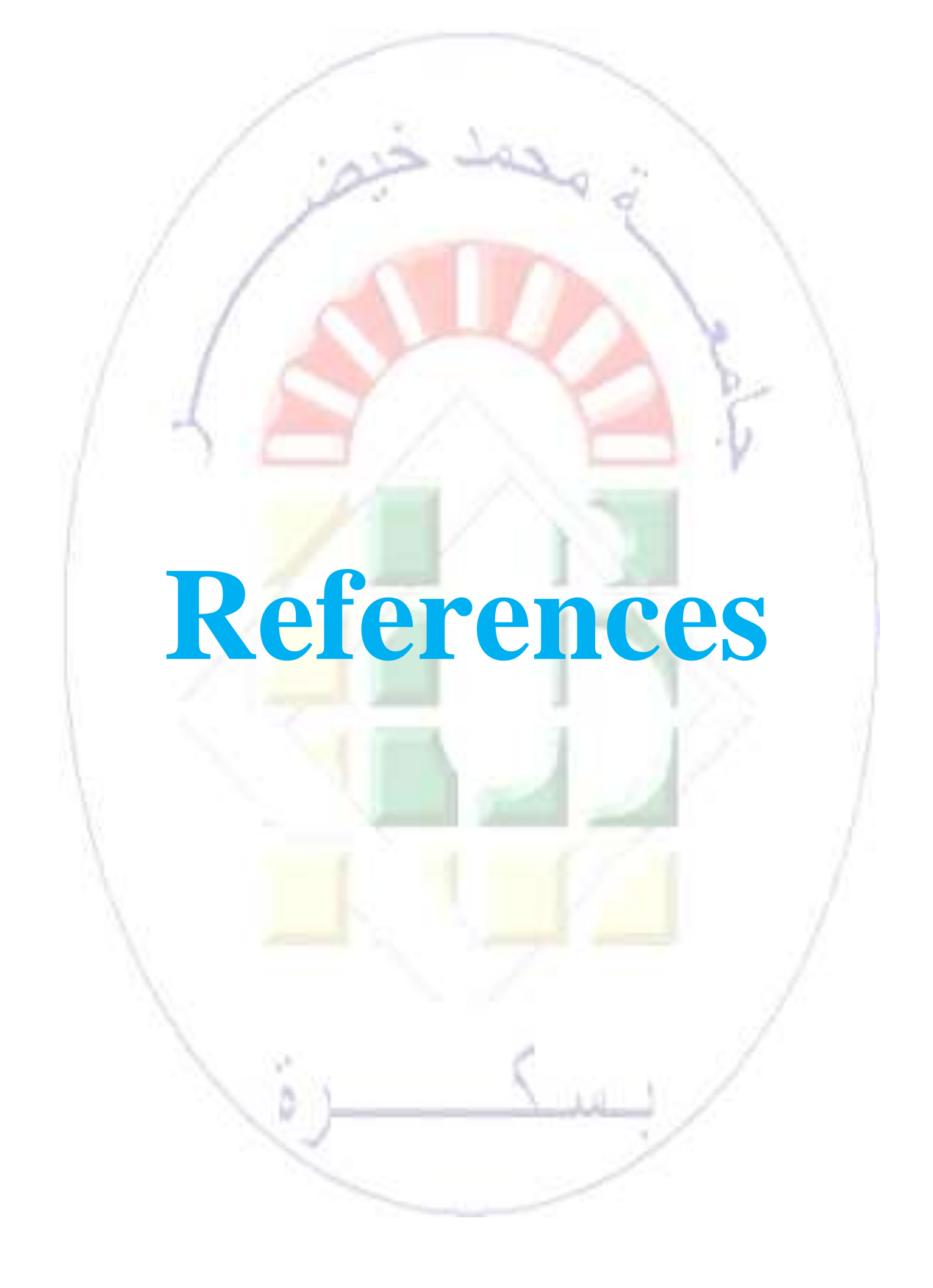


Figure III-25: Changes in electrical conductivity and Strain as a function of the substrate.

Figure III-25 illustrates the variations in electrical resistivity and grain-level distortions as a function of the deposited substrates. An increase in electrical resistivity is observed, which is attributed to changes in structural properties such as the increase in defects and lattice distortions caused by macrostrain, as revealed by X-ray diffraction analysis. The increase in grain distortions leads to a reduction in the effects of grain boundaries, as these boundaries hinder the charge carrier transport mechanism, which explains the observed rise in resistivity [24].



Chapter III......Results and Discussion

References

- [1] M. Dahnoun, "Preparation and characterization of Titanium dioxide and Zinc oxide thin films via Sol-Gel (spin coating) technique for optoelectronic application", Doctoral Thises, Mohamed Khider University of Biskra-Algeria, 2020.
- [2] V. Drozd, V. Titov, I. Kasatkin, L. Basov, A. Lisachenko, O. Stroyuk and S. Kuchmiy, "Structure, optical properties and visible-light-induced photochemical activity of nanocrystalline ZnO films deposited by atomic layer deposition onto Si(100)", Thin Solid Films, p. 128–133, 2 April, 2014.
- [3] S. Jana, S. Mandal, S. Roy, M. Saifuddin and S. Hazra, "Sputter-cleaning modified interfacial energetic and molecular structure of DNTT thin film on ITO substrate", Applied Surface Science, 2024.
- [4] R. Bel Hadj Tahar, B. Takayuki, O.Yutaka and Y. Takahashi, "Tin doped indium oxide thin films, Electrical properties" p. 2631–2645 doi.org/10.1063/1.367025, 1 March, 1998.
- [5] I. Deghiche, Effect of solution concentration on the properties of ZnO thin films prepared by the sol-gel method, Masters dessertation, Mehamed Khider University of Biskra-Algeria, 2018.
- [6] M. Ohring, "Materials science of thin films, Deposition and structure", Academic press, Department of Material Science and Engineering, Stevens Institute of Technology.
- [7] S. Naceur, "Elaboration, characterization and simulation of thin film transistors based on Zinc Oxide", Doctoral Thises, Mohamed Khider University of Biskra-Algeria, 2023.
- [8] A. Taabouche, A. Bouabellou, F. Kermiche, F. Hanini and S. Menakh, "Effect of Substrates on the Properties of ZnO Thin Films Grown by Pulsed Laser Deposition" Advances in Materials Physics and Chemistry, pp. 209-213, doi.org/10.4236.34031, 2013.

[9] W. Chebil, A. Fouzri, B. Azeza, N. Sakly, R. Mghaieth, A. lusson and V. Sallet, "Comparison of ZnO thin films on different substrates obtained by sol-gel process and deposited by spin coating technique" Indian Journal of pure Applied Physics, vol. 53, pp. 521-529, 2015.

- [10] D. Aryanto, W. Jannah, Masturi, T. Sudiro, A. Wismogroho, P. Sebayang, Sugianto and P. Marwoto, "Preparation and structural characterization of ZnO thin films by sol-gel method" IOP Publishing, pp. 1-7, doi: 10.1088/1742-6596/817/1/012025,2017.
- [11] M. Firdaus Malek, M. Hafiz Mamat, M. Zainizan Sahdan, M. Mohamed Zahidi, Z. Khusaimi and M. Rusop Mahmood, "Influence of various sol concentrations on stress/strain and properties of ZnO thin films synthesised by sol-gel technique" Thin Solid Films, vol. 527, pp. 102-109, DOI.org /10.1016/J.tsf.2012. 11.095, 2013.
- [12] A. Amri, A. Louiza, A. Meftah and A. Latif, "Effect of aluminum doping on the structural, optical and electrical properties of ZnO thin films processed under thermal shock conditions" Results in Optics 100426, results-in-optics, 2023.
- [13] D. J. Haneen, A. F. Makram, A. Mohammed Jalal, S. D. Omar, T. Evan, H. Forat and U. Hashim, "Effect of Different Etching Time on Fabrication of an Optoelectronic Device Based on GaN/Psi" Journal of Renewable Materials, vol. 11, no. 03, DOI: 10.32604/jrm.2023.023698, 2023.
- [14] G. williamsont and w. hall, "X-ray line broadening from filed aluminium and wolfram" metallurgica, vol. 01, pp. 23-31, 1953.
- [15] A. Latif, Elaboration of pure and doped ZnO powders with the sol gel method, Doctorale Thesis, University Mohamed Khider of Biskra -Algeria, 2024.
- [16] N. Ben Amar, "Effect of catalyst concentration on the properties of ZnO thin films prepared by the sol-gel method", Masters dessertation, Mohamed Khider University of Biskra, 2018.
- [17] H. Belkacemi, "Deposition and Characterization of ZnO Thin Films with Different Zinc Sources", Masters dessertation, Mohamed Khider University of Biskra-Algeria, 2011.

[18] A. Amri, "Elaboration des couches minces à base de ZnO pour transistors couches minces TFTs", Doctorat Theses, Mohamed Khider University of Biskra-Algeria, 2024.

- [19] M. Othmane, "Synthesis and characterization of Zinc Oxide (ZnO) Thin films deposited by spray pyrolysis for applying, electronics and photonics", Doctoral Thesis, Mohamed Khider University of Biskra -Algeria, 2018.
- [20] Y. Boudiaf and W. Rahab, "Elaboration and Characterization of Pure and Ga-Doped ZnO Nanopowders by the Sol-Gel Method", Masters dessertation, Mohamed Khider University of Biskra-Algeria, 2020.
- [21] H. Nezzal and N. H. Redjouh, "Elaboration of pure and Bi-doped ZnO nano-powders with the sol-gel method", Master dessertation, Mohamed Khider University of Biskra -Algeria, 2022.
- [22] K. Butcher, H. Hirshy, R. Perks, M. Wintrebert-Fouquet and P.-T. Chen, "Stoichiometry effects and the Moss–Burstein effect for InN" physica status solidi, no. 01, pp. 66-74, DOI 10.1002/pssa.200563504, 2006.
- [23] A. Rosmalini, M. Nurmalina, W. Wan Rosmaria, A. Anees and Z. Ahmad Sabirin, "Effect of substrates on Zinc Oxide thin films fabrication using sol-gel method" Materials Science and Engineering, vol. 340, pp. 1-5, DOI:10.1088/1757-899X/340/1/012002, 2018.
- [24] A. Derbali, A. Attaf, H. Saidi, H. Benamra, M. Nouadji, M. Aida, N. Attaf and H. Ezzaouia, "Investigation of structural optical and electrical properties of ZnO thin films prepared by ultrasonic spray technique for photovoltaic applications" Optik, vol. 154, pp. 286-293,DOI.org/10.1016/j.ijleo.2017.10.034, 2018.
- [25] R. Ghosh, D. Basak and S. FUjihara, "Effect of substrate-induced strain on the structural, electrical, and optical properties of polycrystalline ZnO thin films" Additional information on J. Appl. Phys, vol. 96, no. 5, pp. 2689-2692, DOI: 10.1063/1.1769598, 2004.

Chapter III......Results and Discussion

[26] E. Saeed , B. Andrew and I. Agis A, "Study of Conductivity Type of Undoped ZnO films Grown on n and p-type (100) Si Substrates by Pulsed Laser Deposition" P,1-2, 2011.



General Conclusion

Nanostructured zinc oxide (ZnO) has attracted great attention over the recent years because of its interesting properties making this material particularly appealing for a wide range of applications in several technological fields, like optoelectronics and biochemical sensing. This is also evidenced by the huge number of scientific publications about this material. Based on this approach, we prepared high-quality Zinc Oxide thin films within the nanometer scale using a simple and cost-effective sol-gel chemical method. This was achieved through spin coating at low temperatures, with solution preparation times at from 30 and 60 min.

The main objective of this experimental work is to study the effect of glass, silicon p-type, and indium tin oxide (ITO) substrates on the structural, optical, and electrical properties of undoped Zinc Oxide films deposited.

The crystal structure of Zinc Oxide (ZnO) thin films was determined using X-ray diffraction (XRD), which revealed that ZnO crystallizes in a hexagonal wurtzite polycrystalline structure. The grain size was calculated to range from 30,3656 nm to a maximum value of 47,6956 nm on various substrates. Macrostrain was observed within the crystal lattice, with the lowest strain value reaching on p-type silicon substrates, reaching 1,1553x10⁻³, indicating the high quality of ZnO grains and the degree of lattice parameter matching between the films and the substrate. Furthermore, this technique revealed the presence of dislocations in the crystal lattice, with the highest dislocation density estimated at 10,845 nm⁻² on glass substrates.

The optical properties of the zinc oxide thin films were examined using UV-Vis spectrophotometer. It indicated the presence of a distinct band gap, approximately of **3,2888 (eV)** for the thin films deposited on glass substrates at tg =30 min. The highest transmittance was recorded for the glass substrates, reaching a value of **95%** compared to indium tin oxide (ITO) substrates. Additionally, the films exhibited low Urbach energy values with slight variations between different substrates. The extinction coefficient values were also determined, with the highest value recorded at **11,8451**, indicating greater absorption of incident light on the indium tin oxide (ITO) substrates.

General conclusion

As for the electrical properties, the four-point probe technique was used to record various values of electrical resistance, with the lowest value being $4,4871x10^3$ (Ω). Additionally, the best electrical conductivity value achieved was 4,0485 (Ω .cm)⁻¹ on p-type silicon substrate.

Abstract

Effect of Substrates on the properties of ZnO thin films elaborated with the sol-gel method

In this experimental work, we prepared thin films of undoped Zinc Oxide at low temperatures using the Sol-gel chemical method. Seven successive layers were deposited on different substrates including glass, silicon type-p, and indium tin oxide (ITO). The films deposited using the Spin-coating technique. We studied the influence of the different substrates on the structural, optical, and even electrical properties of the films. X-ray diffraction revealed that the films possess a polycrystalline structure with a hexagonal wurtzite phase. Optical property analysis using UV-Vis spectroscopy showed that glass substrates exhibited very high transparency compared to indium tin oxide (ITO) substrates. Additionally, the four-probe technique revealed good electrical conductivity for the silicon substrate, while the other substrates showed higher resistivity.

Key words: Zinc Oxide, Sol-gel, spin coating, Thin films, Substrates, X-ray diffraction, UV-Vis spectrometers, four-probe technique.

ملخص

تأثير الركائز على خصائص الاغشية الرقيقة من أكسيد الزنك المحضرة بطريقة الصول-جل

لقد قمنا في هذا العمل التجريبي بتحضير طبقات رقيقة من اكسيد الزنك الغير مطعم في درجات حرارة منخفضة بالاعتماد على الطريقة الكيميائية سائل-هلام تم ترسيب سبعة طبقات متتالية على ركائز مختلفة من الزجاج والسيليكون بالإضافة الى ركائز الاكسيد الانديوم باستخدام تقنية الطلاء الدوراني ودراسة مدى تأثير الركائز المختلفة على الخصائص البنيوية والبصرية وحتى الكهربائية. كشفت حيود الاشعة السينية على ان الاغشية لها بنية متعددة البلورات على شكل ورتزايت سداسي كما تبين من دراسة الخصائص البصرية باستخدام الاشعة الفوق بنفسجية المرئية ان ركائز الزجاج تتمتع بشفافية عالية مقارنة بركائز أكسيد الانديوم فيما أظهرت تقنية النقاط الأربعة خصائص كهربائية جيدة بالنسبة لركائز السيليكون ومقاومية عالية لبقية الركائز.

الكلمات المفتاحية أكسيد الزنك- سائل هلام- الطلاء الدوراني- الشرائح الرقيقة- الركائز- حيود الاشعة السينية -الاشعة الفوق بنفسجية المرئية- تقنية النقاط الأربعة.

Résumé

Effet des substrats sur les propriétés des films minces de ZnO élaborés par la méthode sol-gel

Dans ce travail expérimental, nous avons préparé des couches minces de ZnO non dope à basse température en utilisant la méthode chimique sol-gel. Sept couches consécutives ont été déposées sur différents substrats en verre, en silicone ainsi que sur des substrats en ITO, en utilisant la technique du spin coating. Nous avons étudié l'effet des différents substrats sur les propriétés structurales, optiques et même électriques des couches. La diffraction des rayons X a révélé que les films ont une structure poly cristalline de type wurtzite hexagonale. L'étude des propretés optiques par spectroscopie UV-Visible a montré que les substrats en verre présentent une transparence plus élevée par rapport aux substrats ITO. En revanche, la méthode des quatre points a révélé de bonnes propriétés électriques pour les substrats en silicone et une résistivité élevée pour les autres substrats.

Mots clés : Oxide de Zinc, Sol-gel, Spin coating, Couches minces, Substrats, La diffraction des rayons X, spectromètres UV-Visible, la méthode des quatre points.

REPUBLIQUE ALGERIENNE DEMOCRATIQUE ET POPULAIRE MINISTERE DE L'ENSEIGNEMENT SUPERIEUR ET DE LA RECHERCHE SCIENTIFIQUE UNIVERSITE MOHAMED KHIDER - BISKRA Faculté des SE.



الجمهورية الجزائرية الديمقراطية الشعبية وزارة التعليم العالي والبحث العلمي جامعة محمط خيصر يسكرة كلية العلوم الدةيونة

Département des Sciences de la matière

Filière: Physique

قسم: علوم المادة

شعبة :الفيزياء

تصريح شرفيي خاص بالالتزام بقواعد النزاهة العلمية لإنجاز بحث (ملحق القرار 1082 المؤرخ في 2021/12/27)



أنا الممضي أسفله،
السيد(ة): حرى حَلْمِقَى عَرَد وَمِنْ السِيدِرة): حراء الحيود.
الصفة: طالب سنة حَالَيْق ماسر تخصص: جَوَرَ حراء الحيود.
الحامل(ة) لبطاقة التعريف الوطنية رقم: 09395456 2 ... الصادرة بتاريخ: 12/6/2013 المسجل بكلية: العلوم الد حَدِقَى قسم: علو مم الحدث : مذكرة والمكلف بانجاز أعمال بحث : مذكرة عنوانها: منظرة المسجل المسجل عنوانها: منظرة المسجل ال

أصرح بشرفي أني ألتزم بمراعاة المعايير العلمية والمنهجية ومعايير الأخلاقيات المهنية والنزاهة الأكاديمية المطلوبة في انجاز البحث المذكور أعلاه وفق ما ينص عليه القرار رقم 1082 المؤرخ في 2021/12/27 المتعلقة بالوقاية من السرقة العلمية ومكافحتها.

التاريخ: 2025/05/22

إمضاء المعني بالأمر